

---

# New Albany Shale, Illinois Basin, USA— Devonian Carbonaceous Mudstone Accumulation in an Epicratonic Sea: Stratigraphic Insights from Outcrop and Subsurface Data

**O. R. Lazar**

*ExxonMobil, 22777 Springwoods Village Parkway, Spring, Texas 77389 (e-mail: ovidiu.remus.lazar@exxonmobil.com)*

**J. Schieber**

*Department of Earth and Atmospheric Sciences, Indiana University, Bloomington, Indiana 47405 (e-mail: jschiebe@indiana.edu)*

*The paucity of fossils has been discouraging, and the uniformity in the character of sediments has been tantalizing, but nevertheless misleading, to stratigraphers. However, the reputed uniformity is more real over hundreds of miles horizontally than in 100 feet vertically.*

—Campbell, 1946, p. 831

## ABSTRACT

Extensive organic-carbon-rich fine-grained rock successions accumulated in the epicontinental seas of Laurentia within sedimentary basins, including the Illinois, Appalachian, and Michigan Basins, during the Middle to Late Devonian. The New Albany Shale of the Illinois Basin illustrates the expression of sequence-stratigraphic surfaces and units in an epeiric, intracratonic sea. Four depositional sequences, bounded by laterally extensive erosion surfaces, are recognized and mapped within the Middle to Upper Devonian New Albany Shale succession. Depositional sequences and their component systems tracts have distinct physical, biogenic, and chemical signatures that translate into distinct source- and reservoir-rock properties. Mudstone units record the interplay of organic production, preservation, and dilution. Depositional sequences and systems tracts vary significantly in thickness vertically and laterally throughout the Illinois Basin. Spatial variation in thickness reflects differences in sediment supply and in accommodation resulting from the changes in paleotopography, sea level, and subsidence.

This chapter illustrates that the sequence-stratigraphic approach provides fundamental insights even when the investigation is based on a fairly limited database consisting of a few cores, outcrops, and gamma-ray well logs acquired over several decades at various (and occasionally insufficient) resolutions. The resulting sequence-stratigraphic framework indicates that the sedimentary record of the New Albany Shale is quite discontinuous. Understanding the character and distribution of source- and reservoir-rock properties within this discontinuous stratigraphic succession is useful for focusing future, more detailed analyses of targeted intervals at different exploration to production phases.

## INTRODUCTION

The Middle to Upper Devonian New Albany Shale is a major source and reservoir of hydrocarbons in the Illinois Basin, having an estimated original gas-in-place of 86–160 Tcf (e.g., National Petroleum Council, 1980, 1992; Cluff et al., 1981; Barrows and Cluff, 1984; Cluff and Byrnes, 1991; Hasenmueller and Comer, 2000; Curtis, 2002; Partin, 2004; Lazar, 2007).

The New Albany Shale has been considered the result of essentially continuous deposition of carbonaceous mud into a largely stratified, anoxic epicontinental sea for more than 20 m.y. (e.g., Lineback, 1970; Cluff, 1980; Beier and Hayes, 1989; Ripley et al., 1990; Frost, 1996). New perspectives emerged through the integration of sedimentologic, paleontological, geochemical, and geophysical data from drilled wells and outcrops (Lazar, 2007):

- Carbonaceous mud accumulated in a relatively low-accommodation setting under the influence of frequent storms, fluctuating sea level, and variable redox conditions.
- The resulting mudstone succession consists of a stack of distinct depositional sequences bounded by erosion surfaces that can be traced throughout the Illinois Basin.

This chapter is based primarily on the detailed study of Lazar (2007) and illustrates the approach and some of the insights gained during the construction of a sequence-stratigraphic framework for the New Albany Shale. The understanding and prediction of the variability in rock properties in the New Albany Shale across the Illinois Basin was enhanced during the process of constructing a sequence-stratigraphic framework for this fine-grained rock succession.

## BACKGROUND

### Geological Context

The Middle to Late Devonian (~392 Ma–361 Ma; Kaufmann, 2006) was characterized by a decline in atmospheric CO<sub>2</sub> concentration (Figure 1A; Berner,

1990; Berner, 1997), an increase in atmospheric oxygen (Figure 1B; Berner, 1999), and a general rise in eustasy (Figure 1C; Vail et al., 1977; Hallam, 1984; Johnson et al., 1985).

Annual average sea surface temperature ranged from 19°C to 24°C (variation ≤ 4°C; ExxonMobil Devonian model). Annual average precipitation/evaporation ratios varied from dry to very dry (very low variation); seas were prone to water-column stratification (ExxonMobil Devonian model). The global climate changed from a warm mode in the late Silurian to latest Devonian to a cool to glacial mode in the latest Devonian to the Mississippian (e.g., Strelc et al., 2000; Joachimski et al., 2009).

Major changes in biotic diversity culminated with the Frasnian–Famennian mass extinction event—considered one of the five greatest biotic crises of the Phanerozoic (e.g., Sepkoski, 1986; Scotese and McKerrow, 1990; Jablonski, 1991; McGhee, 1996; Hallam and Wignall, 1999; House, 2002). Climate change, sea-level change, oceanic anoxia, asteroid impact(s), and environmental perturbations associated with the spread of vascular plants on land have been proposed as singular or combined causes of this biodiversity crisis (e.g., Berner, 1990; Algeo et al., 1995, 2001; McGhee, 1996; Hallam and Wignall, 1999; Joachimski and Buggisch, 2002; McGhee, 2005; Racki, 2005).

The position of the continents during the Middle to Late Devonian has also been a subject of debate. Different paleogeographic reconstructions proposed a range of possibilities—from a close connection to a 3000-km oceanic separation between Laurentia and Gondwana (e.g., van der Voo, 1988; Scotese and McKerrow, 1990; Li et al., 1994; McKerrow et al., 2000; Tait et al., 2000). Paleogeographic reconstructions that propose a relatively narrow oceanic separation suggest that eastern parts of North America were located between approximately 15°S and 30°S latitude (Figure 1D; e.g., Scotese and McKerrow, 1990; Ettensohn, 1992; Day et al., 1996; McKerrow et al., 2000; Blakey, 2006; Markello et al., 2008; Bohacs et al., 2011, 2012).

During the Late Devonian, the area that now spans southern Indiana, western Kentucky, and eastern Illinois was located at a subtropical paleolatitude, between 25°S and 30°S (Figure 1D), on continental

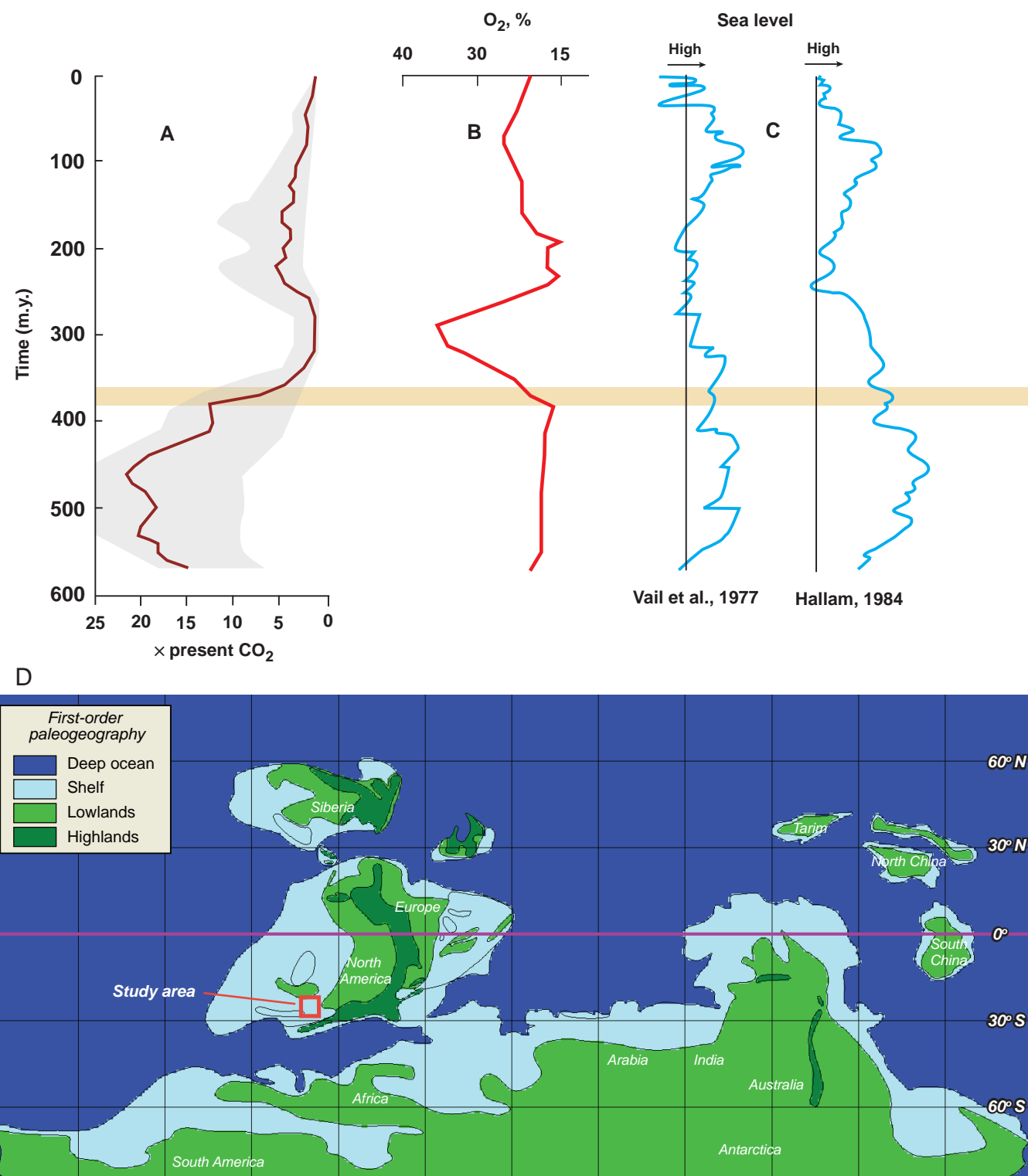


**Figure 1.** (A) Atmospheric  $\text{CO}_2$  versus time; range of errors indicated by shaded area (after Berner, 1997). (B) Atmospheric O<sub>2</sub> versus time (after Berner, 1999). (C) Sea-level curves for the Phanerozoic (after Vail et al., 1977; Hallam, 1984). Horizontal bar (tan) represents the Late Devonian interval. (D) First-order paleogeographic map of the world during the Late Devonian (after Markello et al., 2008; Bohacs et al., 2011, 2012).

crust under an epeiric sea shielded from tropical cyclones (e.g., ExxonMobil Devonian model; Scotese and McKerrow, 1990; Ettensohn, 1992; Day et al., 1996; McKerrow et al., 2000; Blakey, 2006; Markello et al., 2008; Bohacs et al., 2011, 2012). Globally during this time, coral-stromatoporoid-dominated reef platforms were common, and there were minimal skeletal grain producers (Markello et al., 2008; Joachimski et al., 2009; Bohacs et al., 2014). Brachiopods and tentaculitoids provided additional carbonate material (Lazar, 2007; Wittmer and Miller, 2011 and references therein). Primary planktonic producers of organic matter included cyanobacteria and chlorophyta, whereas biogenic SiO<sub>2</sub> producers included radiolaria and siliceous sponges (Markello et al., 2008; Bohacs et al., 2014). There were no primary planktonic CO<sub>2</sub> producers, and vascular plants had recently appeared on land and were spreading into lowlands, updip along braided streams, and downdip along meandering rivers (e.g., Algeo et al., 1995, 2001; Fraticelli et al., 2004, 2006; Bohacs and Fraticelli, 2006, 2008). Weathering-derived detritus from the surrounding catchments included coarse to fine-grained silt composed of clay minerals, quartz, and dolomite (Lazar, 2007; Markello et al., 2008). Much of the detritus in the water column was delivered to the seafloor packaged into aggregate grains (e.g., Lazar, 2007; Schieber and Southard, 2009; Schieber and Yawar, 2009). Once at the seafloor, sediments were commonly reworked by advective processes, and the original depositional fabrics were disrupted by organisms living in the surficial sediment layers (Schieber, 1998a, 2003; Lazar, 2007; Riese, 2014). The potential for dilution by terrigenous clastic yield based on climatic factors was probably moderate to low. As significant volumes of organic carbon were available in the water column, the bottom waters were commonly oxygen depleted, which contributed to enhanced preservation of elevated concentrations of organic carbon in the sediment (up to 25 wt. % total organic carbon [TOC]; e.g., Barrows and Cluff, 1984; Frost and Shaffer, 2000; Curtis, 2002; Schieber and Lazar, 2004; Lazar, 2007).

Extensive organic-carbon-rich fine-grained rock successions accumulated in the epicontinental seas of Laurentia within sedimentary basins, including the Illinois, Appalachian, and Michigan basins during the Middle Devonian to the Early Mississippian (Figure 2; e.g., Conant and Swanson, 1961; Lineback, 1968; Kepferle and Roen, 1981; Catacosinos and Daniels, 1991; Ettensohn, 1992; de Witt et al., 1993; Matthews, 1993; Ettensohn, 1998; Hasenmueller et al., 2000; Lumm et al., 2000; Schieber and Lazar, 2004; Lazar, 2007; Smith et al., 2019). One of these, the Illinois Basin, covers today approximately 155,000 km<sup>2</sup> in parts of Illinois, Indiana, Kentucky,

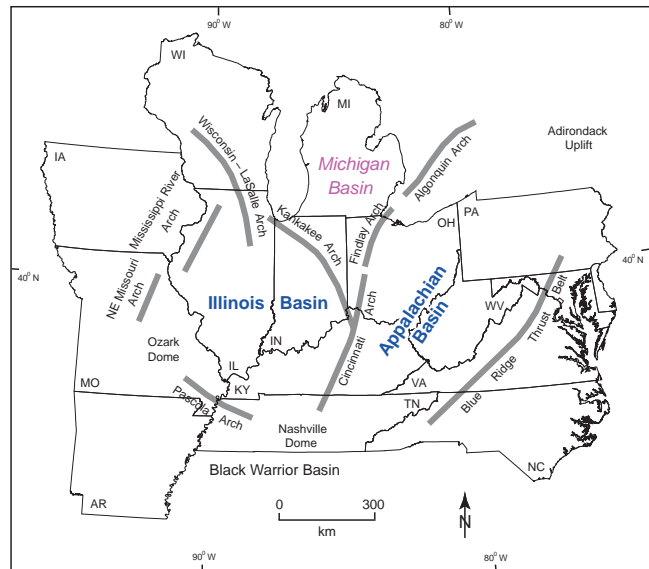


**Figure 2.** Map of the Mideastern United States showing the location of the Illinois Basin and the major structural features that delineate this basin (from Lazar, 2007; after Kepferle and Roen, 1981; Buschbach and Kolata, 1991; Ettensohn, 1992; de Witt et al., 1993; Matthews, 1993; Lumm et al., 2000).

and Tennessee (Figure 2; Barrows and Cluff, 1984; Lumm et al., 2000) and represents a polyhistory basin (Kolata and Nelson, 1991). Following a rift phase that lasted from the early to the middle Cambrian, the basin evolved during the remainder of the Paleozoic into a cratonic basin surrounded by structural arches (Figure 2; Kepferle and Roen, 1981; Barrows and Cluff, 1984; Buschbach and Kolata, 1991; Kolata and Nelson, 1991; Ettensohn, 1992; de Witt et al., 1993; Matthews, 1993; Lumm et al., 2000). The southern part of the Illinois Basin coincides with the northeastern tip of the New Madrid Rift Complex (Buschbach and Kolata, 1991; Kolata and Nelson, 1991; Lumm et al., 2000). Throughout the Devonian, the basin was open to the south (Barrows and Cluff, 1984; Nelson and Marshak, 1996), and erosion of the Acadian Orogen to the east was the principal source of terrigenous clastics for the Upper Devonian mudstones of the eastern United States (Lineback, 1970; Ingall et al., 1993). Eastern- and western-bounding arches (Figure 2) might have been locally active sources of sediment (Lineback, 1970; Cluff, 1980; Lazar, 2007).

The Middle to Upper Devonian New Albany Shale, one of the carbonaceous mudstone successions that developed in the epicontinental seas of Laurentia, occurs in outcrops and in the subsurface throughout much of the Illinois Basin (e.g., Lineback, 1964, 1968, 1970; Hasenmueller and Comer, 2000; Schieber and Lazar, 2004; Lazar, 2007). Studies have addressed the

internal stratigraphy (e.g., Campbell, 1946; Lineback, 1964, 1968, 1970; Ettensohn, 1992; Roen, 1993; Sandberg et al., 1994; Over, 2002; Lazar and Schieber, 2006; Lazar, 2007; Over et al., 2009; Spencer, 2013; Lazar et al., 2015a), geochemistry (e.g., Beier and Hayes, 1989; Hatch et al., 1991; Ingall et al., 1993; Calvert et al., 1996; Frost, 1996; Frost and Shaffer, 2000; Lazar, 2007; Wei et al., 2016; Liu et al., 2019), environments of deposition (e.g., Cluff, 1980; Ettensohn and Barron, 1981; Schieber and Riciputi, 2004; Lazar, 2007; Riese, 2014), and hydrocarbon potential (e.g., Cluff and Byrnes, 1991; Seyler and Cluff, 1991; Hamilton-Smith et al., 2000; Curtis, 2002; Partin, 2004; Gale et al., 2010; Schieber, 2010; Strapoć et al., 2010; Mastalerz et al., 2013; Nuttall, 2013; Nuttall et al., 2015) of the New Albany Shale.

In terms of stratigraphy, based on a combination of fossil content, lithology, and joint patterns, Campbell (1946) proposed the first detailed stratigraphic subdivision of the New Albany Shale into six formations (Figure 3A). Campbell's stratigraphy was significantly revised by Lineback (1964, 1968, 1970), who proposed a lithostratigraphic division of the New Albany Shale into five members and four beds (Figure 3A). Subsequent researchers (e.g., Cluff et al., 1981; Hasenmueller et al., 2000) built on the lithostratigraphic framework of Lineback (1964, 1968, 1970) and defined eight additional members and one formal bed in the New Albany Shale in different parts of the Illinois Basin. As a result, a complex regional lithostratigraphy of 13 members and five beds has been in use for the New Albany Shale (Figure 3B; e.g., Hasenmueller and Comer, 2000). Not all of the 13 members and five beds can be consistently differentiated in the subsurface. Additionally, the use of some of the lithostratigraphic units is locally restricted and in many instances stops at the state boundary between Indiana and Illinois (e.g., Hasenmueller et al., 2000).

## Data, Methods, and Approach

Our information comes from a detailed sequence-stratigraphic study by Lazar (2007) that integrated sedimentologic, paleontological, geochemical, and geophysical data from 219 drilled wells, three cores, two outcrops, and 51 polished thin sections. Outcrops, cores, and thin sections were examined to determine mudstone texture; bedding; composition; degree of bioturbation; type, abundance, and diversity of body and trace fossils; and color. Outcrops and cores are located hundreds of kilometers apart and were chosen to span the full depositional range of the New Albany Shale in the Illinois Basin (Figure 4). We concentrated on Core 57 because it is located approximately in the middle of the Illinois Basin (Figure 4), had almost complete recovery,

and intercepted all four depositional sequences recognized in the New Albany Shale succession.

A set of 219 gamma-ray well logs and two outcrop-measured gamma-ray profiles was available for basinwide stratigraphic correlations. Wells have the same numbers as in Lazar (2007), and well name, operator, and coordinates are given in Table 1. The available dataset comprises gamma-ray logs acquired over several decades at various (and occasionally insufficient) resolutions that did not allow for consistent differentiation of thinner parasequence or lowstand systems tract (LST) packages. In contrast, despite the constraints of data availability and quality, transgressive systems tracts (TSTs) and highstand systems tracts (HSTs) have distinctive gamma-ray responses and were correlated basinwide. These correlations, assisted by the calibration of well-log gamma-ray response to core observations and interpretations, revealed the presence of sequence boundaries and flooding surfaces traceable throughout the Illinois Basin and aided the definition of genetically related stratigraphic units. Based on these correlations, isochore maps of individual systems tracts and depositional sequences were constructed to further understand depositional and thickness trends.

Specific observations that assisted the stratigraphic effort included the following:

- Erosion-related sedimentary features (lag deposits and knife-sharp contacts) between successive mudstone units
- Ultraviolet (UV) light responses in the mudstone succession sampled in cores and associated with variable concentrations of macerals of the liptinite group
- Fossils of biostratigraphic significance (conodonts and *Protosalvinia*) in cores and outcrops
- Total organic carbon contents measured in samples taken from Core 57
- Well- and outcrop-measured gamma-ray profiles (with variability reflecting changes in vertical stacking, stratal geometries, and stratal terminations)

In this chapter, recent information regarding bioturbation (Riese, 2014) and organic-matter type and abundance (Liu et al., 2019) has been added to the data reported in the study by Lazar (2007).

The following paragraphs touch on some of the available data types and their utility for constructing a sequence-stratigraphic framework for the New Albany Shale.

*Lag deposits* are residual accumulations of coarser particles that are produced when underlying units are eroded and winnowed (Figure 5A–C; Schieber, 1998a; Lazar et al., 2015a). Lag deposits have been categorized by the estimated depth of erosion into the underlying strata as *low-energy* lags (silt, conodont,

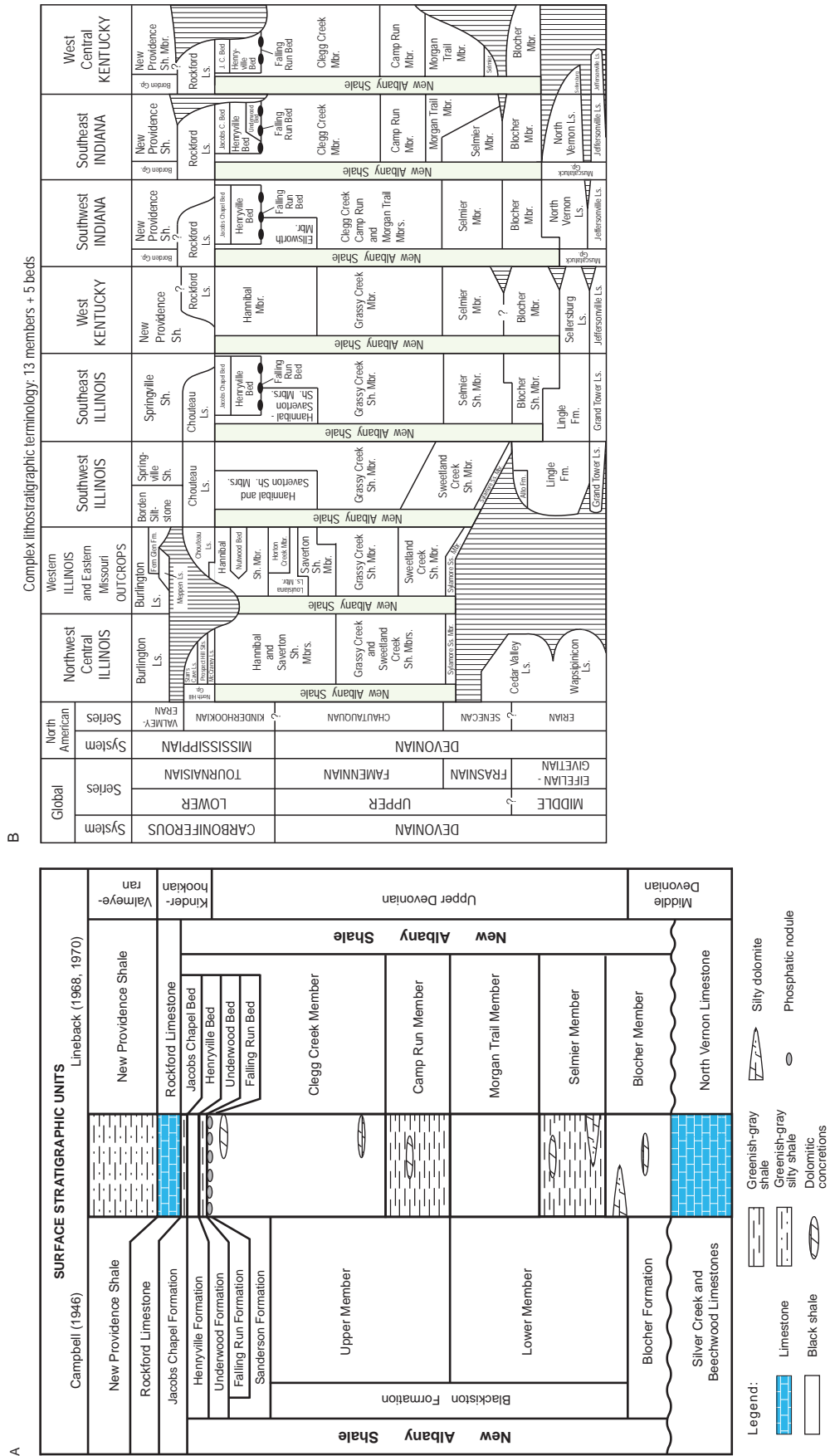


**Figure 3.** (A) Previous lithostratigraphic subdivisions of the New Albany Shale (from Lazar, 2007; after Campbell, 1946, and Lineback, 1968, 1970). (B) Current lithostratigraphic subdivisions of the New Albany Shale (after Hasenmueller et al., 2000).

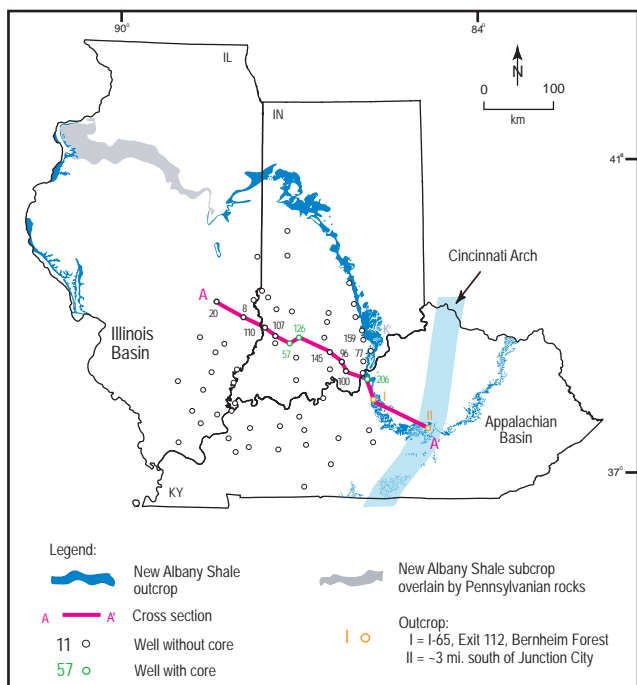


**Figure 4.** Map showing the location of Outcrops I and II; Cores 57, 126, and 206; and cross section A-A' (after Lazar, 2007). Outcrop I is located south of Louisville, Kentucky, on the west side of the I-65 South highway at the intersection with KY-245 ( $37^{\circ} 55' 26''\text{N}$ ,  $85^{\circ} 41' 22''\text{W}$ , WGS84/NAD83, USGS Shepherdsville Quad). Outcrop II is located on the Cincinnati Arch, approximately 3 mi south of Junction City, Kentucky, on the east side of US-127 ( $37^{\circ} 32' 54''\text{N}$ ,  $84^{\circ} 48' 18''\text{W}$ , WGS84/NAD83, USGS Junction City Quad). Detailed descriptions of outcrops I and II are given in Schieber and Lazar (2004). For well information, see Table 1.

and *Lingula* lags) and high-energy lags (bone beds, sand, pyritic, and thick silt lags; Schieber, 1998a). Low-energy lags have been interpreted as a result of more typical and more frequently occurring storms (recurrence on the order of  $10^1$ – $10^2$  years; Schieber, 1998a). High-energy lags have been interpreted as a result of infrequent and exceptionally strong storms (recurrence on the order of  $10^2$ – $10^4$  years), possibly connected to intensified reworking resulting from decreasing accommodation. Formation of high-energy lags implies that significant erosion and winnowing of the underlying mudstone beds took place (Ettenson et al., 1988; Schieber, 1998a; Lazar, 2007). For example, a minimum of a 96-cm thick mudstone with an average pyrite content of 2.5 vol. % had to be completely eroded and winnowed to form a 3-cm pyritic lag that contains 80% reworked pyrite.

Not all erosion surfaces in fine-grained rock successions are marked by a lag deposit, however (Schieber, 1998a; Lazar, 2007). Erosion can also form knife-sharp contacts with an abrupt change in composition at the base of mudstone beds (e.g., Figure 5D; Schieber, 1998a;

Lazar, 2007). By analogy with modern environments, abundance of lags and knife-sharp contacts within a fine-grained succession suggests accumulation in a relatively low-accommodation setting that is affected by storms and sea-level fluctuations (Schieber, 1994a, 1998a, b).

Lag deposits and knife-sharp contacts at the base of mudstone beds are common in the examined cores and outcrops and are interpreted to indicate intermittent erosion within the New Albany Shale succession. Correlation of these erosion-related features assisted the identification of laterally extensive erosion surfaces that separate distinct depositional sequences within the New Albany Shale succession.

Surveys of UV light response were conducted to detect core intervals with high concentrations of macerals of the liptinite group (Taylor et al., 1998). Macerals are the microscopically recognizable individual constituents of organic matter (Taylor et al., 1998). Liptinites originate from relatively hydrogen-rich plant materials (spores, cutin, resins, waxes, fats, and oils), algal cysts (*Tasmanites*), and bacterial degradation products (derived from proteins and cellulose; Taylor et al., 1998). Liptinite particles often show vivid greenish, yellow, and orange fluorescence colors when exposed to UV light (Figure 5E; Taylor et al., 1998; Lazar, 2007). The entire New Albany Shale succession in cores 57, 126, and 206 was examined in UV light using an illumination bench with four 40-watt long-wave (365 nm) UV lamps 126-cm long (Lazar, 2007). Multiple cored intervals showed distinct intervals with bright-yellow UV response, largely because of the presence of abundant *Tasmanites* cysts (Figure 5E–G). As *Tasmanites* cysts are highly resistant to microbial degradation, they can become enriched in the sediment because of either bottom-current reworking or extreme detrital-sediment starvation. During reworking, cysts become concentrated because of removal of clay minerals and other fine-grained matrix materials, and may record significant erosion, such as at sequence boundaries (Lazar, 2007). During sediment starvation, cyst concentrations may form because the lack of detrital input during maximum flooding allows other, more labile organic matter to be effectively degraded by microbes (Schieber, 1998b, 2001; Lazar, 2007). Examination of thin sections from intervals with bright-yellow UV response revealed that fluorescence maxima are largely because of the presence of abundant *Tasmanites* cysts that are either broken or in “pristine” conditions (Figure 5E–G; Lazar, 2007). The variability in the intensity of the UV response assisted the process of identification and correlation of distinct stratigraphic surfaces and units (Lazar, 2007).

Conodonts, toothlike microfossils of calcium phosphate, are the remains of eel-shaped jawless vertebrates (Donoghue et al., 2000; House and Gradstein, 2004) and are an essential tool for biostratigraphic correlation in the Devonian (e.g., Huddle, 1934; Ziegler and Sandberg,

**Table 1.** Well Name, Operator, and Coordinates for the Wells Discussed in This Chapter

Illinois County	Well ID	Well Name	Company	ISGS ID	Section	TWP	Range	1/4	UTM (16, NAD 83)
	Well ID this study								
Crawford	8	Utterback, Mervin 1	Crete Oil Investments, Inc.	120333274900	11	6N	13W	SW SW	428126 4313656
Jasper	20	Thoelle 1	Total Leonard Inc.	120792257600	1	8N	8E	NW	389690 4336470
<b>Indiana</b>									
Daviess	57	1-3 Kavanaugh	Deka Exploration, Inc.	150140	3	2N	6W	NW NE	494611 4276705
Floyd	77	INFL-5	North American Exploration	157987	28	1S	6E	SE SE NE	600642 4250540
Harrison	96	Charles Lorenz C4-29	Jet/Lavanway Exploration, LLC	157728	29	1S	3E	SW NE SE	569743 4250220
Harrison	100	Chinn A3-12	Jet/Lavanway Exploration	157491	12	3S	3E	SE NW NE	575933 4236350
Knox	107	Annetta Hubbard & Densel E. Holting 1	Western Pacific Oil & Gas, Inc.	122888	Don 153	3N	8W	-	474043 4286900
Knox	110	Maurice Jackson 1	Reynolds Resources, Inc.	150128	Loc 176	5N	10W	SW NE SE	459327 4299530
Martin	126	Walton 1-12	Deka Exploration Inc.	158024	12	3N	5W	NE NE	508095 4285090
Orange	145	Cadle-Hollenback Unit 1	Vista Resources Inc.	152616	15	1N	1E	NE NW SW	552537 4263737
Scott	159	SDH-304	Indiana Geological Survey	126939	22	3N	6E	NE SE SW	600724 4282020
<b>Kentucky</b>									
	Well ID this study								
Jefferson	206	Iriquois Park	USGS	-	23-U-45	4225224	606337.62		

ISGS: Illinois State Geological Survey; KGS: Kentucky Geological Survey; USGS: United States Geological Survey.  
Wells have the same numbers as in Lazar, 2007.

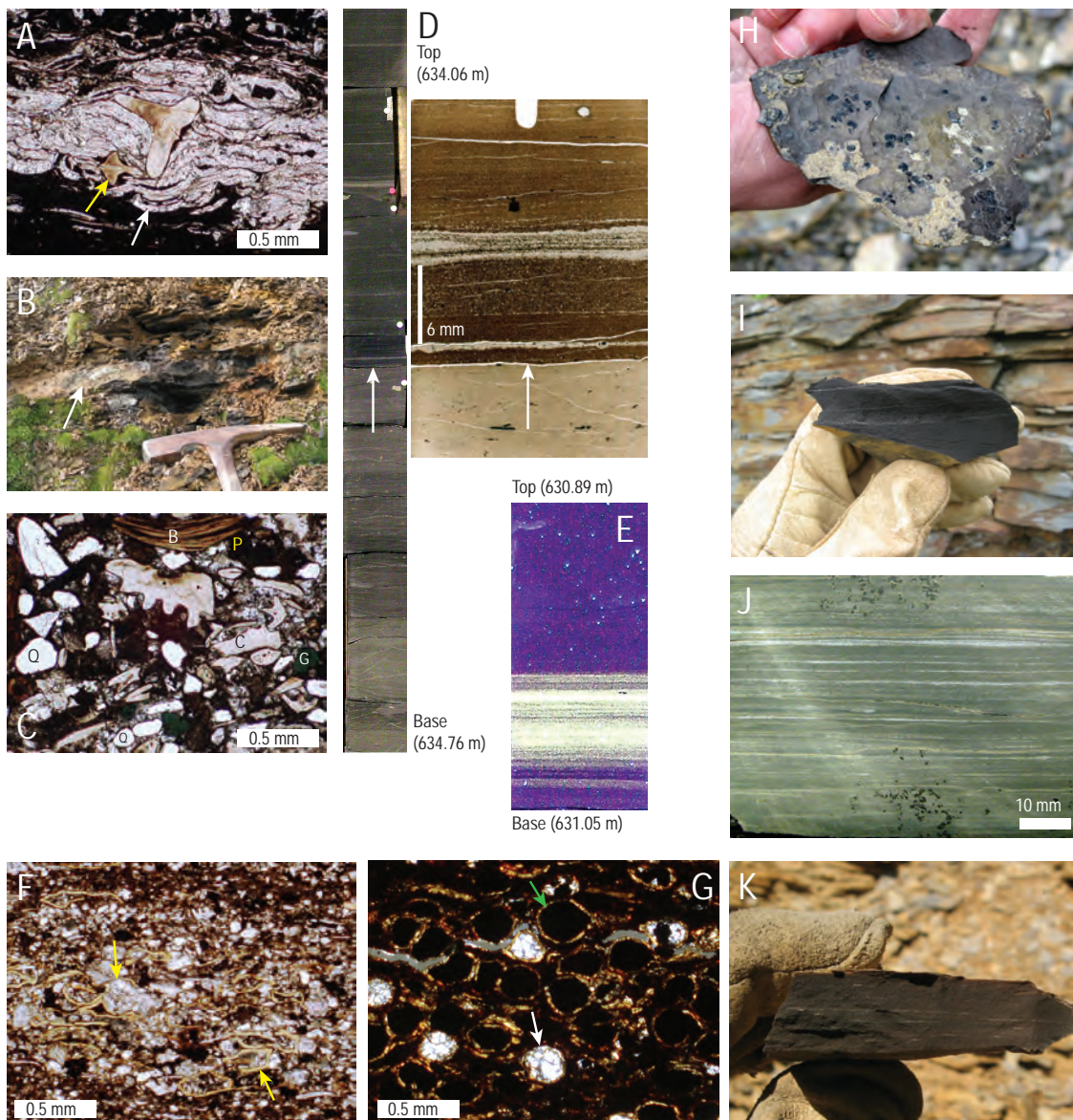


**Figure 5.** Examples of sedimentary features in the New Albany Shale (from Schieber and Lazar, 2004; Lazar, 2007; Lazar et al., 2015a). (A) Photomicrograph (transmitted light) of brownish conodonts (yellow arrow) and white-transparent *Tentaculites* (white arrow) in a lag deposit at 0.9 m above the base of Unit 1 (Depositional Sequence 1) in Core 57. In Upper Devonian “black shales,” a lag like this has been interpreted to be the product of relatively rare and strong storms (e.g., Schieber, 1998b). (B) Lag deposit (white arrow) at the contact between Units 2 and 7 (Depositional Sequences 1 and 3, respectively) in Outcrop I. Outcrop location is shown in Figure 4. (C) Photomicrograph (transmitted light) of the lag deposit in B. This lag deposit is composed of rounded quartz (Q), pyrite (P), glauconite (G), conodonts (C), and brachiopod shell fragments (B). (D) Knife-sharp contact (white arrows) with an abrupt change in composition from gray bioturbated mudstone of FA-6 to black, pyritic mudstone of FA-7 (Core 57, left; thin section, right). Lateral stratigraphic correlations may indicate that such a sharp contact in a core between successive mudstone beds is associated with a significant sequence-stratigraphic surface. (E) Core exposure to ultraviolet (UV) light reveals a bright-yellow fluorescence response. Such a distinct bright-yellow fluorescence under UV light corresponds to enrichment in *Tasmanites* (fossil marine algae) cysts. (F) Enrichment in broken and unrolled, reworked *Tasmanites* cysts filled with detritus (yellow arrows). (G) Enrichment in well-preserved, spherical *Tasmanites* cysts filled with chalcedony (white arrow) or pyrite (green arrow) indicating sediment starvation. (H) *Protosalvinia* is a fossil plant distinguished as small (<5 mm) oval carbonaceous remains on bedding planes in Upper Devonian mudstone successions of eastern United States. Restricted stratigraphic distribution and widespread occurrence make *Protosalvinia* a useful biostratigraphic marker for regional correlations. (I) Graded beds, Depositional Sequence I, Outcrop I. (J) Wave ripple, Depositional Sequence 2, Core 57. (K) Current ripple, Depositional Sequence 1, Outcrop I.

1990; Sandberg et al., 1994; Over, 2002, Lazar, 2007; Over et al., 2009; Over et al., 2019). All of Core 57 and the uppermost 4.6 m of Core 126 were examined for conodonts on bedding planes or in lag deposits (Lazar, 2007). Samples were collected over the entire cored interval and sent for conodont identification to Jeff Over, a Devonian conodont expert from the State University of New York–Geneseo. The resulting conodont zonation was integrated with the conodont zonation for Outcrop I (Over, 2002) and tied in with the Late Devonian absolute timescale of Kaufmann (2006) to construct a conodont-based chronostratigraphic framework. Conodont biostratigraphy provided an independent control of the reliability of basinwide correlations based on physical tracing of major stratigraphic surfaces (flooding and erosion surfaces; Lazar, 2007). In addition, correlation of identified stratal units with the global transgressive-regressive cycles of Johnson et al. (1985) shed light on the role of eustasy in the formation of the New Albany Shale.

*Protosalvinia* (also known as *Foerstia*) is another fossil of biostratigraphic importance for the Upper Devonian “black shales” in the eastern United States. Restricted stratigraphic distribution and widespread occurrence in the Upper Devonian fine-grained rock successions of the eastern United States make *Protosalvinia* an excellent biostratigraphic marker for regional correlations (e.g., Kepferle, 1981; Hasenmueller et al., 1983; Roen, 1993; Schieber and Lazar, 2004; Lazar, 2007; Over et al., 2009; Schieber et al., 2010). *Protosalvinia* is a fossil plant of uncertain botanical affinity regarded as either a marine brown alga or a terrestrial plant (e.g., Schopf and Schwietering, 1970; Niklas and Phillips, 1976; Gray and Boucot, 1977, 1979; Romankiw et al., 1988; Hannibal, 1994; Over et al., 2009). *Protosalvinia* is distinguished on bedding planes as small (<5 mm), oval, and bilobed carbonaceous compression (Figure 5H; Schopf and Schwietering, 1970; Niklas and Phillips, 1976; Schieber and Lazar, 2004; Lazar, 2007). Finding the *Protosalvinia*-bearing interval in Outcrops I and II and in cores 57, 126, and 206 assisted stratigraphic correlations within the New Albany Shale succession.

To assess the geochemical signatures of each stratal unit recognized in the New Albany Shale, 44 samples, each approximately 2 cm in stratigraphic thickness, were collected from Core 57 and analyzed for TOC content using either the LECO C/S 244 elemental analyzer (41 samples) or the Eltra CS-2000 analyzer (3 samples) of the Analytical Geochemistry Laboratory at Indiana University (Lazar, 2007). Total organic carbon values are reported here as weight percentage (wt. %) of the whole rock. Sampling was guided by the recognition of lithological changes, with denser sampling characterizing those intervals that exhibit relatively more common lithologic changes. Samples were removed from a split half of the core and washed with distilled

water to remove surficial contamination caused by coring, splitting, and storage. Dried samples were crushed into small fragments with a hammer, rinsed with  $\text{CH}_2\text{Cl}_2$ , dried, and ground to a powder. Samples were ground with either a synthetic sapphire mortar and pestle or an oil-free SPEX 8000 hardened steel ball mill. Additional TOC values (5 samples) measured using a LECO elemental analyzer and semi-quantitative organic petrographic compositions (33 samples) reported by Liu et al. (2019) further assisted the geochemical characterization of identified stratal units.

The TOC content ranges from essentially nil to approximately 50 wt. % in mudstones; the majority of mudstones, however, have a TOC content of less than 1 wt. % (e.g., Blatt et al., 1980; Lazar et al., 2015a, b). As discussed in Lazar et al. (2022b, Chapter 2 this Memoir), a mudstone with a TOC content between 2 and 25 wt. % is considered to be enriched beyond background values and is defined as “carbonaceous.” In this chapter, we use the terms “subcarbonaceous” and “carbonaceous” to make a distinction between mudstones that have a TOC content ranging from 2 to 10 wt. % and from 10 to 25 wt. %, respectively. We found this grouping useful for the characterization of the observed facies associations in the New Albany Shale.

Gamma-ray profiles have been used frequently as a proxy for stratigraphic correlations (e.g., Slatt et al., 1992; Bohacs and Schwalbach, 1994; Johri and Schieber, 1999; Lazar and Schieber, 2006; Lazar, 2007; Bohacs and Lazar, 2008; case study chapters in this Memoir). Outcrop profiles integrated in this study have been collected with an Exploranium GR-256 gamma-ray spectrometer at 10–30 cm stratigraphic spacing.

Examination of thin sections, cores, outcrops, and gamma-ray profiles revealed considerable stratigraphic variability in the New Albany Shale throughout the Illinois Basin at the bed to depositional-sequence scale (e.g., Schieber and Lazar, 2004; Lazar and Schieber, 2005a, b, 2006; Lazar, 2007). In this chapter, we touch briefly on the bed- to parasequence-scale (facies to facies association) variability and focus mostly on the stratigraphic variability observed at systems-tract to depositional-sequence scales. The next sections summarize the facies to facies association variability observed in the New Albany Shale.

## FACIES

The New Albany Shale contains a variety of facies distinguished by their texture, bedding, composition, degree of bioturbation, trace fossil diversity and abundance, and color. Texture ranges from fine to medium to coarse mudstone to coarse sandstone.

Composition ranges broadly: argillaceous, calcareous, argillaceous-siliceous, siliceous-argillaceous, subcarbonaceous to carbonaceous, and subarkosic.

Bedding styles range from continuous, planar-parallel to discontinuous, wavy nonparallel, with abundant evidence of current and wave sediment erosion, transport, and deposition. Bedding includes graded beds, (starved) wave ripples, (starved) current ripples, combined-flow ripples, scour-based lag deposits, and homogeneous-looking beds (Figure 5; e.g., Schieber and Lazar, 2004; Lazar, 2007; Lazar et al., 2015b). Some mudstones have a “banded” appearance. “Banded” fabric in mudstones is produced by subtle changes in texture, composition, degree of cementation, bioturbation, or color. “Banded” appearance can be generated, for example, by (1) subtle changes from more silt-size-rich to more clay-size-rich textural transitions (e.g., Schieber, 1999); (2) subtle changes in the content of finely disseminated pyrite and organic matter (e.g., Lazar, 2007; Wilson and Schieber, 2017); and (3) bioturbation by short-range meiofauna slightly disrupting water-rich, “soupy” substrates (e.g., Lazar, 2007; Riese, 2014; Wilson and Schieber, 2017). Close examination of lower and upper boundaries of the “banded” fabric can reveal that these boundaries are slightly irregular or subtly wavy with a fuzzy appearance.

The degree of bioturbation ranges from 1 to 5. Observed trace fossils include *Planolites*, *Thalassinoides*, *Chondrites*, *Zoophycos*, *Teichichnus*, *Asterosoma*, *Paleophycus*, escape traces, and biodeformational structures referred to as “mantle and swirl” (e.g., Lineback, 1968, 1970; Cluff, 1980; Lobza and Schieber, 1999; Schieber, 2003; Schieber and Lazar, 2004; Lazar, 2007; Riese, 2014).

Grains include quartz, chalcedony, phyllosilicates (illite, illite-smectite, chlorite), carbonates (calcite, dolomite), feldspars, pyrite (frambooids, euhedral), marcasite, heavy minerals, and phosphates (Lineback, 1968; Calvert et al., 1996; Frost and Shaffer, 2000; Schieber and Lazar, 2004; Lazar, 2007 and references therein; Mastalerz et al., 2013; Spencer, 2013). Total organic carbon content ranges from 0.1 to 25 wt. % (e.g., Barrows and Cluff, 1984; Frost and Shaffer, 2000; Curtis, 2002; Schieber and Lazar, 2004; Lazar, 2007; Liu et al., 2019). Organic matter is mostly marine in origin, dominated by alginite (*Tasmanites*) and amorphous organic matter (AOM; Schieber, 2001; Lazar, 2007 and references therein; Wei et al., 2016; Liu et al., 2017; Liu et al., 2019), with increased content of terrigenous organic matter (vitrinite, inertinite) toward the top of the succession (Lazar et al., 2007 and references therein; Wei et al., 2016; Liu et al., 2017, 2019). *Protosalvinia*, silicified and carbonized logs of *Callixylon*, conodonts, brachiopods (*Lingula*), pteropods, and arthropods, as well as fish fossils have also been found in the New

Albany Shale (e.g., Huddle, 1933, 1934; Lineback, 1968, 1970; Niklas, 1976; Cluff, 1980; Sandberg et al., 1994; Over, 2002; Lazar and Schieber, 2004; Lazar, 2007; Over et al., 2009). Remains of agglutinated benthic foraminifera and benthic fecal pellets are common (e.g., Lazar, 2007; Schieber, 2009; Riese, 2014).

Fecal pellets are excrements of benthic or planktonic organisms. Benthic fecal pellets are often ovoid in shape, densely packed, and resistant to decomposition over time (Cuomo and Bartholomew, 1991). They are dominated by silt- and clay-size particles and may also contain some skeletal debris and organic materials (Cuomo and Bartholomew, 1991). Their inorganic composition resembles that of the bulk sediment (Cuomo and Bartholomew, 1991). In contrast, planktonic fecal pellets are often cylindrical and loosely packed with large pore spaces, and contain mostly biogenic debris and intact tests, pigments, and organic materials (Cuomo and Bartholomew, 1991). In the Devonian mudstones of the Appalachian Basin, benthic fecal pellets are flattened or intact, 80–360 µm long, and lighter in color than the surrounding organic-rich sediment (e.g., Cuomo and Rhoads, 1987; Cuomo and Bartholomew, 1991; Lazar, 2007). Benthic fecal pellets suggest benthic life with a tolerance for low-oxygen conditions in the water-rich surficial muds (Cuomo and Rhoads, 1987; Cuomo and Bartholomew, 1991; Lazar, 2007).

The color of the facies observed in this unit ranges from black to brown to light gray to dark gray to green.

## FACIES ASSOCIATIONS

In this chapter, key facies associations and their characteristics are summarized on the basis of observations made on Core 57 (Figures 4, 6). Facies associations are based on commonly recurring facies with distinctive properties. These properties include texture, bedding, stacking patterns, composition, and component origin observed at hand-specimen scale in Core 57 and augmented by outcrop and thin-section examination. UV light response further assisted the recognition and characterization of facies associations. The protocols used have been discussed in detail in Lazar et al. (2022a, b, Chapters 2 and 3 this Memoir). Facies associations are primarily named for their dominant color, composition, and grain size. Recognized facies associations include the following (Figures 6, 7, Table 2):

### **Facies Association-1 (FA-1)—Black Dolomitic-Argillaceous-Siliceous, Pyritic Fine Mudstone**

Graded beds and starved current ripples are very sparse to sparse in this mostly homogeneous- to

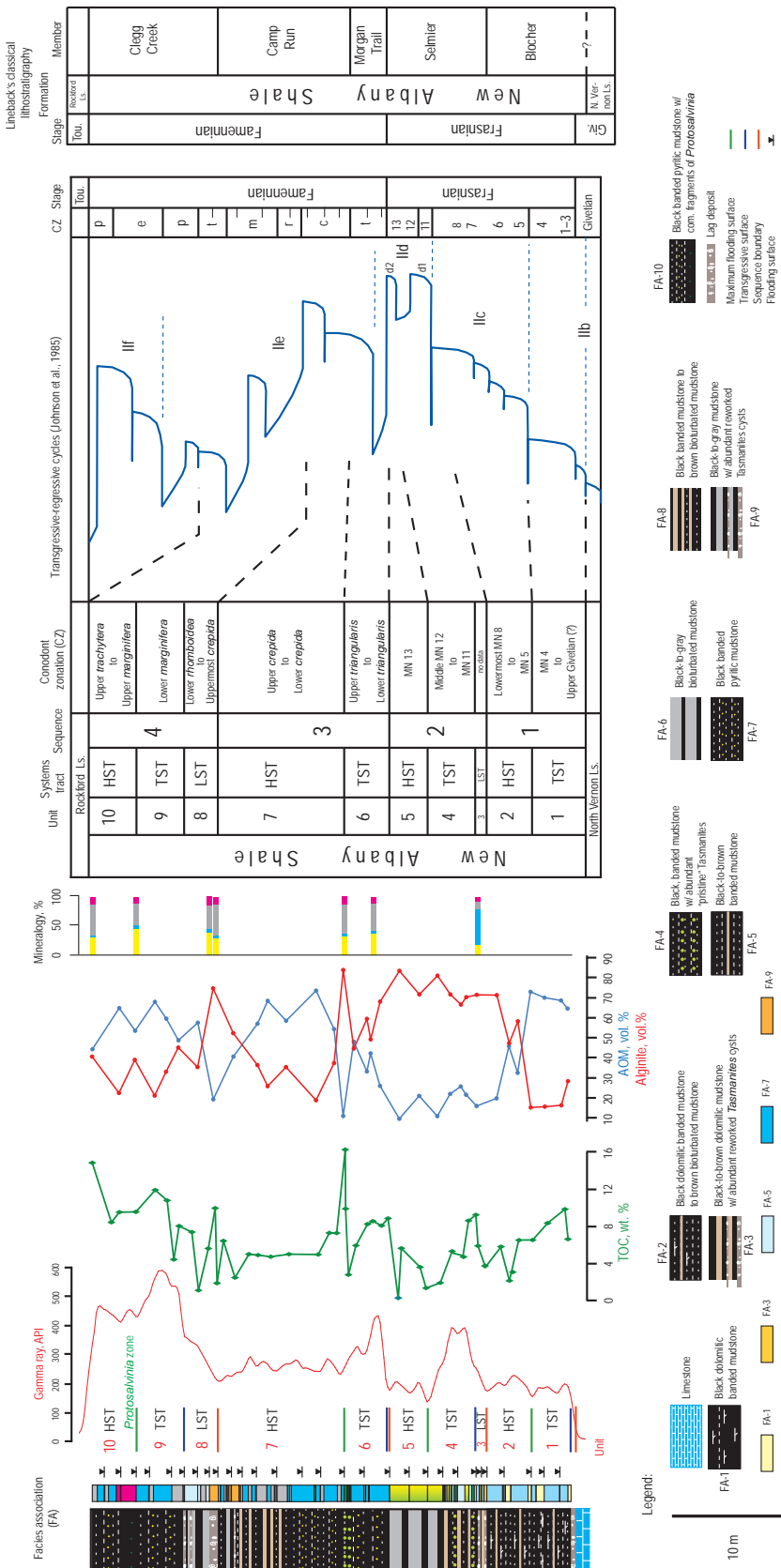


**Figure 6.** Facies association (FA), gamma-ray motif, and sequence stratigraphy of the New Albany Shale succession in Core 57 (after Lazar, 2007). Also shown are total organic carbon (TOC) content and organic-matter type (amorphous organic matter [AOM]; after Lazar, 2007 and Liu et al., 2019), mineralogy as well as the classical lithostratigraphy of Lineback (1964, 1968, 1970). Mudstone sequence-stratigraphic units recognized in Core 57 were related to the transgressive-regressive cycles of Johnson et al. (1985) based on the conodont zonation established by Jeff Over (SUNY-Geneseo). Notice the presence of the biostratigraphic marker *Protoscalvinia* at the base of Unit 10. Conodont zones:  $t = triangularis$ ;  $c = crepida$ ;  $r = rhomboidea$ ;  $m = marginifera$ ;  $p = postera$ ;  $e = expansa$ ;  $P = praesulcata$ . Mineralogy: yellow = quartz; blue = total carbonates; gray = total clay; pink = total feldspar. Core location is shown in Figure 4. API = American Petroleum Institute; HST = highstand systems tract; LST = lowstand systems tract; TST = transgressive systems tract.

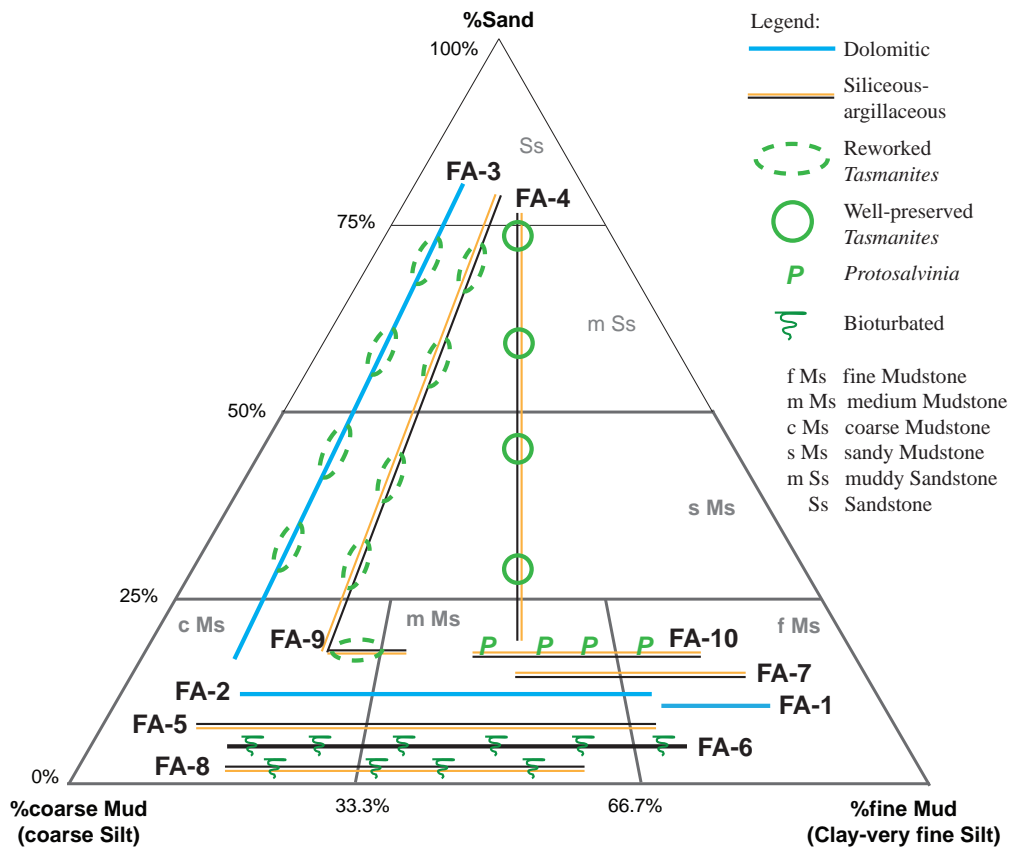


**Figure 7.** Facies association (FA) distribution in Core 57 highlighting common ranges of texture, composition, and bioturbation.

subtly “banded”-looking facies association. Continuous to discontinuous laminae are commonly calcareous or pyritic. Bioturbation index (BI) is commonly 1. “Disseminated” pyrite (scattered pyrite in the form of framboids or dispersed single crystals) together with pyrite concentration in very sparse to common nodules (mostly <5 mm) and very sparse to sparse laminae give this facies association a somewhat “pyritic” appearance at core scale. Organic matter is primarily marine in origin and dominated by AOM and alginite (*Tasmanites*) (Lazar, 2007 and references therein; Wei et al., 2016; Liu et al., 2017).

#### Facies Association 2 (FA-2)—Black to Brown, Dolomitic, Siliceous-Argillaceous to Argillaceous-Siliceous, Subcarbonaceous Fine-Medium to Medium Mudstone Interbedded with Coarse Mudstone to Coarse Sandstone

Graded beds, (starved) current ripples, (starved) wave ripples, combined-flow ripples, and scour-based lag

beds are sparse to common. Lag deposits and laminae are commonly in the coarse mudstone to coarse sandstone textural range and are composed of silt- and sand-size quartz and dolomite grains, *Tasmanites* cysts, conodonts, *Lingula* brachiopod shell fragments, tentaculitoids (small, conical-shaped shelled marine animals; Bond, 2006), and pyrite. Petrographic observations, such as the presence of silt-size dolomicrite (Figure 8A) and rounded cores in euhedral dolomite grains (Figure 8B), indicate that the carbonate grains are detrital in origin and likely derived from carbonate rocks exposed laterally (Schieber and Lazar, 2004; Lazar, 2007). Bioturbation index is commonly 1. The upper parts of some beds have a 4–5 BI, but such beds are very sparse to sparse. Trace fossils include *Planolites* and “mantle and swirl” biodeformational structures (sensu Lobza and Schieber, 1999); some burrows are filled with sand or silt or pyritized. Some core intervals in this facies association appear “banded.” The boundaries of some of these bands have a fuzzy appearance and suggest bioturbation

**Table 2.** Facies Association Summary.

Facies Association	Facies Association Number	TEXTURE	BEDDING	COMPOSITION	COMPONENT ORIGIN	
					Notes	
FA-10 ar-si, "banded" f-m to mMs w/ sp-com. <i>Protosalvinia</i>		muddy Sandstone (ms)		clay, qtz, AOM ± V/I	Pyrite, dol., silica	Reworked <i>Tasmanites</i> , reworked <i>Protosalvinia</i> , reworked <i>Tasmanites</i>
FA-9 ar to ar-si, mMs to cMs to fSS w/ ab. reworked <i>Tasmanites</i>		Sandstone (Ss)		clay, qtz, AOM, macro-fossils	Pyrite, silica	Reworked <i>Tasmanites</i> (UV max), brachiopods, conodonts
FA-8 si-ar to ar-si, f-m to m-c to cMs		coarse Mudstone (cmS)		clay, qtz, AOM, macro-fossils	Pyrite, silica	Moderate diversity/density of trace fossils; brachiopods
FA-7 ar to ar-si to si-ar, "banded", f-m to mMs		medium Mudstone (mMs)		clay, qtz, AOM + Alg, macro-fossils	Pyrite, silica	V+ up to 9.3% of organic matter
FA-6 ar to ar-si, bioturbated, f-m to cMs		fine Mudstone (fMs)		clay, qtz, AOM + Alg, macro-fossils	Pyrite, silica	Bed/bedset-scale changes in BI; high diversity/density of trace fossils; brachiopods
FA-5 si-ar to ar-si, f-mMs to fSS w/ ab. w/ cmMs to mSs		coarse Mudstone (cmS)		clay, qtz, AOM + Alg, macro-fossils	Pyrite, silica	"Pristine" <i>Tasmanites</i> (UV max)
FA-4 ar-si, f-m to mMs to fSS w/ ab.-w. ab. "pristine" <i>Tasmanites</i>		medium Mudstone (mMs)		clay, qtz, AOM + Alg, macro-fossils	Pyrite, silica	"Pristine" <i>Tasmanites</i> (UV max)
FA-3 dl to si-ar, cMs to fSS w/ ab. reworked <i>Tasmanites</i>		muddy Sandstone (ms)		dolomitic	Pyrite, silica	Reworked <i>Tasmanites</i> (UV max), brachiopods, fish bones
FA-2 dl to si-ar, f-m to mMs interbedded w/ cmMs to cSs		coarse Mudstone (cmS)		dolomitic	Pyrite, silica	Conodonts, <i>Lingula</i> , stylolinds, tentaculitids, <i>Tasmanites</i>
FA-1 dl-ar-si, "homogeneous to banded-looking" Ms		medium Mudstone (mMs)		dolomitic	Pyrite, silica	

Legend:

- dominant = black square
- subdominant = grey square
- = continuous
- c = planar; cv = curved; w = wavy
- p = parallel; np = non-parallel

Abbreviations:

- BI = Bioturbation index
- UV max = bright/yellow
- alg = alginite
- AOM = amorphous organic matter
- qtz = quartz
- V/I = vitrinite/finenitrite

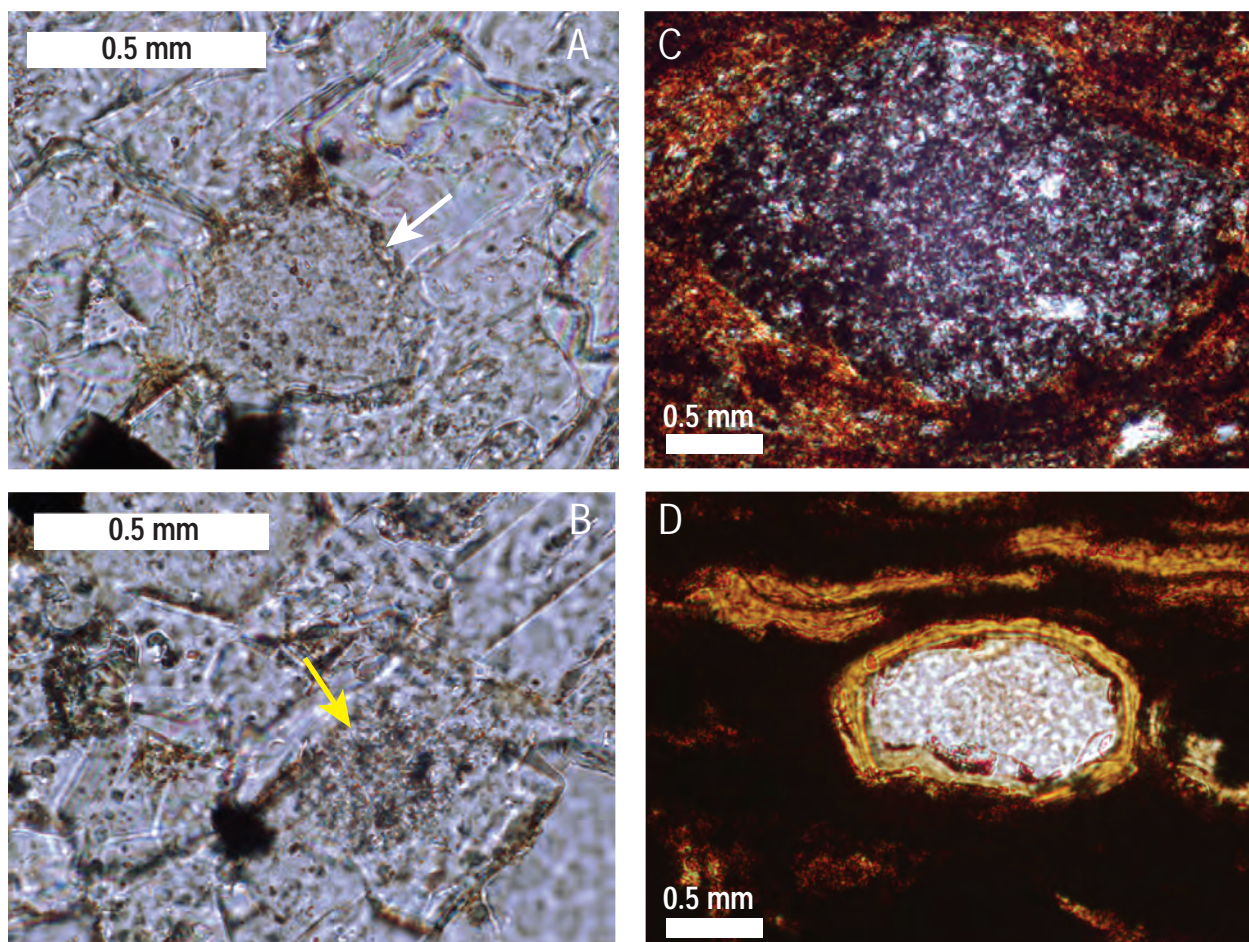


**Figure 8.** (A) Photomicrograph of silt-size dolomicrite (white arrow) in a thin dolomitic lag at the top of Unit 1, Depositional Sequence 1. (B) Rounded core (yellow arrow) in translucent euhedral grains of dolomite in the same dolomitic lag. (C) Photomicrograph of the reworked silica fill of a *Tasmanites* cyst (crossed polarizers). Silica-filled cyst was transported during reworking, and the organic “skin” (the actual cyst) was separated from its early diagenetic fill. (D) Photomicrograph of a *Tasmanites* cyst with silica fill that was not reworked. The yellowish organic cyst wall still surrounds the early diagenetic silica fill (transmitted light).

of surficial muds by millimeter-size metazoans. This cryptobioturbated fabric is common throughout the New Albany Shale (e.g., Schieber, 2003; Schieber and Lazar, 2004; Lazar, 2007; Riese, 2014). Presence of benthic fecal pellets that are ovoid and up to a few hundred microns long and densely packed further suggest benthic life with a tolerance for low-oxygen conditions in the water-rich surficial muds (Cuomo and Rhoads, 1987; Cuomo and Bartholomew, 1991; Lazar, 2007). Differential compaction observed around pellets suggests that they were precompacted by passage through the guts of worms. Pyrite nodules are sparse to common in some intervals. Total organic carbon content ranges between 2 and 4 wt. % in the brown, bioturbated mudstones, and between 7 and 10 wt. %

in the black, less obviously bioturbated mudstones (Lazar, 2007). Organic matter is dominated by AOM and alginite (Lazar, 2007 and references therein; Wei et al., 2016; Liu et al., 2017; Liu et al., 2019).

#### Facies Association 3 (FA-3)—Black to Brown Dolomitic to Siliceous-Argillaceous, Pyritic, Subcarbonaceous Coarse Mudstone to Fine Sandstone with Abundant Reworked *Tasmanites* Cysts

Graded beds, (starved) wave ripples, combined-flow ripples, and scour-based “high-energy” and “low-energy” lags (sensu Schieber, 1998b) are few to abundant. Millimeter-thick lag deposits with basal

scours are composed of dolomite, pyrite, and sand-size, rounded quartz grains; brachiopod shell fragments; fish bones; and abundant to very abundant, reworked, broken, and unrolled *Tasmanites* cysts—these intervals showed distinct fluorescence maxima when exposed to UV light. Cysts along with their silica fill were transported during reworking, and the organic “skin” (the actual cyst) was separated from its early diagenetic fill (Figure 8C; Schieber, 1996; Lazar, 2007). Such reworking and concentration during removal of clay minerals and other fine-grained matrix materials may record significant erosion (Schieber, 1996; Lazar, 2007). Bioturbation index is commonly 0–1; burrows are filled with sand or silt or pyritized. Organic-matter content can be high (up to 9 wt. %) with abundant alginite and relatively higher contents of vitrinite and inertinite than in other facies associations (Figure 6; Lazar, 2007; Liu et al., 2019).

#### **Facies Association 4 (FA-4)—Black Argillaceous-Siliceous, Carbonaceous, Subarkosic Fine-Medium to Medium Mudstone to Fine Sandstone with Abundant to Very Abundant “Pristine” *Tasmanites* Cysts**

Graded beds and (starved) wave ripples are sparse. Bed bases can be scoured or sharp. Some core intervals appear “banded.” This facies association could be described at first sight as a “rather homogeneous-looking black shale.” Core examination under UV light revealed, however, intervals with distinct bright-yellow UV response, largely because of the presence of abundant, “pristine” *Tasmanites* cysts (Figures 5G, 8D; Lazar, 2007). Thin-section examination revealed that the “pristine” *Tasmanites* cysts are well-preserved, spherical cysts filled with chalcedony or pyrite (Figure 5G; Schieber, 1996; Schieber et al., 2000; Schieber and Baird, 2001; Lazar, 2007; Lazar et al., 2015a). Highly resistant to microbial degradation, “pristine” *Tasmanites* cysts likely accumulated in these intervals under extreme sediment starvation (Schieber, 1996; Schieber and Baird, 2001; Lazar, 2007). Bioturbation index is commonly 0–2. Pyrite is disseminated as submillimeter concretionary features or concentrated in laminae or very sparse, millimeter-to-centimeter-wide nodules. Total organic carbon content is relatively high and ranges between 10 and 16 wt. %. Alginite content ranges from abundant to very abundant with mudstone beds containing 80% or more *Tasmanites* cysts by volume (Lazar, 2007; Liu et al., 2019).

#### **Facies Association 5 (FA-5)—Black to Brown Siliceous-Argillaceous to Argillaceous-Siliceous, Subcarbonaceous Fine-Medium Mudstone Interbedded with Coarse Mudstone to Medium Sandstone**

Graded beds, (starved) wave ripples, combined-flow ripples, and scour-based lags are sparse to common. Millimeter-thick lag deposits and laminae are common in the coarse mudstone to medium sandstone textural range and are composed of silt- to sand-size quartz and pyrite. Bed base can be sharp or fuzzy, and some core intervals appear “banded.” Bioturbation index is commonly 1–2. Pyrite is present either disseminated or as very sparse to common pyrite nodules (mostly <5 mm). Total organic carbon content ranges between 5 and 9 wt. %. Organic matter is dominated by alginite (Lazar, 2007; Liu et al., 2019).

#### **Facies Association 6 (FA-6)—Black to Gray Argillaceous to Argillaceous-Siliceous, Subcarbonaceous, Bioturbated Fine-Medium to Coarse Mudstone**

Characteristically, this facies association consists of a succession of centimeter-to-decimeter-thick beds and bedsets characterized by an upward increase in the degree of bioturbation and color change from black or brown to gray or green. Because of extensive bioturbation, sedimentary structures are not well preserved but include graded beds, starved wave ripples, and scour-based, silt- or sand-rich, millimeter-thick lag deposits. Lags are rich in pyrite or shell fragments. Bases of the black mudstone beds are commonly sharp. Bioturbation index is 1–3 in the lower black to brown parts of individual beds or bedsets, whereas the upper gray to green parts of the beds or bedsets have a 4–5 BI. Bioturbation in the black mudstone part of the beds is either easily visible (burrows filled with gray mud and sand) or very subtle. *Planolites*, *Thalassinoides*, *Teichichnus*, *Chondrites*, *Zoophycos*, and *Asterosoma*, escape traces, and commonly present “mantle and swirl” biodeformational structures compose a high diversity and density of trace fossils (Lazar, 2007; Riese, 2014). Some burrows are filled with sand or silt or pyritized. Centimeter to decimeter intervals of this facies association are completely bioturbated and show multiple generations of bioturbation; tiering commonly ranges between 1 and 3 and is relatively shallow in Core 57. Disarticulated (mostly) to articulated calcareous shell fragments of brachiopods are sparse to common in some intervals. These observations have been interpreted to indicate relatively low sedimentation rates;

water-rich, “soupy” substrates; and relatively high bottom-water oxygen concentrations (dysoxic to oxic) for relatively extended time periods (e.g., Schieber, 2003; Schieber and Lazar, 2004; Lazar, 2007; Riese, 2014). Millimeter-to-centimeter-wide pyrite nodules are sparse to few. Total organic carbon content ranges between 0.2 and 6 wt. %. Alginite is abundant to very abundant (Lazar, 2007; Liu et al., 2019). Less bioturbated black to brown mudstones are commonly more organic-matter rich (>5 wt. % TOC), less argillaceous, and pyritic. More bioturbated gray to green mudstones contain less organic matter (<5 wt. % TOC) and are more argillaceous and less pyritic (Schieber and Lazar, 2004; Lazar, 2007; Spencer, 2013).

#### **Facies Association 7 (FA-7)—Black, “Banded,” Argillaceous to Argillaceous-Siliceous to Siliceous-Agillaceous, Subcarbonaceous to Carbonaceous, Subarkosic, Pyritic Fine-Medium to Medium Mudstone**

“Banded” to “faintly banded” fabric is overall common. Combined-flow ripples and starved wave ripples are very sparse, and millimeter-thick pyritic lags are very sparse to few. Bioturbation index commonly ranges between 0 and 1. Shell fragments of brachiopods are present on bedding planes. Remains of agglutinated benthic foraminifera and benthic fecal pellets are very sparse to sparse. Pyrite is sparse to abundant, either disseminated or concentrated in submillimeter-to-millimeter-thick laminae, and 1–26-mm-wide nodules. Organic-matter content ranges from 7 to 15 wt. %. Organic matter is predominantly marine in origin and dominated by alginite and AOM (Lazar, 2007; Liu et al., 2019). Vitrinite and inertinite contents are relatively low in this facies association, typically less than 2 vol.%, with the exception of a sample toward the top of the core, where it reaches 9.3 vol.%, the highest value in the entire New Albany Shale succession (Liu et al., 2019).

#### **Facies Association 8 (FA-8)—Black to Brown Siliceous-Agillaceous, to Argillaceous-Siliceous, Subcarbonaceous, Pyritic, Subarkosic Fine-Medium to Medium-Coarse to Coarse Mudstone**

The fabric of this facies association is commonly “banded” with some bands enhanced in visibility by disseminated fine-crystalline pyrite. Millimeter-thick pyritic lags are very sparse to sparse. Bioturbation index is commonly 1. The upper parts of some beds and bedsets have a 4–5 BI, but these brown

mudstones are overall thinner than the gray, bioturbated mudstones of FA-6. Additionally, the proportion of black, less bioturbated mudstones is overall higher than that of black, less bioturbated mudstones of FA-6. Trace fossils include *Zoophycos*, *Planolites*, *Chondrites*, and *Teichichnus*, and “mantle and swirl” biodeformational structures (Lazar, 2007; Riese, 2014). Remains of agglutinated benthic foraminifera and benthic fecal pellets are sparse. This facies association has a lower ichnodiversity, lower abundance of burrows and biodeformational structures, and lower tiering (1–2) than FA-6 (Lazar, 2007; Riese, 2014). These observations suggest intermittently higher sedimentation rates, more firm substrate, and perhaps shorter durations of dysoxic bottom-water conditions than those during the accumulation of FA-6 (Lazar and Schieber, 2005b; Lazar, 2007). Shell fragments of *Lingula* brachiopods are common on some bedding planes. Pyrite is concentrated in continuous to discontinuous laminae and in mostly small nodules (1–11 mm). Organic-matter content ranges from 1 to 11 wt. %. Organic matter is predominantly marine in origin and dominated by AOM (Lazar, 2007; Liu et al., 2019).

#### **Facies Association 9 (FA-9)—Black to Gray Argillaceous to Argillaceous-Siliceous, Pyritic, Subarkosic, Subcarbonaceous Medium to Coarse Mudstone to Fine Sandstone with Abundant Reworked *Tasmanites* Cysts**

Scour-based, millimeter-to-centimeter-thick lags with thin interbeds of gray to brownish-black bioturbated mudstones and black “banded” mudstones are common to abundant (Figure 9). Graded beds, (starved) wave ripples, and combined-flow ripples are few to abundant. Lag deposits are composed of reworked *Tasmanites* cysts, sand-size rounded to subrounded quartz grains, pyrite, brachiopod shell fragments, and conodonts (Figure 9C, D). A bright-yellow UV response (Figure 9B) is associated with the presence of abundant, reworked, broken, and unrolled *Tasmanites* cysts that became significantly enriched in the sediment likely as a consequence of intensified wave and current erosion and winnowing in a relatively low-accommodation setting (Lazar, 2007; Lazar et al., 2015a). Bioturbation index ranges between 1 and 5; trace fossils are commonly horizontal to subhorizontal and sand- or silt-filled. Pyritic nodules (<5 mm) and laminae are very sparse to sparse. Organic-matter content ranges from 2 to 10 wt. %. Organic matter is predominantly marine in origin and dominated by alginite (Lazar, 2007; Liu et al., 2019).

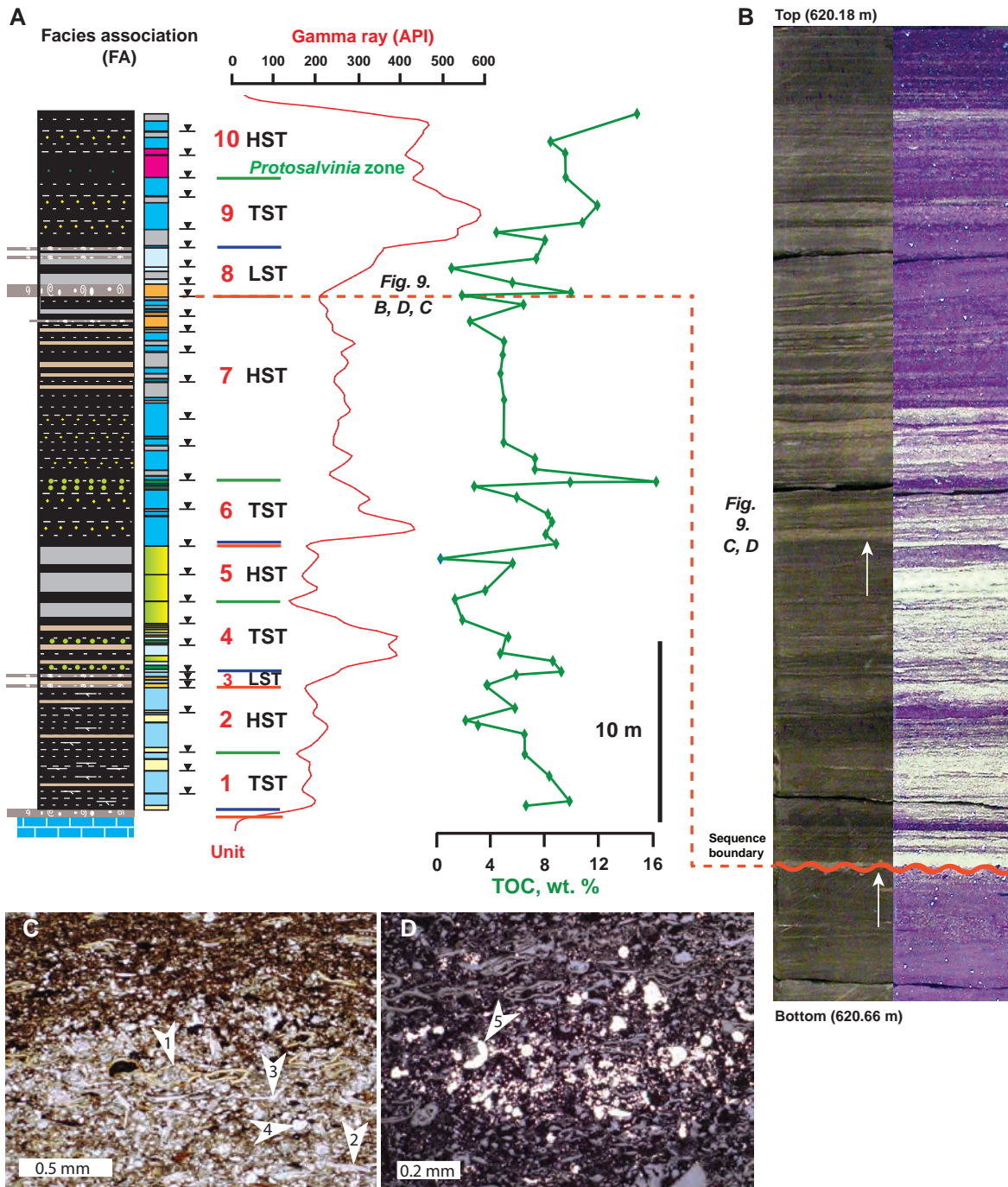


**Figure 9.** (A) Facies associations, gamma-ray response, and total organic carbon (TOC) content of the New Albany Shale in Core 57. Legend for the lithologic column is shown in Figure 6. (B) Centimeter-thick sandy and pyritic lags (white arrows) and fluorescence maxima (bright yellow) that correspond to an abundance of reworked *Tasmanites* cysts mark a sequence boundary between units 7 (HST, Depositional Sequence 3) and 8 (LST, Depositional Sequence 4). (C, D) Photomicrographs of a lag deposit in the basal part of Unit 8. The location of the sample from which thin section was made is shown in B. (C) Transmitted light; the lag deposit is composed of reworked *Tasmanites* cysts (arrow 1), brachiopod shell fragments (arrow 2), conodonts (arrow 3), and rounded quartz grains (arrow 4). (D) Detail (reflected light) showing enrichment in pyrite (bright spots, arrow 5). Blue line = transgressive surface; Green line = maximum flooding downlap surface; Red line = sequence boundary. API = American Petroleum Institute gamma-ray units; HST = highstand systems tract; LST = lowstand systems tract; TST = transgressive systems tract (after Lazar, 2007).

### Facies Association 10 (FA-10)—Black “Banded” Argillaceous-Siliceous, Pyritic, Subcarbonaceous Fine-Medium to Medium Mudstone with Sparse to Common Fragments of *Protosalvinia*

Graded beds and millimeter-to-centimeter-thick pyritic and dolomitic scour-based lags are very sparse to sparse. Some intervals have a “banded” appearance because of subtle reworking by meiofauna of a soupy substrate. The appearance of the “banded” fabric is further enhanced by the presence of submillimeter-to-millimeter-thick laminae at their base and subtle changes in color likely driven by changes in composition (e.g., subtle changes in the content of finely disseminated pyrite) and cementation. In core, *Protosalvinia* is distinguished on bedding planes as oval and bilobed carbonaceous remains that measure 5 mm or less in size. Petrographically, *Protosalvinia*-associated mudstones are characterized by very abundant diagenetic pyrite, cementation by early diagenetic ferroan dolomite and silica, and a profusion of reworked *Tasmanites*. Pyritic nodules (1–13 mm wide) and laminae are very sparse to sparse. Organic-matter content ranges from 9 to 10 wt. %. Organic matter is predominantly marine in origin and dominated by AOM; inertinite and vitrinite contents are relatively higher than in other facies associations reaching 6.9 vol.% (Lazar, 2007; Liu et al., 2019). Bioturbation index commonly ranges from 0 to 1.

The facies associations summarized above record a depositional system with systematic variations in depositional conditions, and bottom-energy and oxygen levels (see detailed discussions in Schieber and Lazar, 2004; Lazar, 2007; Riese, 2014). As discussed in the following section, facies associations stack in recurring successions demarcated by distinct surfaces and interpreted to represent parasequences.

### PARASEQUENCES

Sequence stratigraphy provides an excellent framework within which to integrate the many types and scales of observations that are necessary to elucidate the intricacies of the internal stratigraphy of mudstone successions.

The recognition of parasequences in the New Albany Shale is challenging on gamma-ray logs of different vintages and resolutions. Teasing out parasequences in cores and outcrops is possible, however, by following the standard approach of characterizing the stratal stacking patterns at the multibedset scale (i.e., facies associations) and the attributes of potential bounding surfaces.

Parasequence recognition in Core 57 was facilitated by the identification of (1) distinct boundaries and (2) characteristic bedset-stacking patterns of facies association successions between successive parasequence boundaries. In this section, we detail the expression of two distinct parasequences focusing on their core and gamma-ray characteristics and stratigraphic occurrence and correlation potential (Figures 6, 10). These two parasequences illustrate the range of expression of mud accumulation in variable-accommodation settings in the Illinois Basin.

The first example is that of a 1.3-m-thick parasequence identified at the top of an interval interpreted to represent the TST of Depositional Sequence 2 (see Depositional Sequences section; Figures 6, 10). The lower parasequence boundary is planar and marked by a sharp boundary represented by an abrupt change from brown to gray bioturbated mudstone to black mudstone. Above this lower boundary, the parasequence consists of a succession of centimeter-to-decimeter-thick beds and bedsets composed of the black to gray argillaceous to argillaceous-siliceous, subcarbonaceous, bioturbated, fine-medium to coarse mudstones of FA-6 (Figures 6, 10). Noticeably in the lower 0.5 m of this parasequence, individual beds and bedsets commonly have sharp bases and are composed mostly of black, less obviously bioturbated mudstones (BI = 1–3); the upper part of these beds and bedsets is strongly bioturbated to churned (BI = 4–5). In this lower interval, sedimentary structures include sparse to few graded beds and very sparse starved wave ripples. Millimeter-to-centimeter-wide pyrite nodules are sparse to few. In a strongly bioturbated gray mudstone in this lower 0.5-m-thick interval, organic-matter content is low (1.9 wt. % TOC; Lazar, 2007), and organic-matter type is dominated by alginite (10.9% AOM and 80.3 % alginite; Liu et al., 2019).

In contrast, beds and bedsets in the remaining part of the parasequence above this lower 0.5-m interval are mostly strongly bioturbated to churned (BI = 4–5) and characterized by a marked upward increase in bioturbation. Other characteristics of this interval include the presence of sparse to common disarticulated to articulated calcareous shell fragments of brachiopods and a mudstone color change to various shades of gray. Trace fossils present in this parasequence include *Thalassinoides*, *Teichichnus*, escape traces, and “mantle and swirl” biodeformational structures; some burrows are filled with sand or silt or pyritized. Because of extensive bioturbation, sedimentary structures are not preserved in this upper interval with the exception of a 1-cm-thick lag rich in shell fragments present close to the top of the parasequence. Pyrite nodules are sparse to common. The upper parasequence boundary

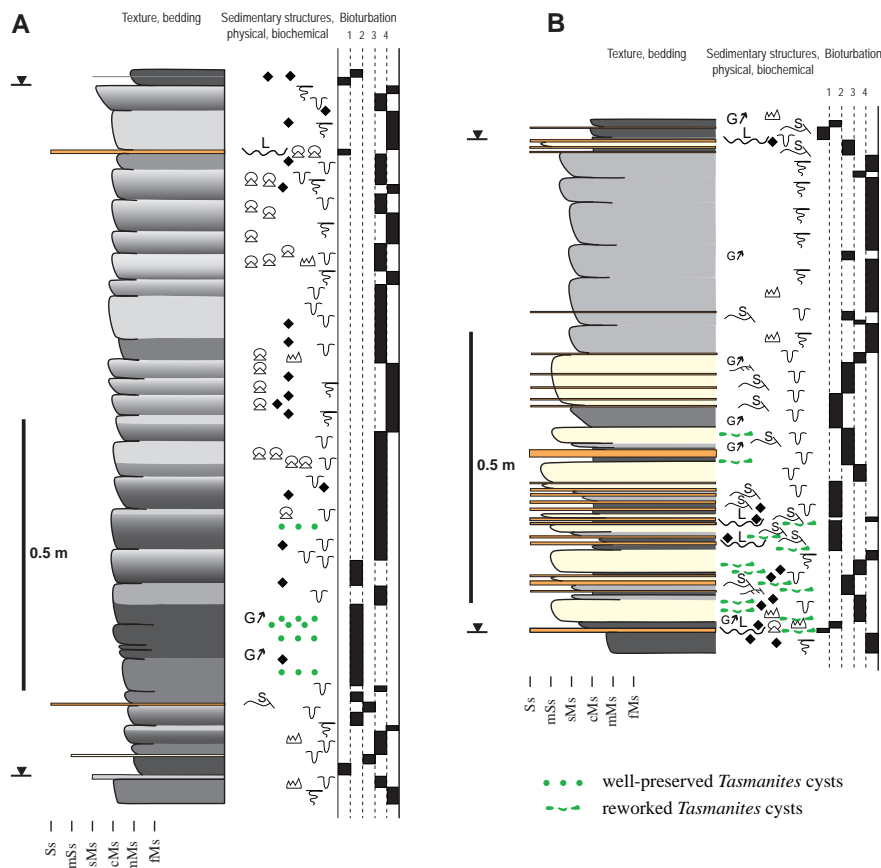


**Figure 10.** Parasequences in Core 57. (A) Example of a parasequence at the top of an interval interpreted to represent the transgressive systems tract of Depositional Sequence 2. (B) Example of a parasequence at the base of an interval interpreted to represent the lowstand systems tract of Depositional Sequence 4. fMs = fine mudstone; mMs = medium mudstone; cMs = coarse mudstone; sMs = sandy mudstone; mSs = muddy sandstone; Ss = sandstone. See Figure 2B in Chapter 3 for symbols.

is planar and sharp, and marks a change to a succession dominated by black, less bioturbated mudstones (Figures 6, 10).

In mudstones of FA-6 sampled in other parasequences, weakly to moderately bioturbated black to brown mudstones are commonly more organic-matter rich (>5 wt. % TOC), less argillaceous, and pyritic. In contrast, the strongly bioturbated to churned gray to green mudstones have less organic matter (<5 wt. % TOC), and are more argillaceous and less pyritic (Schieber and Lazar, 2004; Lazar, 2007).

At the parasequence scale, the total gamma-ray curve lacks a distinct shape other than displaying a rather continuous decrease upward from approximately 275 API to approximately 140 API (Figure 6). Based on the data available for this parasequence and similar parasequences within the New Albany Shale succession, we posit that this upward decrease in total gamma-ray response most likely reflects an upward decrease in TOC content (and associated uranium concentration) corresponding to the overall upward increase in the presence of more bioturbated gray mudstones. In the absence of core information, recognition and correlation of this type of parasequence based solely on the total gamma-ray response are

challenging, especially when available well logs are of different vintages and resolutions.

Regarding depositional conditions, we interpret that the lower 0.5-m succession of this parasequence may be the result of mud accumulation in a marine setting with relatively higher sedimentation rates and lower bottom-water oxygen concentrations (dysoxic to intermittently suboxic or anoxic). Depositional conditions for mud accumulation in the upper 0.8 m of the parasequence appear to have changed to a setting with relatively lower sedimentation rates; water-rich, “soupy” substrates; and relatively higher bottom-water oxygen concentrations (dysoxic to oxic) for relatively longer time periods. Parasequences with upward-decreasing sediment-accumulation rates have also been identified in the Monterey Formation (see Bohacs and Ferrin, 2022, Chapter 13 this Memoir).

The second example is a 0.9-m-thick parasequence identified at the base of an interval interpreted to represent the LST of Depositional Sequence 4 in the New Albany Shale succession (see Depositional Sequences section; Figures 6, 10). The lower boundary of this second parasequence is marked by a change from a succession composed of black, “banded,” pyritic, fine-medium to medium mudstones of FA-7 and

black to brown interbedded, fine-medium to medium-coarse to coarse mudstones of FA-8 to a succession of black to gray, medium to coarse mudstones to fine sandstones with abundant reworked *Tasmanites* cysts and common lag deposits of FA-9 (Figures 6, 10). The lower parasequence boundary itself is marked by a scour surface overlain by a high-energy lag (*sensu* Schieber, 1998b; Figures 5, 9).

Sedimentary structures are well preserved in the 0.38-m interval above the lower parasequence boundary (Figures 6, 10). For example, (starved) wave ripples, combined-flow ripples, and graded beds are few to abundant. In addition, scour-based, millimeter-to-centimeter-thick lags with thin interbeds of gray to brownish-black sparsely to strongly bioturbated mudstones and black “banded” mudstones are common to abundant (Figures 6, 9; Lazar, 2007). Thin-section examination revealed that lag deposits are composed of sand-size rounded to subrounded quartz grains, pyrite, brachiopod shell fragments, and conodonts, as well as abundant, reworked, broken, and unrolled *Tasmanites* cysts (Figure 9C, D; Lazar, 2007). A bright-yellow UV response (Figure 9B) is associated with the presence of *Tasmanites* cysts that became significantly enriched in the sediment likely as a consequence of intensified wave and current erosion and winnowing in a relatively low-accommodation setting (Lazar, 2007; Lazar et al., 2015a). Organic-matter content ranges from 2 to 10 wt. %. Organic matter is predominantly marine in origin and dominated by alginite (Figure 6; Lazar, 2007; Liu et al., 2019).

The remaining 0.53 m of this second example of a parasequence consists of beds and bedsets that stack in a succession characterized by an upward increase in the degree of bioturbation. This upper interval consists mostly of gray to brownish bioturbated mudstones; black “banded” mudstones are more common in the lower part of this interval. Ripples and graded beds are sparse to few, bioturbation index ranges between 3 and 5, and trace fossils are commonly horizontal to subhorizontal and filled with sand and silt. One sample only was analyzed for organic-matter content (5.6 wt. % TOC; Figure 6). Noticeably, this upper interval lacks the distinct fluorescence maxima associated with enrichment or reworked *Tasmanites* cysts. Throughout this second parasequence, pyritic nodules (<5 mm) and laminae are very sparse to sparse. The upper parasequence boundary is planar and sharp, and marks a change to a succession composed of black to brown fine-medium mudstones interbedded with coarse mudstone to medium sandstone of FA-5 (Figures 6, 10).

The total gamma-ray activity is lowest at the base of this second parasequence (107 API) and increases

constantly upward (245 API; Figure 6). Other than a continuous increase upward, the total gamma-ray log does not resolve the bed-to-bedset variability observed in core and also lacks a distinct response that would be needed for log-based regional correlation in the absence of core information. Other parasequences recognized in core have, however, a more distinct gamma-ray response that assisted regional stratigraphic correlations (e.g., parasequences 1 and 2 in the candidate HST of Depositional Sequence 2; see Depositional Sequences section; Figure 6).

We interpret that the second parasequence exemplified here accumulated in a relatively lower accommodation, more energetic depositional setting than that of the first parasequence. By analogy with modern environments, presence of common to abundant lag deposits, especially in the lower part of the parasequence, implies that significant erosion and winnowing of the underlying mudstone beds or of more elevated basinal areas (such as the Cincinnati Arch to the east, Figure 2) or of both took place. We speculate that intensified current and wave reworking enhanced by infrequent and exceptionally strong storms controlled sediment erosion, transport, and deposition in such lower accommodation setting and led to the formation of the second parasequence (Schieber, 1998a, b, 1994a; Lazar, 2007). The interpretation of an energetic, relatively low-accommodation setting is further supported by the presence of strongly bioturbated to churned mudstones dominating parts of this parasequence. The common presence of lag deposits in the lower part of this parasequence and the overall decrease in preserved sedimentary structures and upward increase in the degree of bioturbation at parasequence scale suggest a setting in which, with time, sedimentation rates decreased and bottom-water oxygen concentrations (dysoxic to oxic) increased upward.

## DEPOSITIONAL SEQUENCES

The New Albany Shale comprises at least four depositional sequences (Figure 6; Lazar, 2007). Each depositional sequence is bounded by laterally extensive erosion surfaces that record considerable truncation of the underlying strata. Depositional sequences are relatively thin (5–14 m) and consist of one to three stratigraphic units interpreted to represent systems tracts that have distinct physical, biogenic, and chemical signatures within a robust conodont-based chronostratigraphic framework (Figure 6; Lazar, 2007). A transgressive systems tract (TST) or a highstand systems tract (HST) may be the only preserved part of any given depositional sequence. Lowstand systems tracts (LSTs) tend

to be either thin (a few centimeters to about 3 m) or not deposited. As the available dataset comprises gamma-ray logs acquired over several decades at various (and occasionally insufficient) resolutions, it was not possible to consistently differentiate and map the thin LST packages throughout the basin. In contrast, despite the constraints of data availability and quality, TSTs and HSTs of the lower three depositional sequences were mapped throughout the Illinois Basin. In many older wells, the detailed gamma-ray response of a significant part of or the entire Depositional Sequence 4 (located at the top of the New Albany Shale) was not available because of clipping by the chart recorders above 200 or 300 API. As a result, it was not possible to consistently differentiate and map systems tracts of Depositional Sequence 4 throughout the Illinois Basin; instead, we mapped Depositional Sequence 4 as a whole.

In the following sections, we first present the main attributes and stratigraphic interpretations made vertically in Core 57 for Depositional Sequence 4 within which we identified all three classical systems tracts (Figure 6). Next, we explore lateral stratigraphic variability at the systems-tract-to-depositional-sequence scale along cross section A-A' (Figure 11). Then, we discuss stratigraphic variability revealed by thickness maps of TSTs, HSTs and Depositional Sequence 4, and compare these maps with the thickness map for the entire New Albany Shale. As discussed in the following sections, systems tracts and depositional sequences vary in thickness and character both vertically and laterally. Stratigraphic variability is interpreted to reflect differences in sediment supply and accommodation because of changes in paleotopography, sea level, and subsidence. Identification, characterization, and mapping of key stratigraphic units and surfaces enabled basinwide recognition of the discontinuous nature of New Albany Shale and provided key stratigraphic insights useful for the prediction of variability in source-and reservoir-rock properties.

### **Vertical Distribution and Character**

Observations made in the approximately 40-m-thick Core 57 taken from Well 57, located approximately in the middle of the Illinois Basin, illustrate significant vertical stratigraphic variability in the New Albany Shale (Figures 4, 6; Lazar, 2007). A detailed discussion of the proposed stratigraphy based on observations in Core 57 is given in Lazar (2007). Key for this chapter is that all the four depositional sequences recognized in the New Albany Shale succession have been identified in Core 57 (Figure 6). Principal attributes of these four depositional sequences and associated systems tracts

as interpreted in Core 57 are summarized in Figure 6. These attributes include the presence of distinct facies and facies associations, characteristic gamma-ray and UV responses, and unique conodont assemblages (Figure 6).

In this section, to illustrate the details of the observed vertical stratigraphic variability, the discussion focuses on the attributes and interpretations made for Depositional Sequence 4 located at the top of the Devonian New Albany Shale succession. Depositional Sequence 4 is 10.8 m thick and is composed of all three classical systems tracts (LST, TST, and HST; Figure 6). This is followed by a discussion of core-to-log calibration and key features that can help validate and correlate candidate surfaces and stratal units proposed in Core 57 along cross section A-A' and throughout the basin. Later in the chapter, the derived insights are tested by exploring basinwide stratigraphic variability.

Just below the sequence boundary at the base of Depositional Sequence 4 is Unit 7, a 10.6-m-thick interval of the upper part of Depositional Sequence 3, composed of mudstones of FA-7, FA-8, and FA-9 (Figure 6; Lazar, 2007). These mudstones contain conodonts indicative of an age range from the Lower *crepida* Zone to the Upper *crepida* Zone (Figure 6). This early to middle Famennian conodont age suggests mud deposition during the upper part of the first transgressive pulse of the transgressive-regressive (T-R) cycle IIe, when the sea level has been interpreted to have reached a relative maximum for the Late Devonian (Figure 6; Johnson et al., 1985). Unit 7 is interpreted as an HST.

The boundary between units 7 and 8, marked by a high-energy lag (*sensu* Schieber, 1998b; Figure 9A) with abundant, reworked *Tasmanites* cysts, sand-size rounded and subrounded quartz grains, pyrite grains, brachiopod shell fragments, and conodonts is inferred to represent an erosion surface and is interpreted as a likely candidate for a regional sequence boundary (Figures 6, 9; Lazar, 2007). A bright yellow UV response is associated with the presence of abundant, broken, and unrolled *Tasmanites* cysts (Figure 9B). Unit 8 above this surface has been interpreted as an LST (Figure 6; Lazar, 2007). This unit is relatively thin (3.1 m). The basal parasequence in the LST succession is composed of interbedded gray to brownish-black bioturbated mudstones and sandstones of FA-9 (Figures 6, 7, 9). Scour-based, millimeter-to-centimeter-thick, and reworked *Tasmanites* cyst-rich lag deposits are common to abundant, whereas (starved) wave ripples, combined-flow ripples, and graded beds are few to abundant; degree of bioturbation increases upward (Figure 10). The number of lag deposits decreases

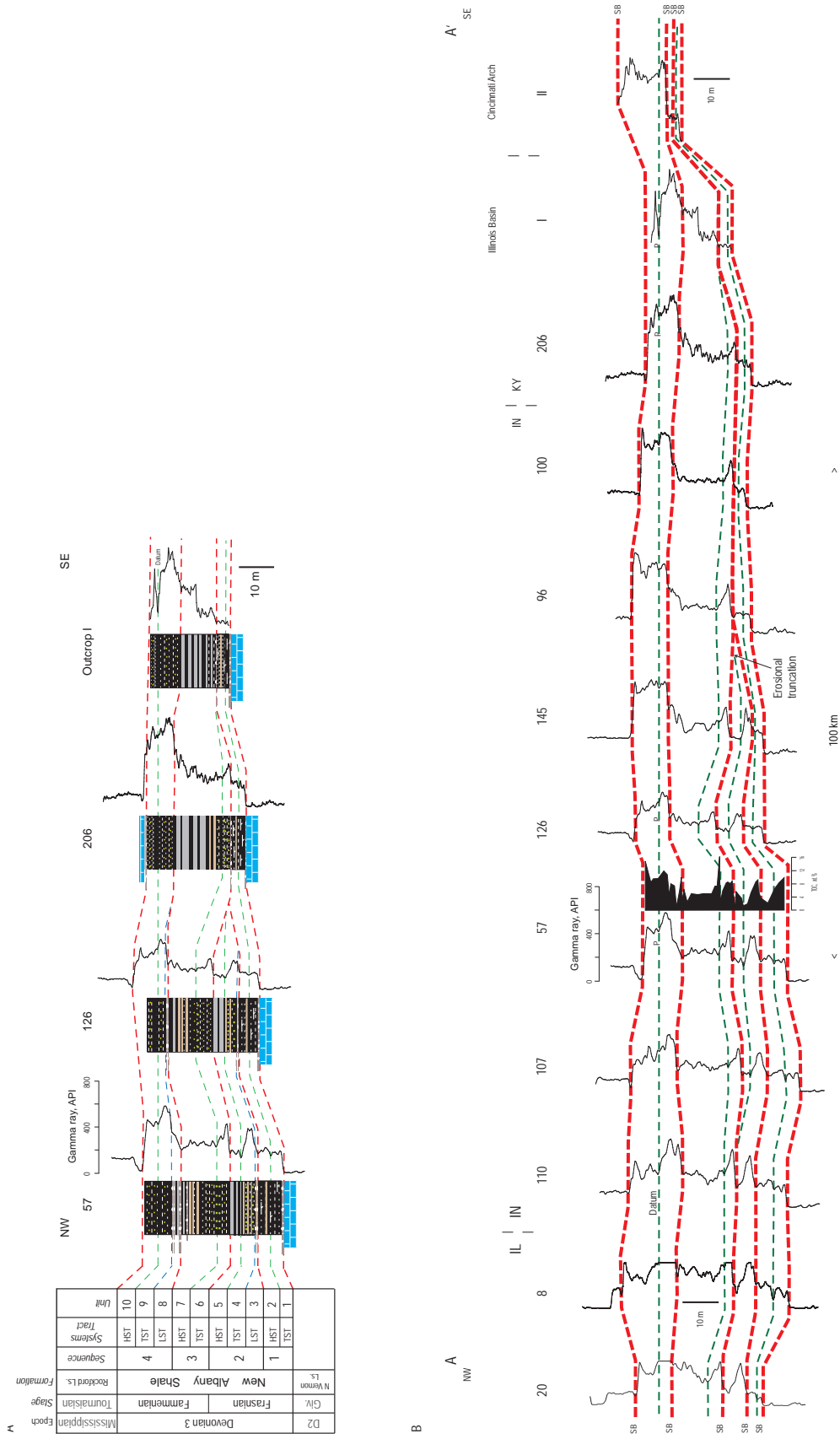


**Figure 11.** Stratigraphic cross section A-A' through cores 57, 126, and 206; outcrops I and II; and wells 20, 8, 110, 107, 145, 96, and 100 (after Lazar, 2007). Datum on the maximum flooding downlap surface of Depositional Sequence 4. Notice the effect of Cincinnati Arch on the deposition of the New Albany Shale. D2 = Middle Devonian; D3 = Late Devonian; Fam. = Famennian; Frs. = Frasnian; Giv. = Givetian; HST = highstand systems tract; LST = lowstand systems tract; TST = transgressive systems tract.

upward within the overlying two parasequences. These two parasequences are composed of interbedded and variably bioturbated mudstones and sandstones of FA-5 and FA-8 (Figure 6). By analogy with modern environments, lag deposits could be interpreted to represent sediment accumulation in a relatively low-accommodation, high-energy setting that was affected by infrequent and exceptionally strong storms (Schieber, 1994a, 1998a, b; Lazar, 2007). The composition and abundance of lag deposits in the lower part of Unit 8 implies that significant erosion and winnowing of the underlying mudstone beds or of more elevated basinal areas (such as the eastern-located Cincinnati Arch; Figure 2) took place possibly in association with intensified current and wave reworking in a low-accommodation setting. Such an interpretation is further supported by the presence of a strongly bioturbated to churned facies in this mudstone interval. Conodonts yielded an Uppermost *crepida* Zone to Lower *rhomboidea* Zone age for Unit 8 (Figure 6; Lazar, 2007), an age range that coincides with the lower part of a significant regression that dominated most of the upper half of the Famennian T-R cycle IIe of Johnson et al. (1985). In conjunction with the abundance of lag deposits and the implicitly high-energy levels of lag formation, deposition during a significant decrease in accommodation associated with a global sea-level drop supports the interpretation of Unit 8 as an LST of Depositional Sequence 4. The total gamma-ray activity is lowest at the base of the LST and increases almost constantly upward (Figure 6). Other than an increase upward with a change in slope within the upper parasequence, the total-gamma-ray log does not resolve the bed to bedset to parasequence variability observed in core (Figure 6). In addition, the gamma-ray log signature is not distinctive enough for a parasequence to systems-tract scale, log-based regional correlation in the absence of core information.

Unit 9, above Unit 8, is 3.7 m thick and consists of three parasequences in a succession of black, "banded," pyritic, weakly to not bioturbated mudstones (FA-7) and black to brown, pyritic, weakly bioturbated to churned, interbedded subcarbonaceous to carbonaceous mudstones (FA-8; Figure 6). The base of Unit 9 is marked by a sharp increase in gamma-ray intensity (Figure 6), suggestive of a flooding surface. Flooding surfaces are commonly marked by a significant, sometimes sharp increase in gamma-ray intensity associated with the accumulation of organically enriched mudstones above the surface following a decrease in coarse sediment supply and increased accumulation of authigenic and pelagic components (Bohacs, 1998; Bohacs et al., 2004; Lazar, 2007). Unit 9 shows the strongest gamma-ray response in the entire New Albany Shale succession preserved

in Core 57 (Figure 6). The high gamma-ray intensity is likely resulting from high uranium contents associated with high organic-matter contents (Figure 6). In turn, organic-matter enrichment is interpreted to reflect favorable organic-matter production and preservation conditions during mud accumulation in the course of rising sea level and increased accommodation (Bohacs, 1998; Lazar, 2007). Conodonts indicate a Lower *marginifera* Zone age, a time interval during which the global sea level rose significantly (Johnson et al., 1985). The conodont age assessment indicates that Unit 9 was deposited in a higher accommodation time during the first part of the second transgressive pulse of T-R cycle IIe of Johnson et al. (1985; Figure 6). Based on the sharp increase of gamma-ray intensity and relatively high organic-matter content at the base of Unit 9 and throughout Unit 9, together with facies association properties and distribution, and conodont age assessment, we interpret Unit 9 as a TST bounded by a candidate transgressive surface at its base.

Unit 10, above Unit 9, is 4 m thick and largely composed of black, "banded," pyritic, subcarbonaceous to carbonaceous mudstones of FA-7, FA-8, and FA-10 (Figure 6). The biostratigraphic marker *Protosalvinia* occurs in the base of Unit 10 over a 1.3-m-thick interval. *Protosalvinia* is a very useful biostratigraphic marker for regional stratigraphic correlations, as discussed in the Data, Methods, and Approach section. Careful examination of cores 57 and 126 resulted in an excellent conodont dataset, which indicates that the *Protosalvinia* Zone correlates with the Upper *marginifera* Zone (Figures 4, 6; Lazar, 2007; Over et al., 2009). Petrographically, mudstones of the *Protosalvinia* Zone are characterized by very abundant diagenetic pyrite, cementation by early diagenetic ferroan dolomite and silica, and a profusion of *Tasmanites* cysts (Schieber, 2004a; Lazar, 2007). Collectively, these features indicate extremely slow deposition and suggest sediment starvation during a significant increase in accommodation (Schieber, 1998a, b; Lazar, 2007). This assessment is corroborated by time estimates for the duration of the Upper *marginifera* Zone. Using the time scale proposed by Kaufmann (2006), the *Protosalvinia* Zone may represent a time span of approximately 0.8 m.y. An estimated net sedimentation rate of approximately 1.6 mm/ka makes the *Protosalvinia*-bearing part of Unit 10 a highly condensed black mudstone interval above a candidate maximum flooding surface between units 9 and 10 identified in Core 57 (Figure 6). The strata above the *Protosalvinia*-rich interval also consist of "banded" and pyritic black mudstones (Figure 6), but pyrite concentrations are lower and diagenetic ferroan carbonate cements are largely absent (J. Schieber, 2006, personal communication; Lazar, 2007). Although conodonts have not yet yielded a tight age determination,

the mudstone succession above the *Protosalvinia* Zone may extend into the Lower *trachytera* Zone, an age range that coincides with a significant regression in the upper part of the Famennian T-R cycle IIe of Johnson et al. (1985) (Figure 6). Position above a presumed maximum flooding surface and accumulation in a decreasing accommodation setting suggest that Unit 10 represents an HST (Figure 6).

The top of Core 57 stops within the New Albany Shale (Figure 6). The sharp decrease in gamma-ray intensity directly above the cored interval in Well 57 suggests that Unit 10 is most likely overlain by the Lower Mississippian Rockford Limestone (Figure 6). If this is correct, then the top of Unit 10 is a significant sequence boundary separating Upper Devonian fine-grained sedimentary rocks from Lower Mississippian rocks. In many places within the Illinois Basin, mudstones considered equivalent to Unit 10 are overlain by the Falling Run Bed (Campbell, 1946; Lineback, 1964, 1968; Hasenmueller, 1993), a lag deposit with abundant reworked phosphate nodules that marks the unconformity with the overlying Mississippian strata (Ettenson et al., 1988; Schieber and Lazar, 2010). This unconformity has been recognized from southern Tennessee to northern Ohio (Schieber, 2004b). Bounded by two candidate sequence boundaries, the succession of Units 8–10 is interpreted to represent Depositional Sequence 4 (Lazar, 2007).

The observations and interpretations made in this section illustrate significant vertical facies and stratigraphic variability within the New Albany Shale. These types of observations and interpretations expanded to the entire Core 57 are essential for core-to-log calibration and regional stratigraphic correlations. Key observations and interpretations along the entire Core 57 are as follows (Figure 6):

- Distinct facies and facies associations can be recognized in the New Albany Shale vertical succession. Some facies associations are present only in some intervals within the cored succession. For example, FA-6 is part of Depositional Sequence 2. Other FAs such as FA-7 and FA-8 are present throughout depositional sequences 3 and 4.
- Facies associations are stacked in relatively thin successions (mostly between <0.5 and <2 m) interpreted to represent parasequences. Some parasequences have distinct gamma-ray log responses that assist stratigraphic correlations (e.g., parasequences 1 and 2, Unit 5-HST, Depositional Sequence 2). Other parasequences do not have a distinct gamma-ray log response, especially those identified in LSTs (e.g., parasequences 1 and 2 in Unit 8-LST, Depositional Sequence 4); this is also the case for some TST or HST parasequences (e.g., parasequence 1, Unit 9-TST, Depositional

Sequence 4; parasequence 2, Unit 10-HST, Depositional Sequence 4).

- Lowstand systems tracts are relatively thin and their gamma-ray log response may not be distinctive enough for consistent differentiation and stratigraphic correlation throughout the basin.
- Candidate transgressive surfaces are marked by a sharp increase in gamma-ray log response. Such a distinctive log response associated with transgressive surfaces has been observed in other fine-grained rock successions (e.g., Bohacs, 1998; Bohacs et al., 2022a, b; Bohacs and Guthrie, 2022, Chapters 6, 8, and 12 this Memoir) and is very useful for stratigraphic correlations. In Core 57, significantly organic-matter-enriched “homogeneous-looking” to “banded” pyritic mudstones accumulated above these flooding surfaces.
- The New Albany Shale is a discontinuous, fine-grained rock succession composed vertically of four depositional sequences that are bounded by candidate sequence boundaries. The gamma-ray log responses of TSTs, HSTs, and especially depositional sequences are distinct. These distinct log responses enabled the identification and correlation of these stratigraphic packages throughout the Illinois Basin. This correlation and mapping exercise revealed the extent of the discontinuous character of the New Albany Shale and may reveal significant lateral and vertical variability between adjacent mudstone units throughout the basin. If this variability is because of the top-truncated gamma-ray motifs, it may be attributed to partial or complete erosional truncation at the top of individual units (Schieber, 2000; Schieber, 2004b; Lazar, 2007) and would confirm the discontinuous nature of the New Albany Shale composed of depositional sequences bounded by laterally extensive erosion surfaces. Alternatively, lateral stratigraphic correlations may invalidate this working hypothesis if gamma-ray profiles measured in other wells show a mudstone succession composed of a stack of stratal units that can be traced continuously, layer cake fashion, throughout the basin. In the next section, we will examine the lateral distribution of the major stratal surfaces and units recognized in Core 57.

### Lateral Distribution and Character

In this section, the vertical sequence-stratigraphic framework established for Core 57 is used as a reference for lateral comparisons with the New Albany Shale stratigraphy along cross section A-A' (Figures 6, 11).

The rationale for this approach includes the following:

- Core 57 intercepted four depositional sequences and their systems-tract components (Figure 6). This broad coverage facilitates comparisons with less complete New Albany Shale successions from other localities in the Illinois Basin.
- The conodont-based chronostratigraphic framework established for the mudstone succession in Core 57 (Figure 6) provides an independent control of subsurface correlations based on physical tracing of erosion and flooding surfaces.
- All the five classical lithostratigraphic members of Lineback (1964, 1968, 1970) are present in Core 57 facilitating a comparison of lithostratigraphic nomenclature with the proposed sequence-stratigraphic framework (Figures 3, 6).

Next, the focus is on general stratigraphic insights derived from cross section A-A', followed by specific examples of stratigraphic character and variability in some of the wells along cross section A-A'. This will be followed by a discussion of the sequence-stratigraphic variability demonstrated by thickness maps at basin scale.

Cross section A-A' illustrates that each depositional sequence is bounded by laterally extensive erosion surfaces that record considerable truncation of underlying strata (Figure 11). As a consequence, only three of the four depositional sequences recognized in Core 57 are present in a southeast direction (toward the Cincinnati Arch) beyond Well 145. At the systems-tract scale, thin LST packages could not be mapped consistently throughout the basin because of the varying quality and (in places insufficient) resolution of the gamma-ray logs (Figure 11). In contrast, despite gamma-ray log limitations, TSTs and HSTs have characteristic gamma-ray responses that can be correlated along cross-section A-A' and throughout the Illinois Basin (Figure 11). Notice, for example, the consistent sharp increase in gamma-ray intensity at the base of the mudstone Unit 6, the TST for Depositional Sequence 3 (Figure 11). After calibration between available cores and corresponding gamma-ray logs, the more distinct gamma-ray signatures of TSTs and HSTs enabled consistent regional stratigraphic correlations (Figure 11; Lazar, 2007). Another relevant observation is that, in places, the TSTs are the only preserved parts of a depositional sequence (e.g., Depositional Sequence 1, Well 145; Depositional Sequence 2, Well 110), a characteristic that has also been observed in the laterally equivalent Chattanooga Shale (Schieber, 1998b, 2004b). Where present, HSTs can be significantly truncated by the

overlying sequence boundary (e.g., Depositional Sequence 2, Wells 20, 8, and 110; Depositional Sequence 4, Outcrop I). Comparison of the gamma-ray logs measured in wells along cross-section A-A' also shows the presence of relatively thicker units above thinner units and vice versa (e.g., compare lateral thickness of Units 6 (TST) and 7 (HST); Figure 11). With thinning interpreted as a consequence of erosional removal of strata, localized thinning thus implies the formation of depressions that subsequently result in increased accommodation during deposition of the overlying stratal unit and illustrate the role of accommodation as a significant control on mud deposition. In addition to these broader characteristics of stratal architecture, further insights emerge from detailed examination of stratigraphic changes in Well 126 and outcrops I and II (Figure 11).

Core 126 was taken from a well located approximately 17 km northeast of Well 57 (Figure 4). All the 10 stratigraphic units recognized in Core 57 are present in Core 126 (Figures 6, 11). Mudstone units are distinguished on the basis of the same criteria that are employed for Core 57 (Figures 6, 11). For example, an abrupt change from black to gray subcarbonaceous, bioturbated mudstones (FA-6) to "banded" subcarbonaceous to carbonaceous, pyritic mudstones (FA-7) marks the boundary between units 5 (HST) and 6 (TST) in both cores (Figure 11). The knife-sharp contact at the base of Unit 6 (TST) also coincides with a sharp increase in gamma-ray intensity as measured in both wells 57 and 126 (Figure 11). Further, a strong UV response marks the boundary between units 6 (TST) and 7 in both cores (HST), resulting from a strong enrichment of "pristine" cysts of *Tasmanites* under conditions of increased accommodation and extreme sediment starvation (Lazar, 2007). Although all stratal units recognized in Core 57 occur in Core 126, the New Albany Shale is about 4 m (~10%) thinner in Core 126, a reflection of considerable thinning of units 2 (HST), 3 (LST), 7 (HST), and 8 (LST) over a relatively short distance (Figure 11). As discussed below, lateral variability in the thickness of mudstone units likely reflects changes in accommodation, which in turn appears controlled by nondeposition and bypass or erosion and removal of units beneath sequence boundaries (Figure 11).

Continuing along cross section A-A', lateral variability in the thickness of depositional sequences and corresponding mudstone units becomes evident in the gamma-ray logs from wells 145, 96, and 100 located farther to the southeast (Figure 11). Unit 2, for example, is almost entirely eroded away in Well 145 under the sequence boundary at the base of Depositional Sequence 2 (Figure 11). Considerable erosion of underlying strata is suggested by the truncation of the

gamma-ray motif in Well 96, where the entire Depositional Sequence 2 (units 3–5) is missing (Figure 11). Complete erosional truncation of units 3–5 and partial truncation of Unit 2 can be recognized farther southeast in Well 100 (Figure 11). Notice also that in addition to erosional truncation of the underlying units, sequence boundaries are also marked by onlap of the overlying units (Figure 11).

Core 206 was taken from a well located approximately 130 km southeast of Core 57 and approximately 31 km northwest of Outcrop I (Figures 4, 11). Examination of Core 206 and stratigraphic correlation along cross section A-A' confirmed the presence of laterally extensive erosional truncation and thinning of underlying mudstone units (Figure 11). By comparison with cores 57 and 126, Core 206 also indicates that facies association characteristics of recognized systems tracts persist over large distances. What may change, however, is the thickness of facies associations and facies association successions and the distribution of specific facies within a particular facies association. For example, in cores 57 and 126, FA-6 consists of a succession of centimeter-to-decimeter-thick beds and bedsets characterized by an upward increase in bioturbation (from weakly to strongly to churned) and facies change from less bioturbated black to brown mudstones to more bioturbated gray to green mudstones. Within FA-6, from a relatively more proximal to distal location, the proportion of the bioturbated gray to green mudstones to less bioturbated black to brown mudstones as well as the abundance and diversity of trace fossils decreases (Figure 11; Schieber and Lazar, 2004; Lazar, 2007; Riese, 2014). A similar observation of facies change is made when comparing the proportion of FA-8 black weakly bioturbated mudstones to brown strongly bioturbated to churned mudstones along the more proximal (Core 206) to more distal (Core 57) transect. The proportion of lighter color and more bioturbated mudstones, and the abundance and diversity of trace fossils increase in a more proximal direction (Figure 11; Schieber and Lazar, 2004; Lazar, 2007; Riese, 2014). These observations are interpreted to reflect mud accumulation under longer duration of dysoxic to oxic bottom-water conditions in a lower accommodation setting toward the Cincinnati Arch, likely an elevated area during the Late Devonian (e.g., Kepferle and Roen, 1981; Barrows and Cluff, 1984; Buschbach and Kolata, 1991; Kolata and Nelson, 1991; Ettenson, 1992; de Witt et al., 1993; Matthews, 1993; Lumm et al., 2000; Schieber and Lazar, 2004; Lazar et al., 2007; Riese, 2014).

The biostratigraphic marker *Protosalvinia* is present within Depositional Sequence 4 in Core 206 as well as in the other examined cores and Outcrop I, and

constitutes a useful marker for stratigraphic correlations from outcrops to subsurface (Figure 11).

A phosphatic lag known as the *Falling Run Bed* (Campbell, 1946; Lineback, 1964, 1968, 1970) is present at the top of Unit 10 in Core 206 (Figure 11). The phosphate nodules that occur in this lag must have been derived from underlying strata. In multiple locations within the Illinois Basin, a phosphate nodule-bearing black mudstone unit occurs at the very top of the New Albany Shale (e.g., Schieber and Lazar, 2004, 2010; Lazar, 2007). This phosphatic black mudstone interval may be a few decimeters to several meters thick and has, for example, been described in wells 77 and 159 that were drilled in southeastern Indiana (J. Schieber, 2006, personal communication). The phosphogenesis of this phosphatic interval has been studied in lateral equivalents in Tennessee and has been linked to slow overall sedimentation rates coupled with mechanical reworking and dissolution-reprecipitation processes in surficial sediments (Li and Schieber, 2015). This phosphatic black mudstone interval was likely eroded and reworked as a result of decrease in accommodation possibly related to the Early Mississippian relative fall of sea level (Johnson et al., 1985) and is the most likely provenance of the phosphate nodules in the lithostratigraphic *Falling Run Bed* (Campbell, 1946; Lineback, 1964, 1968, 1970; Cluff et al., 1981; Hasenmueller, 1993) in Indiana, Kentucky, and in lateral equivalents in Tennessee (J. Schieber, 2004, personal communication). As found in earlier studies (Barrett, 2002; J. Schieber, 2006, personal communication), the interval of phosphatic black mudstones with phosphate nodules exists as erosional remnants in various places within the Illinois Basin. Future establishment of a conodont zonation with detailed facies and facies association description as well as basinwide sequence-stratigraphic mapping of this phosphatic mudstone is needed to formally define additional Upper Devonian mudstone unit(s). Such a future study, integrated with the observation of significant lateral erosion under the phosphatic interval in Tennessee (Schieber, 2004b; Schieber et al., 2010; Li and Schieber, 2015), could result in the recognition and mapping of a fifth depositional sequence in the New Albany Shale of the Illinois Basin (Lazar, 2007).

Lower Mississippian lithostratigraphic beds of fossiliferous, gray and black to brown mudstones known under the names of Underwood, Henryville, and Jacobs Chapel Beds (Campbell, 1946; Lineback, 1964, 1968, 1970; Hasenmueller et al., 2000) occur in various places atop the *Falling Run Bed*. The *Falling Run Bed* overlies an erosion surface that cuts to variable depth into the Upper Devonian black mudstone succession and marks a major sequence boundary that separates Upper Devonian strata from

Lower Mississippian strata. Abovementioned Lower Mississippian mudstone beds have traditionally been included into the New Albany Shale Formation (Campbell, 1946; Lineback, 1964, 1968, 1970; Hasenmueller et al., 2000). From a sequence-stratigraphic perspective, the top of the New Albany Shale is defined here at the top of the last Devonian black mudstone unit recognized below the Falling Run Bed, and the Mississippian beds above the Falling Run Bed are considered part of a genetically different succession (Lazar, 2007).

Toward *outcrops I and II* along cross section A-A', closer to and on the Cincinnati Arch, respectively, the number of stratigraphic units recognized in Core 57 decreases to half (Figures 6, 11).

*Outcrop I* is a roadcut located south of Louisville, Kentucky, approximately 143 km southeast from Core

57 (Figures 4, 12). Examination of the New Albany Shale succession revealed that only 5 of the 10 stratigraphic units recognized in Core 57 are present in Outcrop I over a 22-m-thick interval (Figures 11, 12). Using conodont data from this outcrop (Over, 2002) as well as facies and facies association stacking, we interpret these stratigraphic units as correlatives of units 1 (TST), 2 (HST), 7 (HST), 9 (TST), and 10 (HST) from Core 57, comprising depositional sequences 1, 3, and 4 (Figure 11; Schieber and Lazar, 2004; Lazar, 2007).

Erosion-related features observed at candidate sequence boundaries in Core 57 are also present in Outcrop I (Schieber and Lazar, 2004; Lazar, 2007). For example, a 1- to 2-cm-thick pyritic lag with rounded quartz grains, glauconite, *Lingula* shell fragments, and conodonts occurs at the top of a succession of black to brown dolomitic interbedded mudstones to



**Figure 12.** (A) Outcrop I is a roadcut located south of Louisville, Kentucky, at exit 112 off interstate highway I-65 (Figure 4). The New Albany Shale is visibly draped over the Middle Devonian North Vernon Limestone. (B) Outcrop detail photograph of dolomitic mudstones of units 1 and 2 of the New Albany Shale overlying a crinoid-rich interval at the top of the North Vernon Limestone. (C) The first interval of interbedded black and gray mudstones in the New Albany Shale succession (pink rectangle in [A]) has been considered the Selmier Member in the lithostratigraphic code (Lineback, 1964; Hasenmueller et al., 2000). Presence of a pyritic lag at the base of this interval and conodont data (Over, 2002; Figure 5B, C) reveals, however, a 3 m.y. gap in the rock record, and illustrates that the presence of black-gray interbeds is not an infallible field criterion for correctly identifying shale units. P = *Protosalvinia*-rich interval.

sandstones of FA-2 (Figure 5B, C). According to conodont data, the bulk of these dolomitic black mudstones is of the Middle–Upper Frasnian (Over, 2002), an age assessment that makes them a correlative of Unit 2 (HST, Depositional Sequence 1) as recognized in Core 57 (Figures 6, 11; Lazar, 2007). Tracing of gamma-ray logs suggests that the basal part of the dolomitic black mudstones in Outcrop I is probably correlative to Unit 1 (TST, Depositional Sequence 1) as seen in Core 57 (Figures 6, 11; Lazar, 2007). The lag that tops the dolomitic black mudstones of Unit 2 in Outcrop I (Figure 5B, C) is an example of a thin lag that marks a major gap in the rock record. Conodonts indicate that the overlying mudstone package is of the Lower Famennian (Lower *crepida* Zone; Over, 2002), making it correlative to Unit 7 (HST, Depositional Sequence 3) as recognized in Core 57. Thus, units 3 through 6 are missing in Outcrop I, and following the Kaufmann (2006) timescale, we can estimate that at least 3 m.y. of rock record is missing (Figures 6, 11, 12; Schieber and Lazar, 2004; Lazar, 2007).

Lithostratigraphically, the dolomitic black mudstones in Outcrop I can be assigned to the Blocher Member of the New Albany Shale (Figures 3, 6) because identical strata were described as such by Lineback (1964, 1968, 1970) from exposures a few miles east of Outcrop I. In the lithostratigraphic code for the New Albany Shale, the first interval of interbedded gray and black mudstones above the Blocher Member is called the Selmier Member (Figure 3). Observing that there is a thin interval of interbedded black and gray mudstones in the lower part of Unit 7 in Outcrop I, previous workers have attributed this interval to the Selmier Member of the New Albany Shale (Figure 12C; Lineback, 1964, 1968, 1970; Hasenmueller et al., 2000). The perspective from the conodont record and regional sequence-stratigraphic correlations shows, however, that the Selmier-equivalent rock succession is not present in Outcrop I and that rigid application of lithostratigraphic codification may result in miscorrelations if erosional gaps are not recognized (Schieber and Lazar, 2004; Lazar, 2007). Furthermore, lithostratigraphic units, defined strictly on lithic characteristics, typically span parts of genetically related sequence-stratigraphic units and should not simply be equated with the latter (e.g., Liu et al., 2019).

Significant in the context of the above discussion is also the presence of an approximately 3-m-thick interval dominated by black “homogeneous-looking,” “banded,” and pyritic mudstone (FA-7) that contrasts sharply in outcrop with the interbedded black-to brown to gray mudstones (FA-8) of underlying Unit 7 (Figures 11, 12A; Schieber and Lazar, 2004; Lazar, 2007). The two mudstone units show a sharp contact that is

visible from a distance and can be traced easily across the entire exposure. The base of the mudstone packages above this sharp contact coincides with a twofold increase of gamma-ray intensity (Figure 11; Schieber and Lazar, 2004; Lazar, 2007). Based on strong similarities in facies association and gamma-ray response, this 3-m-thick interval is correlated with Unit 9 from cores 57, 126, and 206 (Figures 6, 11, 12A). Judging from other contacts of this kind in Upper Devonian “black shales” (Schieber, 1998a, b), the knife-sharp contact and marked change in facies association are interpreted to represent a significant erosion surface between Units 7 and 9 in Outcrop I (Figure 11; Schieber and Lazar, 2004; Lazar, 2007; Schieber and Lazar, 2010).

In a recessively weathering groove toward the top of the Outcrop I, fragments of *Protosalvinia* occur in the black pyritic mudstone of FA-10 (Figure 12A; Schieber and Lazar, 2004; Lazar, 2007). This interval is also marked by a shift toward lower gamma-ray intensities (Figure 11). In keeping with subdivisions established for Core 57, the *Protosalvinia*-bearing interval allows correlation with Unit 10 (Figures 6, 11, 12A; Lazar, 2007). In Outcrop I, only the lower part of Unit 10 appears to be present because an erosional truncation separates Unit 10 from the overlying Mississippian New Providence Shale Member of the Borden Formation (Figure 11; J. Schieber, 2004, personal communication). Approximately 10 km (6 mi) north in a quarry near the town of Shepherdsville, and elsewhere in Indiana, stratigraphic intervals similar to Unit 10 are overlain by the phosphatic lag known as the Falling Run Bed (e.g., Campbell, 1946; Lineback, 1964, 1968, 1970; Hasenmueller, 1993; Schieber and Lazar, 2010).

*Outcrop II* is a composite section exposed in two roadcuts located approximately 1 km apart, south of Junction City, Kentucky, and approximately 250 km southeast from Core 57 (Figures 4, 13). Following the approach detailed earlier, examination of the mudstone succession revealed the presence of the five stratigraphic units recognized in Outcrop I but in a succession that is only 17-m thick (~22% thinner than in Outcrop I and 56% thinner than in Core 57; Figure 11; Schieber and Lazar, 2004, 2010; Lazar, 2007). A highlight of Outcrop II is the presence of a large number of fractures, filled with quartz, dolomite, and locally some bitumen, some of which cut vertically for as much as several meters, found in the basal, black dolomitic mudstones of Depositional Sequence 1 (Figure 13B; Dumitrescu et al., 2004; Schieber and Lazar, 2004; Lazar, 2007; Gale et al., 2010, 2014). These fractures range from a few centimeters to 15 cm in width, and have been contorted and telescoped because of post emplacement compaction of the surrounding mudstone. Bitumen occurs in vuggy

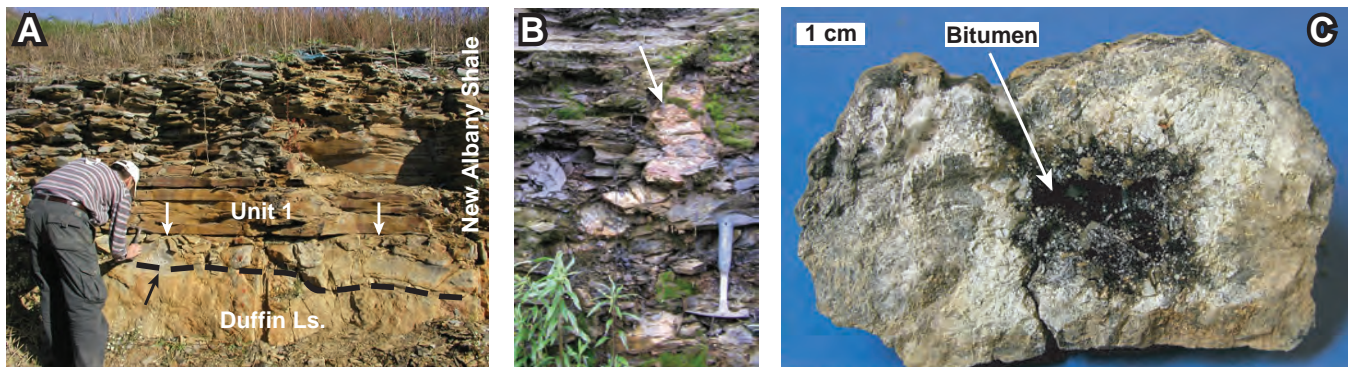


**Figure 13.** Outcrop II is a composite section exposed in two roadcuts located approximately 1 km apart south of Junction City, Kentucky (Figure 4). (A) Base of New Albany Shale succession in Outcrop II (south end) overlying the buff-weathering Middle Devonian Duffin carbonates. A lag deposit (up to 40 cm thick) separates the platy rusty-weathering mudstones of Unit 1 of the New Albany Shale from the Duffin carbonates. The base of the lag (black arrow, dashed line) is undulous and fills in surface irregularities on the Duffin. The upper surface of the lag is even and forms a sharp contact (white arrows) with overlying New Albany Shale (from Schieber and Lazar, 2004). (B) Quartz-dolomite-bitumen contorted fracture (white arrow) in the black dolomitic mudstones at the base of the New Albany Shale (Depositional Sequence 1). The fracture is contorted because of compaction of the surrounding mudstones after their emplacement (from Schieber and Lazar, 2004). (C) Example of bitumen occurrence in a vuggy opening (from Dumitrescu et al., 2004).

openings (Figure 13C; Schieber and Lazar, 2004; Lazar, 2007). A biomarker study on the bitumen from four vuggy openings, a rock sample from the surrounding mudstone, and two oil samples from the Plummer field of Indiana suggest that the bitumen had a different source of organic matter than the host mudstone (Dumitrescu et al., 2004). Dumitrescu et al. (2004) considered that the dolomitic mudstone host could have been hydrofractured during oil generation from older Ordovician or Silurian strata, and that Ordovician or Silurian bitumen migrated along open fractures and then was trapped in veins and vuggy openings as the fractures were mineralized.

Gamma-ray signatures that can be recognized laterally and appear diagnostic for particular stratigraphic units and surfaces allow for robust regional subsurface stratigraphic correlations in the New Albany Shale (Lazar and Schieber, 2006; Lazar, 2007). Observations made along cross section A-A' demonstrate that the New Albany Shale is a discontinuous mudstone succession of significant vertical and lateral stratigraphic variability (Figures 6, 11). Stratigraphic variability is evident in both cores and gamma-ray motifs and is primarily the result of facies association variability and partial or complete erosional truncation at the top of underlying units (Figure 11). Sequence boundaries are also marked by onlap of overlying units (Figure 11).

The New Albany Shale varies considerably in thickness across the Illinois Basin from less than 10 m in the vicinity of the Cincinnati Arch up to 108 m in

the Rough Creek Graben and the Wabash Valley Fault System area (Figure 14). We constructed a set of *isochore maps* to further explore stratigraphic variability in the New Albany Shale succession (Figure 14; Lazar, 2007). These thickness maps were constructed at systems-tract (with the exception of LSTs) and depositional-sequence scales. LSTs (mudstone units 3 and 8; Figure 6) are often too thin (a few centimeters to a couple of meters thick) and lack a distinct gamma-ray response to be identified confidently and consistently on the available gamma-ray logs acquired at various resolutions over several decades. Therefore, when making the isochore maps, the thin LST Units 3 and 8 were included with their overlying TSTs (units 4 and 9, respectively). In addition, in many older wells, the gamma-ray response of a significant part of or the entire Depositional Sequence 4 has not been available because of original clipping of gamma-ray values above 200 or 300 API. Consequently, we did not correlate basinwide the systems tracts of Depositional Sequence 4.

Regional correlations support the premise that the New Albany Shale consists of a stack of distinct depositional sequences that are bounded by laterally extensive erosion surfaces (Lazar, 2007). Depositional sequences and corresponding systems tracts can be correlated tens to hundreds of kilometers from outcrops to subsurface across the Illinois Basin and beyond (Figure 14; Schieber, 1998a, b; Schieber, 2004b; Lazar, 2007). Mapped mudstone units show significant variability in thickness (from <1 m to 27 m;

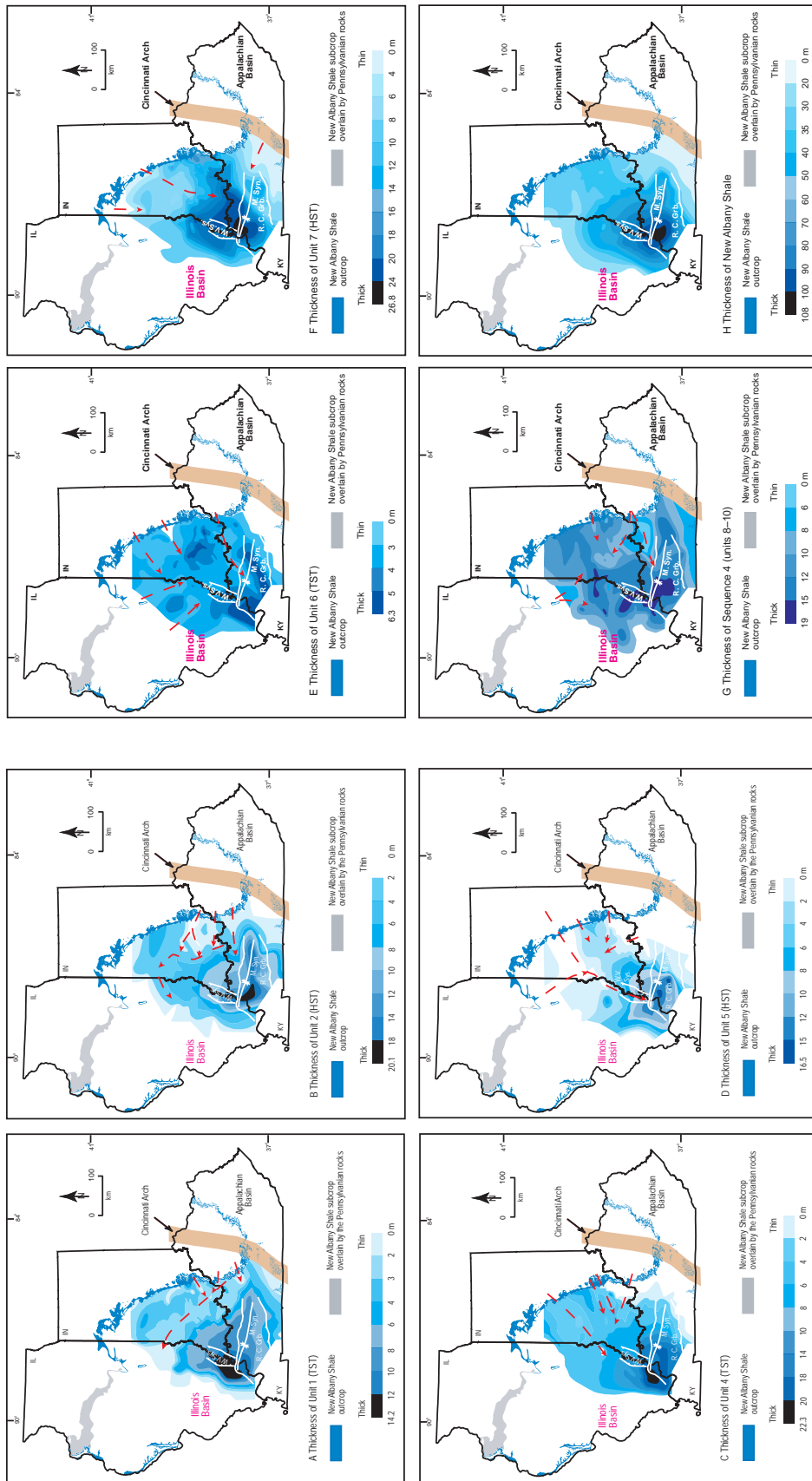


**Figure 14.** Thickness maps of systems tracts, Depositional Sequence 4, and the New Albany Shale (after Lazar, 2007). Red dashed arrows highlight areas of relatively thinner shale interpreted to reflect basinal current circulation, "local" erosion, and/or less deposition. HST = highstand systems tract; TST = transgressive systems tract. Structural features: M.Syn. = Mormon Syncline; R.C.Gr. = Rough Creek Graben; W.V.Sys. = Wabash Valley Fault System.

Figure 14). Depositional sequences and corresponding mudstone units are generally thicker in southeastern Illinois, western Kentucky, and southwestern Indiana (Figure 14A–H). Stratal units vary in thickness laterally, and where one unit thins, the overlying unit tends to be thicker and vice versa (Figures 11, 14). Depositional sequences 1–3 generally diminish in thickness or disappear completely toward the Cincinnati Arch in the east, whereas Depositional Sequence 4 thickens or has a thickness comparable with more basinal locations (Figure 14). The variability in the thickness of Depositional Sequence 4 (from 3.8 m to 19 m) across most of the basin suggests substantial erosional truncation of its upper part (Figure 14G). Depositional sequences and their corresponding units also diminish in thickness or disappear toward central Illinois, southwestern Illinois, and northern parts of the Illinois Basin (Figure 14). Changes in thickness were controlled by sediment supply and by accommodation, which in turn was controlled by paleotopography, relative changes in sea level, and subsidence.

The role of *paleotopography* is most clearly seen in areas where the New Albany Shale drapes over pre-existing highs and lows of underlying carbonate units. For example, Figure 12 illustrates the influence that the North Vernon Limestone paleotopography had on the accumulation of Depositional Sequence 1 and corresponding TST and HST (Units 1 and 2) in the eastern parts of the Illinois Basin. Figure 14A shows that the thickness of basal Unit 1 changes over relatively short distances along the Indiana outcrop belt, further illustrating the influence that the North Vernon Limestone paleotopography had on the deposition of the basal stratal units of the New Albany Shale. (Similar effects of preexisting topography were seen in the units discussed in Bohacs and Ferrin, 2022; Bohacs and Guthrie, 2022; Bohacs et al., 2022a, c; Potma et al., 2022; Chapters 6, 8, 10, 11, and 13 this Memoir.)

The influence of paleotopography at a larger scale is indicated by the presence of erosional truncation of underlying strata and onlap of overlying units toward the Cincinnati Arch. These stratal relations suggest that the arch was a positive geomorphologic feature and that the vicinity of the arch was a shallower, more energetic depositional setting (e.g., Figures 11, 14; Lazar, 2007).

Thickness changes may also reflect *ocean-current circulation and sediment depositional pathways* in the basin (Figure 14). This point is supported by the presence of relatively narrow areas of thinner mudstone units on the isochore maps. These areas are oriented approximately perpendicular to structural arches (e.g., Cincinnati Arch, a paleohigh during the Late Devonian) and may constitute submarine channels through which eroded sediment (from the Cincinnati

Arch) was carried into settings of higher accommodation (red arrows, Figure 14B, D, F). In other places, these narrow areas approximately parallel basin topography and may reflect bottom-current circulation along bathymetric contours (Figure 14A, B; Lazar, 2007). These narrow areas were likely characterized by higher energy conditions and “local” erosion or smaller rates of mud deposition.

A decrease in accommodation can result from a *relative fall of sea level*. Such a decrease in accommodation is commonly accompanied by an increase in the energy levels of the depositional setting, which, in turn, can cause laterally extensive, partial, or complete erosional truncation of underlying mudstone units as seen atop depositional sequences 1 and 3 (Figure 11, 14).

The active role of *subsidence* in accommodation change is strongly suggested by the increase in the thickness of mudstone units in or around the Rough Creek Graben and the Wabash Valley Fault System (Figure 14). The Rough Creek Graben is asymmetrical, with greater displacements along its east–west-trending northern margin (Nelson, 1991). The Wabash Valley Fault System consists of a series of high-angle normal faults that strike north–northeasterly in southeastern Illinois, southwestern Indiana, and western Kentucky (Nelson, 1991). Episodic reactivation of faults of the Rough Creek Graben and the Wabash Valley Fault System at the time of accumulation of depositional sequences 1 and 2 (Units 1, 2, 4, and 5), for example, likely generated the necessary space for greater sediment accumulation and may explain the location and shape of depocenters within these two structural features (Figures 14, 15). Comparison of thickness maps reveals that depocenters of each systems tract shifted spatially through time and filled up remaining accommodation following the accumulation of the underlying unit (Figure 15; Lazar, 2007). (Similar influence of fault-associated subsidence on stratal distribution in the Kimmeridge Clay Formation is discussed in Bohacs et al., 2022c, Chapter 11 this Memoir.) Sediment deposition was enhanced wherever space for deposition was available, that is, not only in the area of the Rough Creek Graben and the Wabash Valley Fault System but also wherever a thinner unit is present above a thicker unit, as shown in Figure 11.

The role of *sediment supply* is apparent in the distribution of Unit 7 (HST, Depositional Sequence 3). This unit is relatively thicker in many parts of the basin (Figures 6, 11, 14). Based on the data from Core 57, it is probably the result of the highest average sedimentation rate in the entire New Albany Shale succession (corrected sedimentation rate of 0.76 cm/ka versus 0.14–0.39 cm/ka for the rest of the New Albany Shale succession; Lazar, 2007).

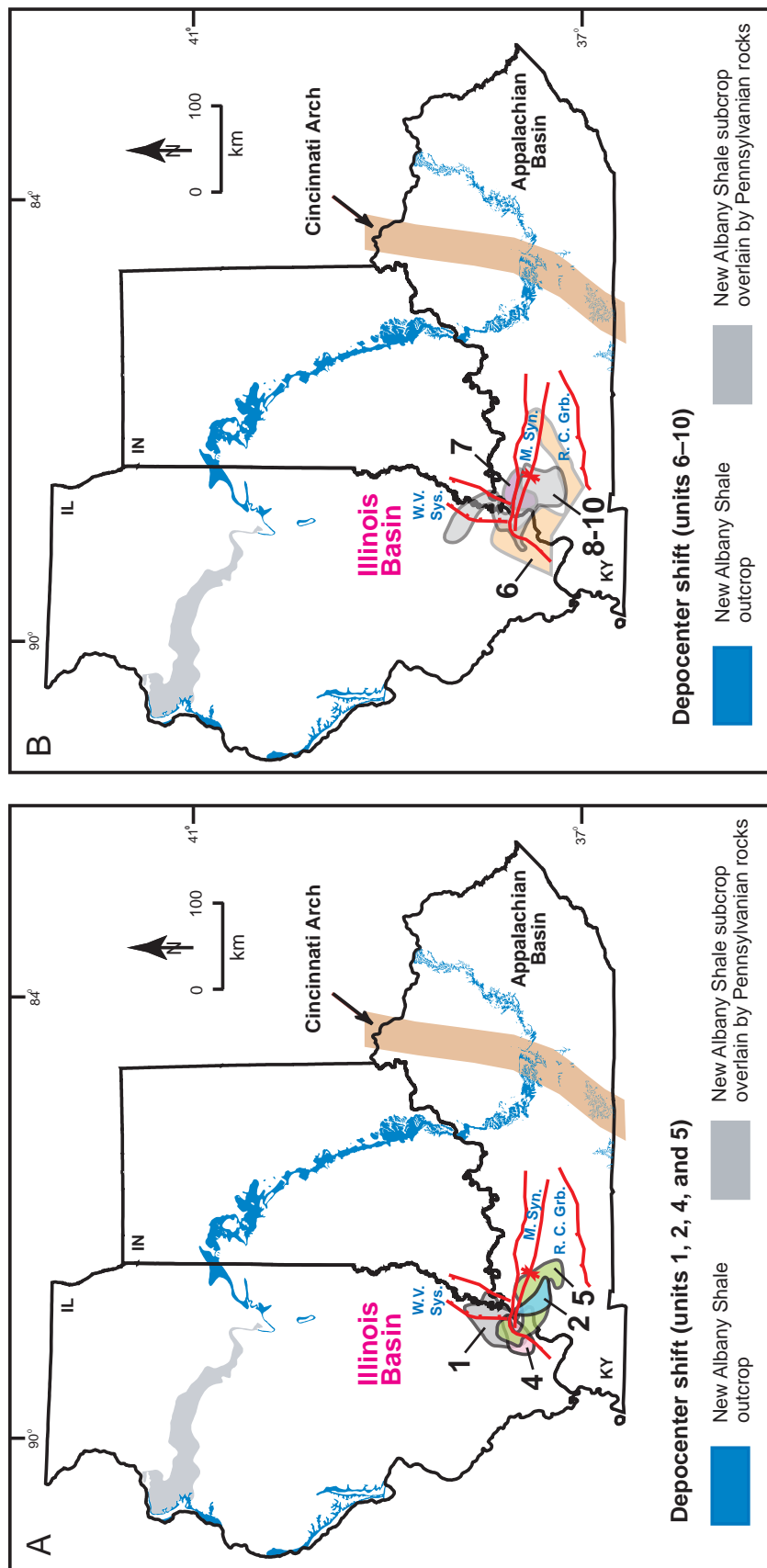


Figure 15. (A) Depocenter shift during deposition of units 1, 2, 4, and 5. (B) Depocenter shift during deposition of units 6–10. M.Syn. = Mormon Syncline; R.C.Gr. = Rough Creek Graben; W.V.Sys. = Wabash Valley System.

Examination of thickness maps of sequence-stratigraphic units also suggests that the Illinois Basin was open to the southwest and that the sea flooded the basin toward the north–northeast and east during the Late Devonian (Figure 14). One can speculate that the age of the lowermost mudstone unit (Unit 1) distinguished in the New Albany Shale succession in Core 57 becomes older in a southwest direction. Available conodont data suggest that the base of Unit 1 may be as old as the upper Givetian in that area (Lazar, 2007). A future conodont study of Unit 1 in the southwestern part of the Illinois Basin may extend the lower age limit of this mudstone unit into the Middle Devonian.

Generation of a thickness map of the entire Upper Devonian New Albany Shale succession and comparison with thickness maps of sequence-stratigraphic units (systems tracts and depositional sequences) provide valuable insights into the course of stratigraphic analysis of a formation of interest. In the case of the Upper Devonian New Albany Shale, thickness maps of individual sequence-stratigraphic units reflect in detail regional stratigraphic spatial variability that resulted from complex interactions of paleotopography, relative change in sea level, sediment supply, and subsidence. In contrast, the thickness map of the entire New Albany Shale succession (such as might be made using only formation tops) spans many systems tracts and depositional sequences, and only illustrates general stratigraphic variability at basin scale (Figure 14). As discussed in the next section, source- and reservoir-rock properties vary at systems-tract and depositional-sequence scales, and a map of the total thickness of the New Albany Shale would not assist identification of the most prospective areas from the perspective of estimating volumes of key rock properties.

## ROCK PROPERTY VARIATIONS WITHIN A SEQUENCE-STRATIGRAPHIC FRAMEWORK

As is illustrated for the marine and lacustrine settings of other case studies in this Memoir, major shifts in rock properties including organic-matter richness of mudstone strata tend to occur at sequence boundaries, transgressive surfaces, and maximum flooding surfaces. These through-going physical surfaces bound mudstone packages such as systems tracts and depositional sequences that have distinct characteristics.

### Source-Rock Potential

The New Albany Shale is a major source rock in the Illinois Basin. The stratigraphic profiles of TOC content

and organic-matter type in Core 57 show significant vertical variations at facies-association, systems-tract, and depositional-sequence scales (Figure 6). The organic matter in the mudstones penetrated by Core 57 likely did not undergo significant thermal maturation ( $R_o = 0.55\%$ ; Strapoć et al., 2010; Liu et al., 2019), and examination of stratigraphic variability of TOC content and organic-matter type in this core assists our understanding of the source-rock potential of the New Albany Shale.

In this section, we discuss stratigraphic variability of organic-matter type and abundance in the context of an investigation of key controls of organic-matter enrichment at the systems-tract scale. For the New Albany Shale, based on the available data, this is the mappable scale that can inform us about the basinwide potential and distribution of source and reservoir rocks.

What controlled the observed variability in organic-matter enrichment in the New Albany Shale? Examination of Core 57, thin sections, and derived stratigraphic profiles of various geochemical and petrographic proxies shows that organic-carbon sequestration at the systems-tract scale is a result of nonlinear interactions of three key factors: organic-matter production, preservation, and dilution (Lazar, 2007). The role of production, preservation, and dilution in organic-carbon sequestration in fine-grained rocks can be defined using the relative terms of “low,” “moderate,” and “high,” and several conceptual pathways can lead to the formation of organic-carbon-rich or organic-carbon-poor mudstones (Figure 16; Lazar, 2007). Examination of Figure 6 shows that TST mudstones generally have relatively higher TOC contents and mostly marine organic matter dominated by alginite or AOM (Lazar, 2007; Liu et al., 2019). A comparison of organic-carbon sequestration in units 9 (TST) and 4 (TST) shows that Unit 9 has overall a higher TOC and AOM content than Unit 4 (Figure 6). This comparison also illustrates that organic-matter enrichment can follow different pathways defined by the complex interactions of biogenic production, destruction, and dilution (Figure 16). For example, the relatively higher TOC content of Unit 9, FA-7 (8.1–11.9 wt. % TOC; black, “banded,” pyritic mudstone) may be a product of generally moderate to high production, low dilution, and high preservation along the conceptual *green or gray* pathways in Figure 16A. In contrast, the relatively lower TOC content of Unit 4, FA-5 (5.3–8.6 wt. % TOC; black to brown mudstone) may be a product of moderate production, low dilution, and moderate preservation (Figures 6, 16A). This pathway is similar to the conceptual *orange* pathway in Figure 16A.

The case of Unit 4 is particularly interesting in detail. Examination of this unit shows that the measured TOC contents are relatively high in the lower

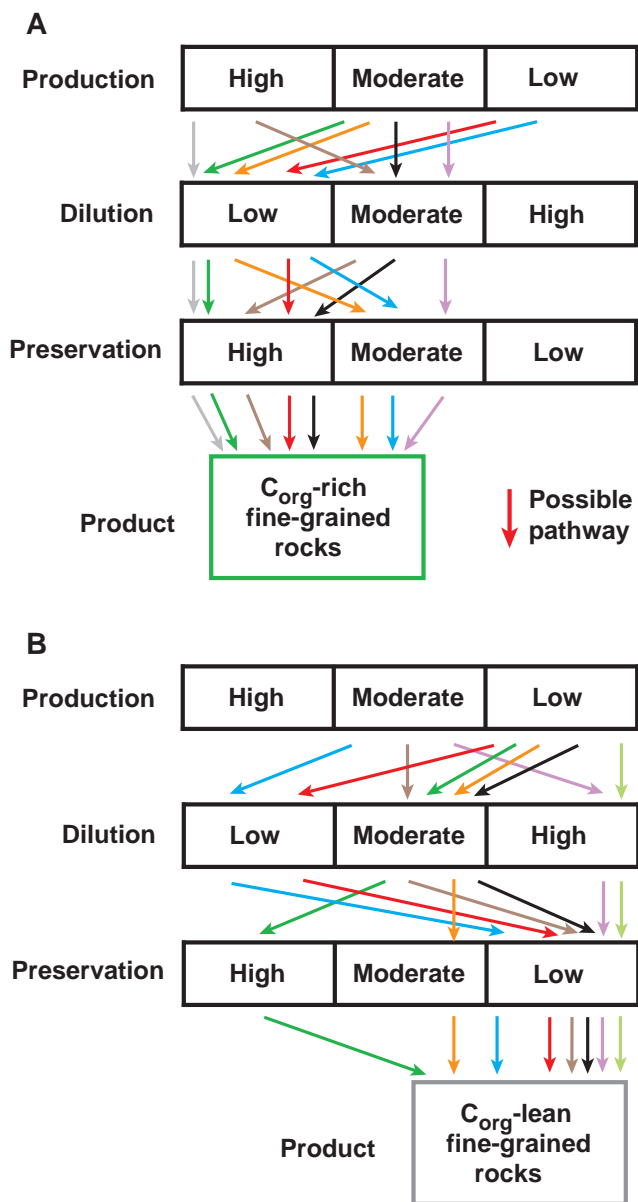


**Figure 16.** Conceptual diagram of the complex interactions of organic preservation, production, and dilution based on Bohacs et al. (2000, 2005), Tyson (1995, 2001, 2005), and Lazar (2007), and references therein. Inputs of preservation, productivity, and dilution are considered in relative terms of low, moderate, and high (from Lazar, 2007). (A) Examples of pathways leading to the formation of organic-carbon-rich fine-grained rocks. Each pathway is marked by a particular color. (B) Examples of pathways leading to the formation of organic-carbon-lean fine-grained rocks.

part of the unit and decrease significantly upsection (Figure 6). The lower half of Unit 4 is dominated by the black, “banded,” “homogeneous-looking,” weakly bioturbated mudstones of FA-4 and the black to brown, weakly to sparsely bioturbated mudstones

interbedded with coarse mudstones and sandstones of FA-5. In contrast, the degree of bioturbation in the upper half of Unit 4 is commonly in the 4–5 range, as this upper part is dominated by the black to gray weakly bioturbated to churned mudstones of FA-6 (1.9–4.6 wt.% TOC; Figure 6). Thus, the 4.5 times lower TOC content toward the top of Unit 4 may primarily reflect an upward decrease of preservation from relatively moderate to relatively low because of either a decrease in sedimentation rate or an increase in paleo-oxygenation levels, or a combination of both (Lazar, 2007). In this case, assuming similar moderate production rates and considering that dilution was relatively low for data points of Unit 4, one can speculate that a change from moderate to low preservation favored different pathways that led to TOC-richer rocks in the lower part of Unit 4 (orange pathway; Figure 16A) and TOC-leaner rocks in the upper part of Unit 4 (blue pathway; Figure 16B). Because a significant difference in preservation may mask the magnitude of initial production, one may also speculate that organic production may have been different throughout. More complex interactions appear if the organic production was different and contributed together with a difference in preservation to the difference in TOC content. For example, organic-matter enrichment in the lower part of Unit 4 could have been the result of moderate production, low dilution, and high preservation (green pathway; Figure 16A), whereas organic-matter enrichment in the upper part of Unit 4 could have been the result of low production, low dilution, and low preservation (red pathway; Figure 16B).

The above analysis can be further extended to discuss organic-carbon sequestration in HST mudstones. For example, Unit 10 (HST) has, on average, a four times higher TOC content than Unit 5 (HST; Figure 6). This large difference in the TOC content between units 10 and 5 has been interpreted as a result of the combined influence of organic-matter preservation and production (Lazar, 2007). Unit 10 has the highest average concentration of TOC in black, “banded,” pyritic mudstones of FA-7 and FA-10 (9.5–14.9 wt. % TOC; Figure 6). The observed organic-carbon enrichment in Unit 10 may be a product of relatively high production, low dilution, and high preservation under what may have been the most oxygen-deprived conditions during the deposition of the New Albany Shale (Figures 6, 16A). This pathway is similar to the conceptual gray pathway in Figure 16A. The lower TOC content of the black to gray, bioturbated mudstones of FA-6, Unit 5 (3.6–5.7 wt.% TOC), may be a product of relatively low to moderate production, moderate to low dilution, and low preservation (Figures 6, 16). These pathways are similar to the conceptual red and brown pathways in Figure 16B.

The above considerations illustrate that TOC content in the New Albany Shale succession is a result of complex and multiple interactions of preservation, production, and dilution. Examination in relative terms of “low,” “moderate,” and “high” of the interactions between these key controls reveals their varying importance in the accumulation of organic matter in the New Albany Shale. Several pathways of organic-carbon sequestration are possible (Figure 16; Lazar, 2007). It is noteworthy that an optimum of organic-matter accumulation in the New Albany Shale apparently resulted from relatively moderate to high production, moderate to low dilution, and high preservation (e.g., Unit 9-TST and Unit 10-HST; Figure 17). In contrast, relatively moderate to low organic production and moderate clastic dilution, coupled with bottom-water conditions that were mostly oxygenated during mud deposition, likely resulted in a relatively low TOC content (e.g., Unit 5-HST; Figure 17; Lazar, 2007). Other studies have also argued that organic-carbon production, preservation, and clastic dilution are fundamental and interrelated factors that have unequal influences in various settings (e.g., Bohacs et al., 2000, 2005; Sageman et al., 2003; Harris, 2005; Bohacs and Ferrin, 2022; Bohacs and Guthrie, 2022; Bohacs et al., 2022b; Chapters 8, 12, and 13 this Memoir; and references therein).

### Hydrocarbon Reservoir Potential

The New Albany Shale is also an important reservoir of hydrocarbons in the Illinois Basin (e.g., Hamilton-Smith et al., 2000; Hill and Nelson, 2000; Curtis, 2002; Partin, 2004). Hydrocarbon gases contained in the New Albany Shale consist of thermogenic gas evolved from thermally mature organic material as well as biogenic methane resulting from bacterial digestion of carbon compounds (e.g., Walter et al., 2000; Curtis, 2002; Comer et al., 2006; Crockett and Morse, 2010; Strapoć et al., 2010). New Albany Shale gas wells were first drilled in the Indiana part of the Illinois Basin in Harrison County, near the Ohio River, more than 100 years ago (Sorgenfrei, 1952; Sullivan, 1995; Hamilton-Smith et al., 2000; Partin, 2004). Gas production has been reported from New Albany Shale reservoirs associated with folds, faults, and draping over the underlying limestone (e.g., Sorgenfrei, 1952; Hamilton-Smith et al., 2000; Partin, 2004). Fractures and veins are common in the New Albany Shale (e.g., Carr, 1981; Hamilton-Smith et al., 2000; Dumitrescu et al., 2004; Schieber and Lazar, 2004; Gale et al., 2010, 2014 and references therein), and its most effective mudstone reservoirs are those that are

fractured naturally. In the outcrops discussed in this chapter, fractures are vertical to subvertical, generally oriented in the northwest–southeast direction, and present mostly in Units 1-TST and 2-HST (Outcrop II) and Unit 7-HST (Outcrop I; Schieber and Lazar, 2004; Lazar, 2007). The most productive gas-producing zone in Harrison County, Indiana, is within Depositional Sequence 4 (mostly 8–19 m thick; Figure 14) at the top of the New Albany Shale (Sorgenfrei, 1952; Partin, 2004; Lazar, 2007). Depositional Sequence 4 has some of the best source rocks in the New Albany Shale succession (Units 9-TST and 10-HST; Figures 6, 17) that can translate into relatively higher organic porosity where mudstones are overmature (Figure 17; Schieber, 2010; Mastalerz et al., 2013). In addition, some of the associated mudstones (FA-7, FA-8, and FA-10) contain up to 46% quartz and carbonate (Figure 6) and might be amenable to induced stimulation. Detailed maps of fracture distribution together with thickness, maturity, and porosity maps can be overlain to identify the most suitable areas for gas exploitation. Such favorable areas would be enhanced where positive structural anomalies are present. This exercise can be extended to the entire New Albany Shale succession to determine areas where key shale-gas parameters are present: an optimum stack of mudstone reservoir facies with sufficient thickness, porosity, and permeability, as well as appropriate maturity, mechanical strength, and present-day pressure (cf. Ottmann and Bohacs, 2014). In addition to facies associations of Depositional Sequence 4, other favorable mudstone reservoir facies include, for example, the dolomitic, subcarbonaceous FA-2 in the TST of Depositional Sequence 1, the interbedded subcarbonaceous FA-5 in the TST of Depositional Sequence 2, and the siliceous-argillaceous, subcarbonaceous FA-7 in the TST of Depositional Sequence 3 (Figure 17; Lazar, 2007; Bohacs et al., 2008).

### CONCLUSIONS

An integrated sequence-stratigraphic framework is proposed for the Middle to Upper Devonian New Albany Shale of the Illinois Basin. This framework is founded on observations in cores, outcrops, and gamma-ray logs. Core and outcrop information was critical for calibration of gamma-ray response and basinwide recognition and correlation of sequence-stratigraphic units. In this context, early integration of biostratigraphic age constraints assisted physical stratigraphic correlations and established ties to extrinsic controls such as eustasy. In the absence of core and outcrop information, recognition and correlation of parasequences based solely on the total gamma-ray response

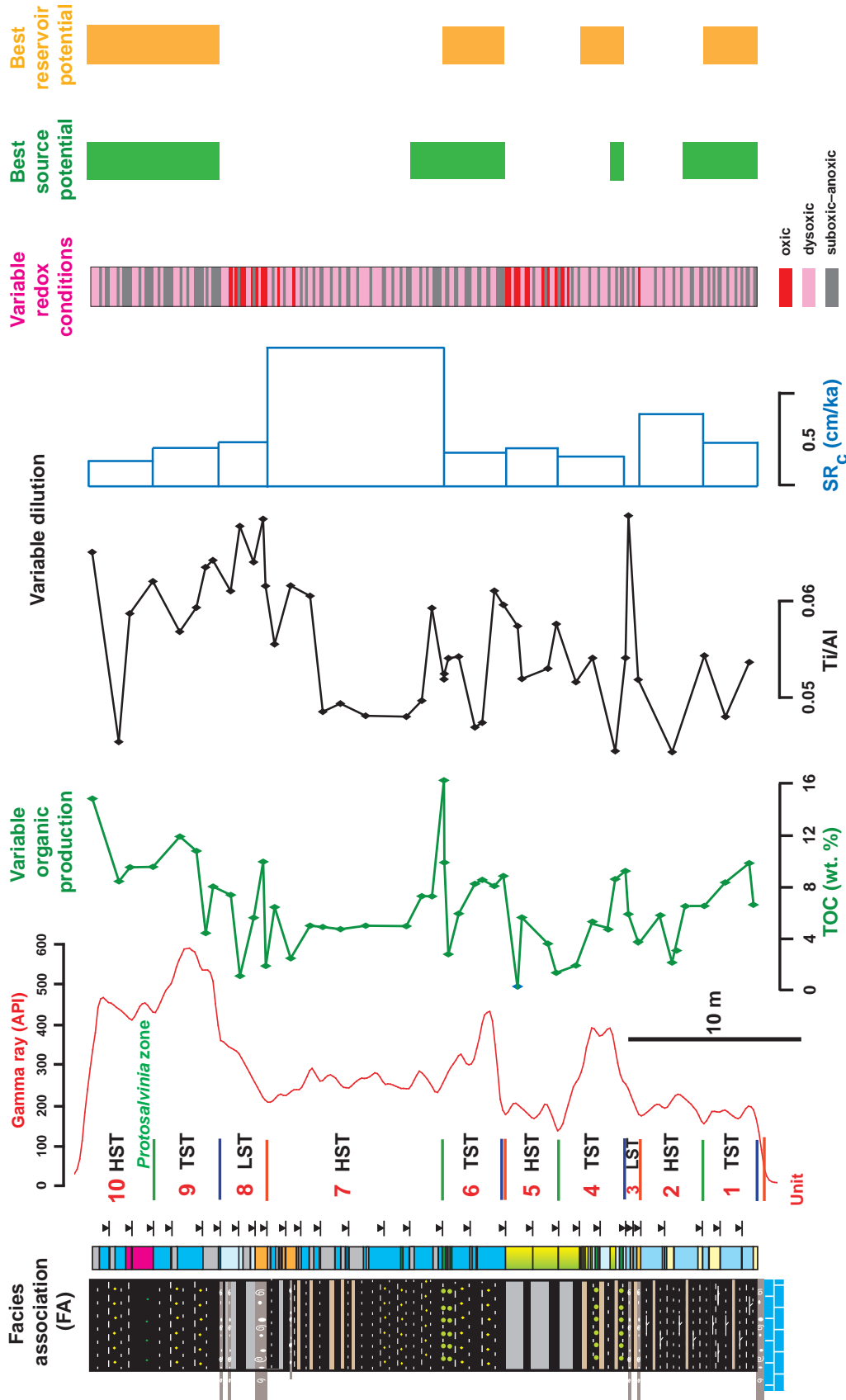


**Figure 17.** Distribution of best source and reservoir rocks in the New Albany Shale (after Lazar, 2007). See Figure 6 for legend of facies association (FA). Oxygen terminology after Tyson and Pearson (1991). API = American Petroleum Institute; HST = highstand systems tract; LST = lowstand systems tract; TST = transgressive systems tract. SR<sub>c</sub> = corrected sedimentation rate.

is challenging especially when available well logs are of different vintages and resolutions.

The proposed sequence-stratigraphic framework provides a unified and internally consistent view of the stratigraphy of the New Albany Shale throughout the Illinois Basin. Within this framework, four depositional sequences bounded by laterally extensive erosion surfaces are recognized and mapped. Depositional sequences, ranging in thickness from a few meters to a few tens of meters, are composed of distinct mudstone units interpreted to be systems tracts. Systems tracts are relatively thin successions ( $<1 - >10$  m) of distinct facies and facies association. A transgressive systems tract (TST) or a highstand systems tract (HST) may be the only preserved parts of a depositional sequence. If present, a lowstand systems tract (LST) can be thin (a few centimeters to a few meters). Depositional sequences and systems tracts are recognized and correlated based on distinct physical, biogenic, and chemical signatures within a robust conodont-based chronostratigraphic framework. Spatial variability of stratal thickness of mudstone units was influenced by paleotopography, ocean-current circulation, and sediment depositional pathways in the basin, as well as sea-level changes and fault-associated subsidence.

Systems tracts and depositional sequences have distinct source- and reservoir-rock properties that vary basinwide as a result of carbonaceous mud accumulation in a relatively low-accommodation setting under the influence of frequent storms, fluctuating sea level, and variable redox conditions. Identification of the most prospective areas for hydrocarbon exploration and production is enhanced by a detailed understanding of regional stratigraphic variability of key rock properties.

The presence of depositional sequences and their constituent mudstone units demonstrates that the sedimentary record of the New Albany Shale is discontinuous. It also indicates that complex, non-linear interactions among organic-matter production, preservation, and clastic dilution controlled organic-carbon sequestration and source- and reservoir-rock properties and distribution in the New Albany Shale succession. This view differs from the long-held belief that the New Albany Shale represents quasi continuous deposition under persistently anoxic bottom-water conditions for a time span exceeding 20 m.y.

The lessons learned here regarding the stratigraphy and the formation of the New Albany Shale could be helpful when studying other mudstone successions. Such lessons include the following:

- Recognition and correlation of parasequences and systems tracts based solely on the total gamma-ray response in the absence of core calibration can be challenging especially when available well logs are of different vintages and resolutions. One can, however, use the sequence-stratigraphic approach even in successions where key stratal units are challenging to identify and not obviously expressed.
- Distance from the mainland shoreline does not necessarily correlate with water depth or bottom energy. Erosional truncation many meters deep can occur hundreds of kilometers away from major land masses.
- It is essential to integrate biostratigraphic age control to provide additional evidence for physical correlations and to tie to extrinsic controls such as eustasy.

*Black shales, correspondingly, should not be assigned to any general condition, but each black shale formation should receive interpretation on the basis of the characteristics of that black shale formation.*

—Twenhofel, 1939, p. 1197

## ACKNOWLEDGMENTS

We thank Jon Kaufman, Taury Smith, and Joao Trabucho Alexandre for their helpful and timely reviews of this chapter. We gratefully acknowledge Kevin Bohacs of ExxonMobil Upstream Research Company for his continuous support of this contribution.

We thank Jeff Over (State University of New York–Geneseo) for his crucial assistance with conodont identification and establishment of the essential conodont zonation.

We are grateful to John Rupp, John Steinmetz, Charles Zuppann, Sherry Cazee (Indiana Geological Survey), David Morse (Illinois State Geological Survey), and Sue Rimmer (University of Kentucky) for their support of this research through facilitating access to cores and gamma-ray logs.

This research has been supported by a grant from the donors of the Petroleum Research Fund, administered by the American Chemical Society awarded to Juergen Schieber, and by grants from the Department of Geological Sciences of Indiana University and from Indiana Geological Survey awarded to Remus Lazar. A National Science Foundation equipment grant to Juergen Schieber provided funds for the purchase of the analytical scanning electron microscope (SEM) that was used for acquiring relevant petrographic information.

## REFERENCES CITED

- Algeo, T. J., R. A. Berner, J. B. Maynard, and S. E. Scheckler, 1995, Late Devonian oceanic anoxic events and biotic crises: "Rooted" in the evolution of vascular land plants?: *GSA Today*, v. 5, p. 63–66.
- Algeo, T. J., S. E. Scheckler, and J. B. Maynard, 2001, Effects of the Middle to Late Devonian spread of vascular land plants on weathering regimes, marine biotas, and global climate, in P. G. Gensel, and D. Edwards, eds., *Plants invade the land: Evolutionary and environmental perspectives*: New York, Columbia University Press, p. 213–236.
- Barrett, T. L., 2002, Detailed correlation of the New Albany Shale in southeastern Indiana with emphasis on erosion surfaces, M.S. thesis, University of Texas–Arlington, Arlington, Texas, 80 p.
- Barrows, M. H., and R. M. Cluff, 1984, New Albany Shale Group (Devonian-Mississippian) source rocks and hydrocarbon generation in the Illinois Basin, in G. Demaison, and R. J. Morris, eds., *Petroleum geochemistry and basin evaluation*, AAPG Memoir 35, p. 111–138.
- Beier, J. A., and J. M. Hayes, 1989, Geochemical and isotopic evidence for paleoredox conditions during deposition of the Devonian-Mississippian New Albany Shale, southern Indiana: *GSA Bulletin*, v. 101, p. 774–782.
- Berner, R. A., 1990, Atmospheric carbon dioxide levels over Phanerozoic time: *Science*, v. 249, p. 1382–1386.
- Berner, R. A., 1997, The rise of plants and their effect on weathering and atmospheric CO<sub>2</sub>: *Science*, v. 276, p. 544–546.
- Berner, R. A., 1999, Atmospheric oxygen over Phanerozoic time: *Proceedings of the National Academy of Science, USA*, v. 96, p. 10955–10957.
- Blakey, R. C., 2006, Sedimentation, Tectonics, and Paleogeography of the North Atlantic Region website (<http://www4.nau.edu/geology>; accessed 1 April 2006).
- Blatt, H., G. Middleton, and R. Murray, 1980, *Origin of sedimentary rocks*, Second Edition: Englewood Cliffs, New Jersey, Prentice-Hall, 782 p.
- Bohacs, K. M., 1998, Contrasting expressions of depositional sequences in mudrocks from marine to non-marine environs, in J. Schieber, W. Zimmerle, and P. Sethi, eds., *Shales and mudstones I*: Stuttgart, Germany, E. Schweizerbart'sche Verlagsbuchhandlung (Nägele u. Obermiller), p. 33–78.
- Bohacs, K. M., A. R. Carroll, J. E. Neal, and P. J. Mankiewicz, 2000, Lake-basin type, source potential, and hydrocarbon character: An integrated sequence-stratigraphic-geochemical framework, in E. H. Gierlowski-Kordesch and K. R. Kelts, eds., *Lake basins through space and time*: AAPG Studies in Geology 46, p. 3–34.
- Bohacs, K. M., and A. Ferrin, 2022, Monterey Formation, Miocene, California, USA—A Cenozoic biosiliceous-dominated continental slope to basin setting: A billion-barrel deep-water mudstone reservoir and source rock, in K. M. Bohacs and O. R. Lazar, eds., *Sequence stratigraphy: Applications to fine-grained rocks*: AAPG Memoir 126, p. 475–504.
- Bohacs, K. M., G. J. Grabowski Jr., and J. E. Neal, 2004, Unlocking geological history: The key roles of mudstones and sequence stratigraphy, in J. Schieber, and R. O. Lazar, eds., *Devonian black shales of the eastern US: New Insights into Sedimentology and Stratigraphy from the Subsurface and Outcrops in the Illinois and Appalachian Basins*: Indiana Geological Survey Open File Study 04-05, p. 78.
- Bohacs, K. M., G. J. J. Grabowski, A. R. Carroll, P. J. Mankiewicz, K. J. Miskell-Gerhardt, J. R. Schwalbach, M. B. Wegner, and J. A. Simo, 2005, Production, destruction, and dilution—The many paths to source-rock development, in N. B. Harris, ed., *The deposition of organic-carbon-rich sediments: Models, mechanisms, and consequences*: SEPM Special Publication 82, p. 61–101.
- Bohacs, K. M., and J. M. Guthrie, 2022, Chimney Rock Shale Member, Paradox Formation, Utah: Paleozoic, shallow carbonate-dominated shelf-to-basin billion-barrel source rocks, in K. M. Bohacs and O. R. Lazar, eds., *Sequence stratigraphy: Applications to fine-grained rocks*: AAPG Memoir 126, p. 223–248.
- Bohacs, K. M., and C. M. Fraticelli, 2006, The critical role of contingency, scaling, and conditioning in applying earth systems models to continental settings: Joint SEPM-GSL Research Conference, *The Application of Earth System Modelling to Exploration Abstract Volume*, Snowbird, Utah, July 11–13, 2006, p. 9–10.
- Bohacs, K. M., and C. Fraticelli, 2008, Paleo-environmental reconstruction and analysis (paleogeography, paleoclimate, paleo-oceanography, paleobiology) as part of integrated source rock prediction: IPTC Paper Number 12257, p. 1–10.
- Bohacs, K. M., and O. R. Lazar, 2008, The role of sequence stratigraphy in unraveling and applying the complex controls from mudstone reservoir properties: AAPG Annual Convention and Exhibition, Program with Abstracts, v. 17, p. 21.
- Bohacs, K. M., O. R. Lazar, R. Klimentides, J. D. Ottmann, J. Markello, M. Hardy, J. O'Leary, and J. Celerier, 2014, Changes in mudstone properties and "shale" reservoir potential through geological time—The impact of biological and oceanic evolution: AAPG Search and Discovery Article #90189.
- Bohacs, K. M., O. R. Lazar, and J. D. Ottman, 2022a, Parasequence sets and depositional sequences, in K. M. Bohacs and O. R. Lazar, eds., *Sequence stratigraphy: Applications to fine-grained rocks*: AAPG Memoir 126, p. 149–194.
- Bohacs, K. M., O. R. Lazar, R. D. Wilson, and J. H. S. Macquaker, 2022b, Mowry Shale–Belle Fourche Shale, Bighorn Basin, Wyoming, USA—A Mesozoic clastic-biosiliceous shelf system: A prolific source rock with associated mudstone reservoir potential, in K. M. Bohacs and O. R. Lazar, eds., *Sequence stratigraphy: Applications to fine-grained rocks*: AAPG Memoir 126, p. 395–474.
- Bohacs, K. M., J. H. S. Macquaker, and O. R. Lazar, 2022c, Kimmeridge Clay Formation, United Kingdom—A Mesozoic clastic-carbonate shelf-to-intrashelf basin system: An outcrop-to-subsurface analog for the Haynesville, Vaca

- Muerta, and Bazhenov formations, *in* K. M. Bohacs and O. R. Lazar, eds., Sequence stratigraphy: Applications to fine-grained rocks: AAPG Memoir 126, p. 345–394.
- Bohacs, K. M., I. O. Norton, D. Gilbert, J. E. Neal, M. Kennedy, W. Borkowski, M. Rottman, and T. Burke, 2012, The accumulation of organic-matter-rich rocks within an earth systems framework: The integrated roles of plate tectonics, atmosphere, ocean, and biota through the Phanerozoic, *in* D. G. Roberts, and A. W. Bally, eds., Regional geology and tectonics: Principles of Geologic Analysis: Amsterdam, the Netherlands, Elsevier, p. 646–678.
- Bohacs, K. M., and J. R. Schwalbach, 1994, Natural gamma-ray spectrometry of the Monterey Formation at Naples Beach, California: Insights into lithology, stratigraphy, and source-rock quality, *in* J. S. Hornafius, ed., Field guide to the Monterey Formation between Santa Barbara and Gaviota: California, The Pacific Section SEPM meeting, May 5–7, 1994, Ventura, California, 123 p.
- Bohacs, K. M., B. West, and G. J. J. Grabowski, 2011, Predicting source occurrence, character, and distribution in frontier settings using paleo-environmental factors: The SourceRER modeling system (Source Retrodiction and Environmental Reconstruction): Geological Society (London) Source Rock Symposium, London, September 12–14, 2011.
- Bond, D., 2006, The fate of the homocatenids (*Tentaculitoidea*) during the Frasnian–Famennian mass extinction (Late Devonian): *Geobiology*, v. 4, p. 167–177.
- Buschbach, T. C., and D. R. Kolata, 1991, Regional setting of Illinois Basin, *in* M. W. Leighton, D. R. Kolata, D. F. Oltz, and J. J. Eidel, eds., Interior cratonic basins: AAPG Memoir 51, p. 29–55.
- Calvert, S. E., R. M. Bustin, and E. D. Ingall, 1996, Influence of water column anoxia and sediment supply on the burial and preservation of organic carbon in marine shales: *Geochimica et Cosmochimica Acta*, v. 60, p. 1577–1593.
- Campbell, G., 1946, New Albany Shale: *GSA Bulletin*, v. 57, p. 829–903.
- Carr, D., 1981, Lineament analysis, *in* N. R. Hasenmueller, and G. S. Woodard, eds., Studies of the New Albany Shale (Devonian and Mississippian) and equivalent strata in Indiana: Morgantown, Western Virginia: US Department of Energy, Morgantown Energy Research Center, DE-AC 21-76MC05204, p. 62–69.
- Catacosinos, P. A., and P. A. J. Daniels, 1991, Early sedimentary evolution of the Michigan Basin: *GSA Special Paper* 256, 248 p.
- Cluff, R. M., 1980, Paleoenvironment of the New Albany Shale group (Devonian–Mississippian) of Illinois: *Journal of Sedimentary Petrology*, v. 50, p. 0767–0780.
- Cluff, R. M., and A. P. Byrnes, 1991, Lopatin analysis of maturation and petroleum generation in the Illinois Basin, *in* M. W. Leighton, D. R. Kolata, D. F. Oltz, and J. J. Eidel, eds., Interior cratonic basins: AAPG Memoir 51, p. 425–454.
- Cluff, R. M., M. L. Reinbold, and J. A. Lineback, 1981, The New Albany Shale group of Illinois: *Illinois State Geological Survey Circular* 518, 83 p.
- Comer, J. B., N. R. Hasenmueller, M. D. Mastalerz, J. A. Rupp, N. R. Shaffer, and C. W. Zuppann, 2006, The New Albany Shale gas play in southern Indiana: AAPG Search and Discovery Article #90059.
- Conant, L. C., and V. E. Swanson, 1961, Chattanooga shale and related rocks of central Tennessee and nearby areas: US Geological Survey Professional Paper 357, 91 p. <https://doi.org/10.3133/pp357>.
- Crockett, J., and D. Morse, 2010, The New Albany Shale in Illinois: Emerging play or prolific source: *Oil and Gas Journal*, v. 108, p. 72–79.
- Cuomo, M. C., and P. R. Bartholomew, 1991, Pelletal black shale fabrics: Their origin and significance, *in* R. V. Tyson, and T. H. Pearson, eds., Modern and ancient continental shelf anoxia: GSA Special Publication 58, p. 221–232.
- Cuomo, M. C., and D. Rhoads, 1987, Biogenic sedimentary fabrics associated with pioneering polychaete assemblages: Modern and ancient: *Journal of Sedimentary Petrology*, v. 57, p. 537–543.
- Curtis, J. B., 2002, Fractured shale-gas systems: AAPG Bulletin, v. 86, p. 1921–1938.
- Day, J., T. Uyeno, W. Norris, B. J. Witzke, and B. J. Bunker, 1996, Middle-Upper Devonian relative sea-level histories of central and western North American interior basin, *in* B. J. Witzke, G. A. Ludvigson, and J. Day, eds., Paleozoic sequence stratigraphy: Views from the North American Craton: GSA Special Publication 306, p. 259–275.
- de Witt, W. J., J. B. Roen, and Wallace, L. G. 1993, Stratigraphy of Devonian black shales and associated rocks in the Appalachian basin, *in* Roen, J. B. and Kepferle, R. C. eds., Petroleum geology of the Devonian and Mississippian black shale of eastern North America: US Geological Survey Bulletin 1909, p. B1–B57.
- Donoghue, P. C. J., P. L. Forey, and R. J. Aldridge, 2000, Conodont affinity and chordate phylogeny: *Biological Review*, v. 75, p. 191–251.
- Dumitrescu, M., D. B. Finkelstein, O. R. Lazar, J. Schieber, and S. C. Brassell, 2004, Origin and history of bitumen in geodes of the New Albany Shale, *in* J. Schieber, and O. R. Lazar, eds., Devonian black shales of the eastern US: New insights into sedimentology and stratigraphy from the subsurface and outcrops in the Illinois and Appalachian basins: Indiana Geological Survey Open File Study 04-05, p. 61–67.
- Ettensohn, F. R., 1992, Changing interpretations of Kentucky geology—Layer-cake facies, flexure, and eustacy: Miscellaneous Report No. 5, Field Trip 15 for the Annual Meeting of the GSA, p. 184.
- Ettensohn, F. R., 1998, Compressional tectonic controls on epicontinental black-shale deposition: Devonian–Mississippian examples from North America, *in* J. Schieber, W. Zimmerle, and P. Sethi, eds., Shales and mudstones I: Stuttgart, Germany, E. Schweizerbart'sche Verlagsbuchhandlung, p. 109–128.
- Ettensohn, F. R., and L. S. Barron, 1981, Depositional model for the Devonian–Mississippian black shale sequence of North America: A tectono-climatic approach: US Department of Energy, Morgantown Energy Technology Center, v. 12040-2, p. 80.

- Ettensohn, F. R., M. L. Miller, S. B. Dillman, T. D. Elam, K. L. Geller, D. R. Swager, G. Markowitz, R. D. Wock, and L. S. Barron, 1988, Characterization and implications of the Devonian–Mississippian black shale sequence, eastern and central Kentucky, USA: Pycnolines, transgression, regression, and tectonism, in N. J. McMillan, A. F. Embry, and D. J. Glass, eds., Devonian of the World: Proceedings of the 2nd International Symposium on the Devonian System — Canadian Society of Petroleum Geologists Memoir 14, p. 323–345.
- Fraticelli, C. M., K. M. Bohacs, and B. P. West, 2006, Vegetation-climate interactions drive sedimentologic evolution through the Phanerozoic: AAPG Search and Discovery article #2006.06088.
- Fraticelli, C. M., B. P. West, K. M. Bohacs, P. E. Patterson, and W. A. Heins, 2004, Vegetation-precipitation interactions drive palaeoenvironmental evolution: Eos Transactions of the American Geophysical Union, Fall Meeting, Supplementary Abstract H54A-06, v. 85, no. 47.
- Frost, J. K., 1996, Geochemistry of black shales of the New Albany Group (Devonian-Mississippian) in the Illinois Basin: Relationships between lithofacies and the carbon, sulfur, and iron contents: Department of Natural Resources Illinois State Geological Survey, Circular 557, p. 1–24.
- Frost, J. K., and N. R. Shaffer, 2000, Mineralogy and geochemistry, in N. R. Hasenmueller, and J. B. Comer, eds., Gas potential of the New Albany Shale (Devonian and Mississippian) in the Illinois Basin: Gas Research Institute, GRI-00/0068, p. 41–46.
- Gale, J. F. W., W. E. Laubach, and L. J. Fidler, 2010, Natural fractures in the New Albany Shale, Illinois Basin, and their importance for Shale-Gas production: AAPG Search and Discovery article #80120.
- Gale, J. F. W., W. E. Laubach, J. E. Olson, P. Eichhubl, and A. Fall, 2014, Natural fractures in shale: A review and new observations: AAPG Bulletin, v. 98, no. 11, p. 2165–2216.
- Gray, J., and A. J. Boucot, 1977, Early vascular land plants: Proof and conjecture: *Lethaia*, v. 10, p. 145–174.
- Gray, J., and A. J. Boucot, 1979, The Devonian land plant *Protosalvinia*: *Lethaia*, v. 12, p. 57–63.
- Hallam, A., 1984, Pre-quaternary sea level changes: Annual Review of Earth and Planetary Sciences, v. 12, p. 205–243.
- Hallam, A., and P. B. Wignall, 1999, Mass extinctions and sea-level changes: Earth-Science Reviews, v. 48, p. 217–250.
- Hamilton-Smith, T., N. R. Hasenmueller, W. S. Boberg, Z. Smidchens, and W. T. Frankie, 2000, Gas production, in N. R. Hasenmueller, and J. B. Comer, eds., Gas potential of the New Albany Shale (Devonian and Mississippian) in the Illinois Basin: Gas Research Institute, GRI-00/0068, p. 23–40.
- Hannibal, J. T., 1994, Methods for distinguishing carbonized specimens of the presumed cephalopod aptychus *Sidetes (Spathiocaris)* from the plant *Protosalvinia (Foerstia)*: Journal of Paleontology, v. 68, p. 671–673.
- Harris, N. B., 2005, The deposition of organic-carbon-rich sediments: Models, mechanisms, and consequences—introduction, in N. B. Harris, ed., The deposition of organic-carbon-rich sediments: Models, mechanisms, and consequences: SEPM Special Publication 82, p. 1–5.
- Hasenmueller, N. R., 1993, New Albany Shale (Devonian and Mississippian) of the Illinois Basin, in J. B. Roen and R. C. Kepferle, Petroleum geology of the Devonian and Mississippian black shale of eastern North America: US Geological Survey Bulletin 1909, p. C1–C19.
- Hasenmueller, N. R., and J. B. Comer, 2000, Gas potential of the New Albany Shale (Devonian and Mississippian) in the Illinois Basin: Gas Research Institute GRI-00/0068, 83 p.
- Hasenmueller, N. R., W. S. Boberg, D. K. Lumm, W. T. Frankie, T. Hamilton-Smith, and J. B. Comer, 2000, Stratigraphy, in N. R. Hasenmueller, and J. B. Comer, eds., Gas potential of the New Albany Shale (Devonian and Mississippian) in the Illinois Basin: Gas Research Institute GRI-00/0068, p. 13–22.
- Hasenmueller, N. R., R. D. Matthews, R. C. Kepferle, and D. Pollock, 1983, *Foerstia (Protosalvinia)* in Devonian shales of the Appalachian, Illinois, and Michigan Basins, eastern United States: in Eastern Oil Shale Symposium Proceedings, Lexington, Kentucky, October 1–2 1983, University of Kentucky Institute for Mining and Mineral Research Report IMMR83-089, p. 41–58.
- Hatch, J. R., J. D. King, and J. B. Risatti, 1991, Geochemistry of Illinois Basin oils and hydrocarbon source rocks, in M. W. Leighton, D. R. Kolata, D. F. Oltz, and J. J. Eidel, eds., Interior cratonic basins: AAPG Memoir 51, p. 403–423.
- Hill, D. G., and Nelson, C. R. 2000, Gas-productive fractured shales—An overview and update: Gas Tips, v. 6, no. 3, p. 4–13.
- House, M. R., 2002, Strength, timing, setting and cause of Mid-Paleozoic extinctions: Palaeogeography, Palaeoclimatology, Palaeoecology, v. 181, p. 5–25.
- House, M. R., and F. M. Gradstein, 2004, The Devonian period, in F. M. Gradstein, J. G. Ogg, and A. G. Smith, eds., A geologic time scale 2004: Cambridge, U.K., Cambridge University Press, p. 202–221.
- Huddle, J. W., 1933, Marine fossils from the top of the New Albany Shale of Indiana: American Journal of Science, v. 25, p. 303–314.
- Huddle, J. W., 1934, Conodonts from the New Albany Shale of Indiana: Bulletins of American Paleontology, v. 21, p. 189–324.
- Ingall, E. D., R. M. Bustin, and P. Van Cappellen, 1993, Influence of water column anoxia on the burial and preservation of carbon and phosphorus in marine shales: *Geochimica et Cosmochimica Acta*, v. 57, p. 303–316.
- Jablonski, D., 1991, Extinctions: A paleontological perspective: *Science*, v. 253, p. 754–757.
- Joachimski, M. M., and W. Buggisch, 2002, Conodont apatite  $\delta^{18}\text{O}$  signatures indicate climate cooling as a trigger of the Late Devonian mass extinction: *Geology*, v. 30, p. 711–714.
- Joachimski, M. M., S. Breisig, W. Buggisch, J. A. Talent, R. Mawson, M. Gereke, J. R. Morrow, J. Day, and K. Weddige, 2009, Devonian climate and reef evolution: Insights from oxygen isotopes in apatite: *Earth and Planetary Science Letters*, v. 284, p. 599–609.

- Johnson, J. G., G. Klapper, and C. A. Sandberg, 1985, Devonian eustatic fluctuations in Euramerica: GSA Bulletin, v. 96, p. 567–587.
- Johri, P., and J. Schieber, 1999, A detailed study of gamma ray logs from the Laconia field in southern Indiana: Internal stratigraphy of the New Albany Shale and implications for sequence stratigraphy: GSA Abstracts with Programs, v. 31, p. A-10.
- Kaufmann, B., 2006, Calibrating the Devonian time scale: A synthesis of U-Pb ID-TIMS ages and conodont stratigraphy: Earth-Science Reviews, v. 76, p. 175–190.
- Kepferle, R. C., 1981, Correlation of Devonian shale between the Appalachian and the Illinois Basins facilitated by *Foerstia (Protosalvinia)*, in T. G. Roberts, ed., GSA Cincinnati '81 Field Trip Guidebooks, Volume II: Economic geology, structure: American Geological Institute, p. 334–335.
- Kepferle, R. C., and J. B. Roen, 1981, Chattanooga and Ohio Shales of the southern Appalachian Basin (Field Trip No. 3), in T. G. Roberts, ed., GSA Cincinnati '81 Field Trip Guidebooks, Volume II: Economic geology, structure: American Geological Institute, p. 259–407.
- Kolata, D. R., and W. J. Nelson, 1991, Tectonic history of the Illinois Basin, in M. W. Leighton, D. R. Kolata, D. F. Oltz, and J. J. Eidel, eds., Interior cratonic basins: AAPG Memoir 51, p. 263–285.
- Lazar, O. R., 2007, Redefinition of the New Albany Shale of the Illinois basin: An integrated, stratigraphic, sedimentologic, and geochemical study, Ph.D. thesis, Indiana University, Bloomington, Indiana, 336 p.
- Lazar, O. R., K. M. Bohacs, J. Schieber, J. H. S. Macquaker, and T. M. Demko, 2015a, Mudstone primer: Lithofacies variations, diagnostic criteria, and sedimentologic/stratigraphic implications at lamina to bedset scale: SEPM Concepts in Sedimentology and Paleontology 12, 204 p.
- Lazar, O. R., K. M. Bohacs, J. H. S. Macquaker, and J. Schieber, and T. M. Demko, 2015b, Capturing key attributes of fine-grained sedimentary rocks in outcrops, cores, and thin sections: Nomenclature and description guidelines: Journal of Sedimentary Research, v. 85, p. 230–246.
- Lazar, O. R., K. M. Bohacs, J. Schieber, J. H. S. Macquaker, and T. M. Demko, 2022a, Tools and techniques for studying mudstones, in K. M. Bohacs and O. R. Lazar, eds., Sequence stratigraphy: Applications to fine-grained rocks: AAPG Memoir 126, p. 35–88.
- Lazar, O. R., K. M. Bohacs, J. Schieber, J. H. S. Macquaker, and T. M. Demko, 2022b, Mudstone nomenclature, in K. M. Bohacs and O. R. Lazar, eds., Sequence stratigraphy: Applications to fine-grained rocks: AAPG Memoir 126, p. 21–34.
- Lazar, O. R., and J. Schieber, 2004, New Albany and Ohio Shales: An introduction, in J. Schieber, and O. R. Lazar, eds., Devonian Black Shales of the eastern U.S.: New insights into sedimentology and stratigraphy from the subsurface and outcrops in the Illinois and Appalachian basins: Indiana Geological Survey Open File Study 04-05, p. 31–34.
- Lazar, O. R., and J. Schieber, 2005a, A coherent and genetically based stratigraphic framework for the New Albany Shale succession: Methods and results: AAPG Search and Discovery article #90039.
- Lazar, O. R., and J. Schieber, 2005b, Paleo-redox conditions during deposition of the Devonian New Albany Shale, Illinois Basin: Results of a multi-proxy investigation: AAPG Search and Discovery article #90039.
- Lazar, O. R., and J. Schieber, 2006, Stratigraphic insights into Late Devonian black shales of the Illinois and Appalachian Basins: Outcrop to subsurface examples: AAPG Annual Convention, Houston, April 9–12, 2006, Abstracts Volume, p. 62.
- Li, Y., and J. Schieber, 2015, On the origin of a phosphate enriched interval in the Chattanooga Shale (Upper Devonian) of Tennessee—A combined sedimentologic, petrographic, and geochemical study: Sedimentary Geology, v. 329, p. 40–61.
- Li, Z. X., C. M. Powell, and A. Trench, 1994, Paleozoic global reconstructions, in J. A. Long, ed., Paleozoic vertebrate biostratigraphy and biogeography: Baltimore, Maryland, The Johns Hopkins University Press, p. 25–53.
- Lineback, J. A., 1964, Stratigraphy and depositional environment of the New Albany Shale (Upper Devonian and Lower Mississippian) in Indiana, Ph.D. thesis, Indiana University, Bloomington, Indiana, p. 136.
- Lineback, J. A., 1968, Subdivisions and depositional environments of New Albany Shale (Devonian-Mississippian) in Indiana: AAPG Bulletin, v. 52, p. 1291–1303.
- Lineback, J. A., 1970, Stratigraphy of the New Albany Shale in Indiana: State of Indiana Department of Natural Resources Geological Survey Bulletin, v. 44, p. 73.
- Liu, B., J. Schieber, and M. Mastalerz, 2017, Combined SEM and reflected light petrography of organic matter in the New Albany Shale (Devonian-Mississippian) in the Illinois Basin: A perspective on organic pore development with thermal maturation: International Journal of Coal Geology, v. 184, p. 57–72.
- Liu, B., J. Schieber, M. Mastalerz, and J. Teng, 2019, Organic matter content and type variation in the sequence stratigraphic context of the Upper Devonian New Albany Shale, Illinois Basin: Sedimentary Geology, v. 383, p. 101–120.
- Lobza, V., and J. Schieber, 1999, Biogenic sedimentary structures produced by worms in soupy, soft muds: Observations from the Chattanooga Shale (Upper Devonian) and experiments: Journal of Sedimentary Research, v. 69, p. 1041–1049.
- Lumm, D. K., W. T. Frankie, N. R. Hasenmueller, and T. Hamilton-Smith, 2000, Illinois Basin geologic setting, in N. R. Hasenmueller, and J. B. Comer, eds., Gas potential of the New Albany Shale (Devonian and Mississippian) in the Illinois Basin: Gas Research Institute, GRI-00/0068, p. 9–12.
- Markello, J. R., R. B. Koepnick, L. E. Waite, and J. F. Collins, 2008, The carbonate analogs through time (CATT) Hypothesis and the global atlas of carbonate fields—A systematic and predictive look at Phanerozoic carbonate systems, in J. Lukasik, and J. A. Simo, eds., Controls on carbonate platform and reef development: SEPM Special Publication 89, p. 15–45.
- Mastalerz, M., A. Schimmelmann, A. Drobniak, and Y. Chen, 2013, Porosity of Devonian and Mississippian New

- Albany Shale across a maturation gradient: Insights from organic petrology, gas adsorption, and mercury intrusion: AAPG Bulletin, v. 97, no. 10, p. 1621–1643.
- Matthews, R. D., 1993, Review and revision of the Devonian-Mississippian stratigraphy in the Michigan Basin, in J. B. Roen, and R. C. Kepferle, eds., Petroleum geology of the Devonian and Mississippian black shale of eastern North America: US Geological Survey Bulletin 1909, p. D1–D85.
- McGhee, G. R. J., 1996, The Late Devonian mass extinction: The Frasnian/Famennian crisis: New York, Columbia University Press, p. 303.
- McGhee, G. R. J., 2005, Modelling Late Devonian extinction hypotheses, in D. J. Over, J. R. Morrow, and P. B. Wignall, eds., Understanding Late Devonian and Permian-Triassic biotic and climatic events: Towards an integrated approach: Amsterdam, Elsevier B.V., p. 37–50.
- McKerrow, W. S., C. Mac Niocaill, P. E. Ahlberg, G. Clayton, C. J. Cleal, and R. M. C. Eager, 2000, The Late Paleozoic relations between Gondwana and Laurasia, in W. Franke, V. Haak, O. Oncken, and D. Tanner, eds., Orogenic processes: Quantification and modelling in the Variscan Belt: Geological Society (London) Special Publication 179, p. 9–20.
- National Petroleum Council, 1980, Devonian shale, in J. F. Bookout, chairman, Unconventional gas sources: Washington, D.C., National Petroleum Council, p. D3.
- National Petroleum Council, 1992, Source and supply, in F. H. Richardson, chairman, The potential for natural gas in the United States: Washington, D.C., National Petroleum Council, p. 91–142.
- Nelson, W. J., 1991, Structural styles of the Illinois Basin, in M. W. Leighton, D. R. Kolata, D. F. Oltz, and J. J. Eidel, eds., Interior cratonic basins: AAPG Memoir 51, p. 209–243.
- Nelson, W. J., and S. Marshak, 1996, Devonian tectonism of the Illinois basin region, US continental interior, in B. A. van der Pluijm, and P. A. Catacosinos, eds., Basement and basins of eastern North America: GSA Special Paper 308, p. 169–179.
- Niklas, K. J., 1976, Organic chemistry of *Protosalvinia* (=*Foerstia*) from the Chattanooga and New Albany Shales: Review of Palaeobotany and Palynology, v. 22, p. 265–279.
- Niklas, K. J., and T. L. Phillips, 1976, Morphology of *Protosalvinia* from the Upper Devonian of Ohio and Kentucky: American Journal of Botany, v. 63, p. 9–29.
- Nuttall, B. C., 2013, Middle and Late Devonian New Albany Shale in the Kentucky Geological Survey Marvin Blan No. 1 Well, Hancock County, Kentucky: Report of Investigations 17, Series XII, Kentucky Geological Survey.
- Nuttall, B. C., T. M. Parris, G. Beck, D. C. Willette, M. Mastalerz, and J. Crockett, 2015, Oil production from low-maturity organic-rich shale: An example from the Devonian New Albany Shale in the Illinois Basin, Breckinridge County, Kentucky: AAPG Search and Discovery article #51196.
- Ottmann, J. D., and K. M. Bohacs, 2014, Conventional reservoirs hold keys to the ‘Un’s: AAPG Explorer, February 2014, p. 42.
- Over, D. J., 2002, The Frasnian/Famennian boundary in central and eastern United States: Palaeogeography, Palaeoclimatology, Palaeoecology, v. 181, p. 153–169.
- Over, D. J., E. Hauf, J. Wallace, J. Chiarello, J. S. Over, G. J. Gilleaudeau, Y. Song, and T. J. Algeo, 2019, Conodont biostratigraphy and magnetic susceptibility of Upper Devonian Chattanooga Shale, eastern United States: Evidence for episodic deposition and disconformities: Palaeogeography, Palaeoclimatology, Palaeoecology, v. 524, p. 137–149.
- Over, D. J., O. R. Lazar, G. C. Baird, J. Schieber, and F. P. Ettensohn, 2009, *Protosalvinia* Dawson and associated conodonts of the upper *Trachytera* Zone, Famennian, Upper Devonian, in the eastern United States: Journal of Paleontology, v. 83, p. 70–79.
- Partin, T. H., 2004, Demand and high price spurs a new era of drilling for the New Albany Shale gas wells in Harrison County, Indiana, in J. Schieber and O. R. Lazar, eds., Devonian Black Shales of the eastern US: New insights into sedimentology and stratigraphy from the subsurface and outcrops in the Illinois and Appalachian Basins: Indiana Geological Survey Open File Study 04-05, p. 68–76.
- Potma, K., R. Jonk, and K. M. Bohacs, 2022, Canol Formation, Northwest Territories, Canada—An outcrop-to-subsurface analog for the Paleozoic Horn River Shale-gas play, in K. M. Bohacs and O. R. Lazar, eds., Sequence stratigraphy: Applications to fine-grained rocks: AAPG Memoir 126, p. 295–344.
- Racki, G., 2005, Toward understanding Late Devonian global events: Few answers, many questions, in D. J. Over, J. R. Morrow, and P. B. Wignall, eds., Understanding Late Devonian and Permian-Triassic biotic and climatic events: Towards an integrated approach: Amsterdam, Elsevier B.V., p. 5–36.
- Riese, D. J., 2014, The significance of crypto- and macrobioturbation in the New Albany Shale for the interpretation of depositional histories: An integrated approach using core descriptions, CT scans, neoichnology experiments, and geochemistry, Ph.D. thesis, Indiana University, Bloomington, Indiana, 301 p.
- Ripley, E. M., N. R. Shaffer, and M. S. Gilstrap, 1990, Distribution and geochemical characteristics of metal enrichment in the New Albany Shale (Devonian-Mississippian), Indiana: Economic Geology, v. 85, p. 1790–1807.
- Roen, J. B., 1993, Introductory review—Devonian and Mississippian black shales, eastern North America, in J. B. Roen, and R. C. Kepferle, eds., Petroleum geology of the Devonian and Mississippian black shale of eastern North America: US Geological Survey Bulletin 1909, p. A1–A8.
- Romankiw, L. A., P. G. Hatcher, and J. B. Roen, 1988, Evidence of land plant affinity for the Devonian fossil *Protosalvinia* (*Foerstia*): *Lethaia*, v. 21, p. 417–423.
- Sageman, B. B., A. E. Murphy, J. P. Werne, C. A. Ver Straeten, D. J. Hollander, and T. W. Lyons, 2003, A tale of shales: The relative roles of production, decomposition, and dilution in the accumulation of organic-rich strata,

- Middle–Upper Devonian, Appalachian basin: Chemical Geology, v. 195, p. 229–273.
- Sandberg, C. A., N. R. Hasenmueller, and C. B. Rexroad, 1994, Conodont biochronology, biostratigraphy, and biofacies of Upper Devonian part of New Albany Shale, Indiana: CFS, v. 168, p. 227–253.
- Schieber, J., 1994a, Evidence for episodic high energy events and shallow water deposition in the Chattanooga Shale, Devonian, central Tennessee, USA: *Sedimentary Geology*, v. 93, p. 193–208.
- Schieber, J., 1996, Early diagenetic silica deposition in algal cysts and spores: A source of sand in black shales?: *Journal of Sedimentary Research*, v. 66, p. 175–183.
- Schieber, J., 1998a, Sedimentary features indicating erosion, condensation, and hiatuses in the Chattanooga Shale of Central Tennessee: Relevance for sedimentary and stratigraphic evolution, in J. Schieber, W. Zimmerle, and P. Sethi, eds., *Shales and mudstones I*: Stuttgart, Germany, E. Schweizerbart'sche Verlagsbuchhandlung (Nägele u. Obermiller), p. 187–215.
- Schieber, J., 1998b, Developing a sequence stratigraphic framework for the Late Devonian Chattanooga Shale of the southeastern USA.: Relevance for the Bakken Shale, in J. E. Christopher, C. F. Gilboy, D. F. Paterson, and S. L. Bend, eds., Eighth International Williston Basin Symposium, Volume 13, Saskatchewan Geological Society Special Publication, p. 58–68.
- Schieber, J., 1999, Distribution and deposition of mudstone facies in the Upper Devonian Sonyea Group of New York: *Journal of Sedimentary Research*, v. 69, p. 909–925.
- Schieber, J., 2000, Sequence stratigraphic correlations in Devonian Black Shales of the eastern US: Relationship to global sea level variations: AAPG Search and Discovery article #90914.
- Schieber, J., 2001, A role for organic petrology in integrated studies of mudrocks: Examples from Devonian black shales of the eastern US: *International Journal of Coal Geology* v. 47, p. 171–187.
- Schieber, J., 2003, Simple gifts and buried treasures—implications of finding bioturbation and erosion surfaces in black shales: *The Sedimentary Record*, v. 1, p. 4–8.
- Schieber, J., 2004a, On the origin and significance of pyrite beds in Devonian black shales from the eastern US: GSA Abstracts with Programs, v. 36, p. 372.
- Schieber, J., 2004b, Connecting the dots: Sequence stratigraphic correlations in Devonian black shales of the eastern US and relationship to global sea-level variations, in J. Schieber, and O. R. Lazar, eds., *Devonian Black Shales of the eastern U.S.: New insights into sedimentology and stratigraphy from the subsurface and outcrops in the Illinois and Appalachian basins*: Indiana Geological Survey Open File Study 04-05, p. 80–82.
- Schieber, J., 2009, Discovery of agglutinated benthic foraminifera in Devonian black shales and their relevance for the redox state of ancient seas: *Palaeogeography, Palaeoclimatology, Palaeoecology*, v. 271, p. 292–300.
- Schieber, J., 2010, Common themes in the formation and preservation of intrinsic porosity in shales and mudstones—Illustrated with examples across the Phanerozoic: SPE-132370, 10 p.
- Schieber, J., and G. Baird, 2001, On the origin and significance of pyrite spheres in Devonian black shales of North America: *Journal of Sedimentary Research*, v. 71, p. 155–166.
- Schieber, J., and O. R. Lazar, 2004, Devonian Black Shales of the eastern U.S.: New insights into sedimentology and stratigraphy from the subsurface and outcrops in the Illinois and Appalachian basins: *Indiana Geological Survey Open File Study 04-05*, p. 8–29.
- Schieber, J., and O. R. Lazar, 2010, Outcrop description: Central Kentucky, in J. Schieber, R. Lazar, and K. Bohacs, eds., *Sedimentology and stratigraphy of shales: Expression and correlation of depositional sequences in the Devonian Tennessee, Kentucky and Indiana*: AAPG Field Guide for Post-Convention Field Trip 10, p. 116–142.
- Schieber, J., and L. Ricupi, 2004, Pyrite ooids in Devonian black shales record intermittent sea-level drop and shallow-water conditions: *Geology*, v. 32, p. 305–308.
- Schieber, J., and J. B. Southard, 2009, Bedload transport of mud by floccule ripples: Direct observation of ripple migration processes and their implications: *Geology*, v. 37, p. 483–486.
- Schieber, J., and Z. Yawar, 2009, A new twist on mud deposition: Mud ripples in experiment and rock record: *The Sedimentary Record*, v. 7, no. 2, p. 4–8.
- Schieber, J., D. Krinsley, and L. Ricupi, 2000, Diagenetic origin of quartz silt in mudstones and implications for silica cycling: *Nature*, v. 406, p. 981–985.
- Schieber, J., O. R. Lazar, and K. M. Bohacs, 2010, *Sedimentology and stratigraphy of shales: Expression and correlation of depositional sequences in the Devonian of Tennessee, Kentucky, and Indiana*: SEPM Field Guidebook for Post-Convention Field Trip 10, 172 p.
- Schopf, J. M., and J. F. Schwietering, 1970, The *Foerstia* zone of the Ohio and Chattanooga Shales: US Geological Survey Bulletin, v. 1294-H, p. H16.
- Scotese, C. R., and W. S. McKerrow, 1990, Revised world maps and introduction, in W. S. McKerrow, and C. R. Scotese, eds., *Palaeozoic palaeogeography and biogeography*: Geological Society (London) Memoir 12, p. 1–21.
- Sepkoski, J. J. J., 1986, Phanerozoic overview of mass extinction, in D. M. Raup, and D. Jablonski, eds., *Patterns and processes in the history of life*: Berlin, Springer-Verlag, p. 277–295.
- Seyler, B., and R. M. Cluff, 1991, Petroleum traps in the Illinois Basin, in M. W. Leighton, D. R. Kolata, D. F. Oltz, and J. J. Eidel, eds., *Interior cratonic basins*: AAPG Memoir 51, p. 361–401.
- Slatt, R. M., D. W. Jordan, A. E. D'Agostino, and R. H. Gillespie, 1992, Outcrop gamma-ray logging to improve understanding of subsurface well log correlations, in A. Hurst, C. M. Griffiths, and P. F. Worthington, eds., *Geological applications of wireline logs II*: GSA Special Publication 65, p. 3–19.

- Smith, L. B., J. Schieber, and R. D. Wilson, 2019, Shallow-water onlap model for the deposition of Devonian black shales in New York, USA: *Geology*, v. 47, p. 279–283.
- Sorgenfrei, H. Jr., 1952, Gas production for the New Albany Shale, M.S. thesis, Indiana University, Bloomington, Indiana, 26 p.
- Spencer, S. C., 2013, A sedimentologic, petrographic, mineralogic, and geochemical investigation of parasequences in the Camp Run Member of the Late Devonian New Albany Shale, M.S. thesis, Indiana University, Bloomington, Indiana, 169 p.
- Strašoć, D., M. Mastalerz, A. Schimmelmann, A. Drobniak, and N. R. Hasenmueller, 2010, Geochemical constraints on the origin and volume of gas in the New Albany Shale (Devonian–Mississippian), eastern Illinois Basin: *AAPG Bulletin*, v. 94, p. 1713–1740. <http://dx.doi.org/10.1306/06301009197>.
- Strelc, M., M. V. Caputo, S. Loboziak, and J. H. G. Melo, 2000, Late Frasnian–Famennian climates based on palynomorph analyses and the question of the Late Devonian glaciations: *Earth-Science Reviews*, v. 52, p. 121–173.
- Sullivan, D. M., 1995, Natural gas fields in Indiana: Indiana Geological Survey Special Report 51, 69 p.
- Tait, J., M. Schatz, V. Bachtadse, and H. Soffel, 2000, Paleomagnetism and Paleozoic paleogeography of Gondwana and European terranes, in W. Franke, V. Haak, O. Oncken, and D. Tanner, eds., *Orogenic processes: Quantification and modelling in the Variscan Belt*, The Geological Society (London) Special Publication 179, p. 21–34.
- Taylor, G. H., M. Teichmuller, A. Davis, C. F. K. Diessel, R. Littke, and P. Robert, 1998, *Organic petrology*: Stuttgart, Germany, Gebrüder Borntraeger, 704 p.
- Twenhofel, W. H., 1939, Environments of origin of black shales: *AAPG Bulletin*, v. 23, p. 1178–1198.
- Tyson, R. V., 1995, Sedimentary organic matter: organic facies and palynofacies: London, Chapman and Hall, 615 p.
- Tyson, R. V., 2001, Sedimentation rate, dilution, preservation and total organic carbon: Some results of a modelling study: *Organic Geochemistry*, v. 32, p. 333–339.
- Tyson, R. V., 2005, The "productivity versus preservation" controversy: Cause, flaws, and resolution, in N. B. Harris, ed., *The deposition of organic-carbon-rich sediments: Models, mechanisms, and consequences*: SEPM Special Publication 82, p. 17–33.
- Tyson, R. V., and T. H. Pearson, 1991, Modern and ancient continental shelf anoxia: An overview, in R. V. Tyson and T. H. Pearson, eds., *Modern and ancient continental shelf anoxia*: GSA Special Publication 58, p. 1–24.
- Vail, P. R., R. M. Mitchum Jr., and S. Thompson III, 1977, Seismic stratigraphy and global changes of sea level. Part 3: Relative changes of sea level from coastal onlap, in C. E. Payton, ed., *Seismic stratigraphy-applications to hydrocarbon exploration*: AAPG Memoir 26, p. 63–81.
- van der Voo, R., 1988, Paleozoic paleogeography of North America, Gondwana, and intervening displaced terranes: Comparisons of paleomagnetism with paleoclimatology and biogeographical patterns: *GSA Bulletin*, v. 100, p. 311–324.
- Walter, L. M., J. C. McIntosh, J. M. Budai, and A. M. Martini, 2000, Hydrogeochemical controls on gas occurrence and production in the New Albany Shale: *GasTIPS*, v. 6, no. 2, p. 14–20.
- Wei, L., Y. Wang, and M. Mastalerz, 2016, Comparative optical properties of macerals and statistical evaluation of mis-identification of vitrinite and solid bitumen from early mature Middle Devonian–Lower Mississippian New Albany Shale: Implications for thermal maturity assessment: *International Journal of Coal Geology*, v. 168, p. 222–236.
- Wilson, R. D., and J. Schieber, 2017, Association between wave- and current-aided hyperpycnites and flooding surfaces in shelfal mudstones: An integrated sedimentologic, sequence stratigraphic, and geochemical approach: *Journal of Sedimentary Research*, v. 87, p. 1143–1155.
- Wittmer, J. M., and A. Miller, 2011, Dissecting the global diversity trajectory of an enigmatic group: The paleogeographic history of tentaculitoids: *Palaeogeography, Palaeoclimatology, Palaeoecology*, v. 312, p. 54–65.
- Ziegler, W., and C. A. Sandberg, 1990, The Late Devonian standard conodont zonation: *Courier Forschungs-Institut Senckenberg*, v. 121, p. 1–115.

